

Alma Mater Studiorum – Università di Bologna

DOTTORATO DI RICERCA in

Biologia Cellulare e Molecolare

Ciclo: 29

Settore Concorsuale di afferenza:O5/E1

Settore Scientifico disciplinare:BIO/10

TITOLO TESI

Mitochondrial DNA deletions:

Quantitative evaluation of single and multiple
deletions generation and expansion in single cells

Presentata da: Selena Trifunov

Coordinatore Dottorato

Prof. Giovanni Capranico

Relatore

Prof. Valerio Carelli

Correlatore

Prof. ssa Michela Rugolo

ABSTRACT

Mitochondria are unique organelles, containing their own, maternally inherited genome. Human mitochondrial DNA (mtDNA) is small, circular and intronless, encoding 37 genes, precisely 13 proteins of the respiratory chain, 22 transfer RNAs (tRNAs) and 2 ribosomal RNAs. Each mitochondrion contains several mtDNA copies. Mitochondrial DNA deletions are pathogenic mutations that remove various portions of mtDNA genome, leading to shorter mtDNA molecules. In patients, there are two classes of mtDNA deletions: single, large-scale deletions that are present from the birth, whereas multiple deletions accumulate with age secondarily to mutations in nuclear genes involved in mtDNA maintenance. Every deleted mtDNA, coexists with other wild type mtDNAs, in an intracellular pool of mitochondrial genomes, determining the condition known as heteroplasmy. Pathogenic mtDNA mutations may become prevalent in certain cells; this process is defined as intracellular clonal expansion. This study investigates clonal expansion patterns of mtDNA deleted genomes, applying for the first time the droplet-digital polymerase chain reaction (ddPCR) approach on single muscle cells collected by laser-capture microdissection from muscle biopsies of patients with different paradigms of mitochondrial disease with single and multiple mtDNA deletions accumulation. The results of this study indicate different patterns of accumulation of clonally expanded mtDNA deletions in patients with single and multiple deletions. It was found that single deletions patients have clonally expanded deletion in all single muscle cell populations, suggesting that the original deletion event occurred at early stage of embryonic development or even along the maternal germline transmission. Importantly, we distinguish localized clonal expansion of mtDNA deletions in patients with mutations in the *OPA1* fusion gene. In conclusion, the ddPCR is a promising new technique for the investigation of clonal expansion by accurate quantifying of the mtDNA heteroplasmy levels.

INDEX

INTRODUCTION.....	1
1. MITOCHONDRIA.....	2
1.1 THE BEGININGS.....	2
1.2 MORPHOLOGY AND ACTIVITY.....	3
1.3 LIFE CYCLE OF THE MITOCHONDRIA: MODERN NETWORKING ORGANELLS.....	4
1.4 OXPPOS SYSTEM.....	6
2. MITOCHONDRIAL GENETICS.....	8
2.1 STRUCTURE OF MITOCHONDRIAL DNA: THE MAGIC CIRCLE.....	8
2.2 MITOCHONDRIAL REPLICATION, TRANSCRIPTION AND TRANSLATION.....	11
2.2.1 MODELS FOR MITOCHONDRIAL DNA REPLICATION.....	11
2.2.2 MITOCHONDRIAL DNA REPLICATION- THE REPLIOSOM.....	13
2.2.3 TRANSCRIPTION.....	15
2.2.4 TRANSLATION.....	17
2.3 INHERITANCE OF MITOCHONDRIAL DNA.....	18
2.4 MITOCHONDRIAL GENETICS AND HUMAN DISEASE.....	19
3. MITOCHONDRIAL DNA DELETIONS.....	20
3.1 MITOCHONDRIAL DNA DELETIONS HETEROPLASMY AND CLONAL EXPANSION	22
3.2 SINGLE MITOCHONDRIAL DNA DELETIONS.....	24
3.3 INHERITANCE OF SINGLE MTDNA DELETIONS.....	26
3.4 MULTIPLE MITOCHONDRIAL DNA DELETIONS.....	28
3.5 MITOCHONDRIAL DNA MAINTENANCE GENES AND MULTIPLE MTDNA DELETIONS.....	30
3.6 MECHANISMS OF MTDNA DELETIONS FORMATION.....	35
3.7 METHODS FOR QUANTITATIVE ANALYSIS OF MTDNA HETEROPLASMY.....	38
AIMS.....	41
MATERIAL AND METHODS.....	43
1. Patients.....	44
2. Southern blot.....	48
3. Preparation of recombinant plasmid for the standard curve	50
4. Quantitative real-time PCR.....	50

5. Transversal and longitudinal muscle biopsy sectioning.....	51
6. Histochemical analysis and classification of individual muscle fibres.....	51
7. Laser Capture Microdissection.....	52
8. Lysis of the single cells.....	52
9. Droplet Digital PCR.....	52
10. Single cell long range PCR.....	54
11. Statistical analysis.....	54
RESULTS.....	55
1. Validation of Droplet Digital PCR.....	56
2. Proportion of COX negative and intermediate fibres throughout different patient groups.....	59
3. Levels of mtDNA deletions in patients with <i>OPA1</i> mutations.....	61
4. Levels of mtDNA deletions in patients with <i>POLG</i> mutations.....	62
5. Levels of mtDNA deletions in patients with single deletions.....	62
6. Comparison of mtDNA deletion accumulation in all patient groups.....	62
7. Deletion levels in longitudinal biopsy sections.....	65
8. MtDNA copy number levels show mtDNA proliferation in certain fibre types.....	67
9. MtDNA deletions presence by single cell long range PCR.....	68
DISCUSSION.....	70
REFERENCES.....	78

INTRODUCTION

1. MITOCHONDRIA

1.1 THE BEGININGS

The very first evidence of intracellular structures that probably represent mitochondria dates back to the 1840s, only a few years after the discovery of the cell nucleus (Brown, R. 1833).

In 1890, Altman first appreciated the recurrence of these structures that he named "bioblasts". His description was: "elementary organisms" living inside cells and carrying out vital functions. The name mitochondrion first appeared in 1898, used by Benda, and it emerges from the Greek "mitos" (thread) and "chondros" (granule), referring to the appearance of these structures during spermatogenesis (Ernster and Schatz, 1981).

Today, more than a century from Altmann's observations, we know that mitochondria are necessary organelles, powerhouses of eukaryotic cells. They produce ATP through the oxidative phosphorylation (OXPHOS). They are unique for containing their own maternally inherited circular genome (Giles, 1980). But, mitochondria have not always been cytoplasmic organelles, once upon a time they were free facultative aerobic bacteria (Ernster and Schatz, 1981).

According to the endosymbiotic theory, first proposed by Lynn Margulis in the 1970s, mitochondria were originally bacteria, engulfed by ancestral cells but not digested. In return for security of host environment, mitochondria became the power supplier of the cell (Margulis, 1975).

When exactly the symbiosis between eukaryotic cell and mitochondrion emerged? Probably between 1.5 and 2 billion years ago (Lane, 2014; Martin, 2015). However, it was at the beginning of the eukaryotic life, which developed with multicellular organisms thanks to the energy produced through mitochondria.

1.2 MORPHOLOGY AND ACTIVITY

From the bacterial ancestor mitochondria inherited, along with many other features, the double membrane system. The outer mitochondrial membrane (OMM) is the boundary to cytoplasm and also a place where mitochondria make contacts with their environment. In that sense, OMM is not just a simple barrier but has multiple roles that are vital for mitochondrial life and death. Maybe the most important is the interaction of OMM with endoplasmic reticulum (ER) at specific sites called mitochondria-associated ER membranes (MAMs). Mitochondria require a regular and synchronized replenishment of membrane lipids to perform the physiological processes and maintain their membrane integrity. OMM and its ER connected sites are involved in many other important roles: calcium signalling, apoptosis, fission, and inflammation (Marchi, 2014).

Voltage dependent anion channel (VDAC), a multispinning β -barrel protein often called mitochondrial porin, which provides high permeability to small molecules and ions, is placed at OMM. Overall, OMM operates like exchange hub for mitochondria.

Between the two mitochondrial membranes there is the inter-membrane space (IMS), hosting a quite large pool of hydrophilic proteins (Marchi, 2014).

The second membrane, the inner mitochondrial membrane (IMM) acts more privately, being impermeable to the majority of ions and smaller molecules.

IMM is the site where energy conversion occurs and there are two structural regions to consider: the “boundary membrane” and the cristae, which are defined by narrow tubular sections named cristae junctions (Frey and Mannella, 2000).

Structurally, a multitude of proteins are embedded in the IMM, most being constituents of the oxidative phosphorylation system (OXPHOS). The core of mitochondria is the matrix, a gel like structure containing enzymes of the tricarboxylic acid cycle and of β -oxidation. The oxidation-reduction reactions occurring mostly in association to the OXPHOS metabolism engage a large number of mitochondrial proteins. The

global mitochondrial proteome is currently estimated to contain up to 1500 proteins, and this number is constantly growing (Mao and Holt, 2009).

As mentioned above, the IMM is highly invaginated to form structures called cristae (Palade, 1952). The tips of these invaginations are juxtaposed to the OMM, held together by the IMM integral protein OPA1. This organisation is important for the activation of apoptosis, because when the mitochondrial membrane potential declines or the intrinsic pathway of apoptosis is activated, the IMM proteases become activated and cleave OPA1. This results in the enlargement of the cristae junctions leading to release of luminal cytochrome c into the IMS (Burke, 2015; Frezza, 2006). However, not only apoptosis is dependent on cristae organization, but recent research highlights how respiratory efficiency and assembly of respiratory supercomplexes are tightly correlated with the cristae morphology (Cogliati, 2013).

1.3 LIFE CYCLE OF THE MITOCHONDRIA: MODERN NETWORKING ORGANELLS

The idea of a discrete mitochondrion, isolated from the rest of the cell by the two membranes, seemed the right one for a long time. The endosymbiotic mitochondria, considered as discrete foreign entities, misled many to think mitochondria to stand alone within the cytoplasm of the cell. By means of tridimensional imaging techniques emerged the evidence that mitochondria are in fact very social organelles (Chan, 2012). Interconnected in highly dynamic networks, they move fast and can be in spotlight of cellular needs for energy. This network allows mitochondria to travel long distances, like along axons, and to be called up at active synapses. In conditions of oxidative stress, or nutrient starvation, the mitochondrial network is hyperfused, opposite to the G1/S cell phase transition, when mitochondria are elongated. So-called “mitochondria-shaping” proteins are in charge for regulation of organelles fusion and fission, two processes that are essential for managing the demanding mitochondrial network (Griparic and van der Bliek, 2001). Mitochondrial fusion is the process by which two mitochondria join to form a single mitochondrion, whereas fission is the process through which a

single mitochondrion divides into two mitochondria (Fig.1) (Chan, 2012). In the OMM, mitofusins (MFN) 1 and 2, dynamin-related proteins that exhibit high homology, in tight cooperation with OPA1, orchestrate fusion (Santel and Fuller, 2001; Chen, 2003; Cipolat, 2004).

The cytoplasmic dynamin-related protein 1 (Drp1) translocates to mitochondria upon dephosphorylation, regulating the process of mitochondrial fission (Cogliati, 2013; Smirnova, 2001).

Recently, it has been shown that mitochondria can even be electrically coupled, without physical exchange of their matrix content, which normally happens during fusion, and this could be a way to simplify the energy transmission (Santo-Domingo, 2013). Further analysis of mitochondrial interactions points out that neighbouring mitochondria interact through specific inter-mitochondrial junction (IMJ) sites, where cristae membranes become structured into coordinated pairs across organelles (Picard, 2015).

This further level of interaction among mitochondria may provide a structural basis for events of electrochemical inter-mitochondrial communication, but further research in this exciting area is needed.

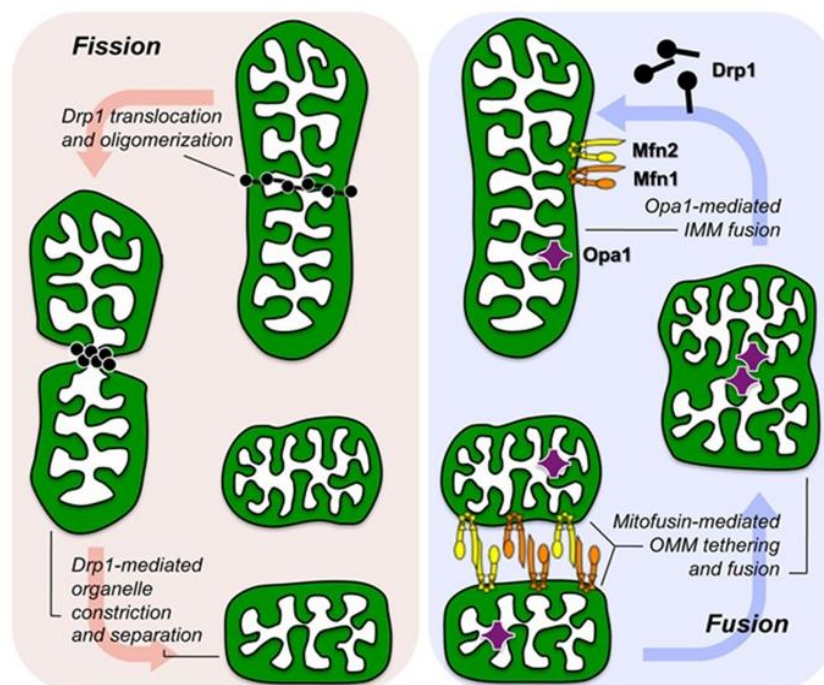


Figure 1. Molecular mechanism of mitochondrial fission and fusion. The three molecular drivers of fission and fusion are shown as they associate with a normal mitochondrion. Fission (left) is initiated by recruitment of cytosolic dynamin-related protein 1 (Drp1) to the organelle, Drp1 oligomerization, and constriction of the parent into two daughters. Fusion (right) requires initial mitofusin 1 (Mfn1)/Mfn2-mediated OM tethering followed by fusion, and finally optic atrophy 1 (Opa1)–mediated IM fusion (from Dorn and Kitsis, 2015).

The maintenance of mitochondrial function is crucial for cellular homeostasis. Balance between fission and fusion is closely related to the homeostatic adjustment of mitochondrial mass to the metabolic needs of different tissues or sensing specific functional needs of cells (Mishra, 2014). Loss of this balance closely relates to regulation of apoptosis and cell death. Thus, maintenance of mitochondrial homeostasis is regulated by mitochondrial biogenesis, which provides newly synthesized organelles, as opposed to the autophagic elimination of damaged mitochondria, called mitophagy (Youle and Narendra 2011). Impaired mitochondrial function caused by different mechanisms may result in a decrease in mitochondrial membrane potential. Depolarized mitochondria become fusion incompetent, they fragment through mitochondrial fission and can be selectively digested by lysosomes (Sarraf, 2013; Dorn and Kitsis, 2015). Mitophagy is part of the quality control system of cells to avoid the accumulation of damaged mitochondria that could eventually lead to apoptosis (Carelli, 2015). In the process of mitophagy, the PTEN-induced kinase 1 (PINK1) and Parkin, a cytosolic E3 ubiquitin ligase, play a crucial role (Narendra, 2010). Mitochondrial fusion is necessary for complementation of mutated mitochondrial DNA (mtDNA) (Chen, 2010). Fusion between damaged and healthy mitochondria has the potential to dilute out the damaged components, thus repairing the damaged organelle through functional complementation (Youle and Van der Bliek, 2012). However, there is always the opposite side of the coin, thus mitochondrial fusion may be considered as a mechanism leading to the pollution of healthy mitochondria, with damaged ones. Thus, it is important to bear in mind that fusion may also be the mechanism for dissemination of mtDNA mutations (Dorn II, 2015).

1.4 OXPHOS

Energy generation and consumption are prerequisite for life itself. This process is elegant, sophisticated and highly complex. In eukaryotes, respiration is a task carried out by the mitochondria.

The OXPHOS system is composed of five enzymatic complexes (CI-V) (Fig.2). It is built up by nearly 100 polypeptides, of which only 13 are encoded by mtDNA, whereas the remaining are coded by the nuclear DNA (nDNA), and only subsequently imported within mitochondria (Carelli V., Chan D., 2014).

Mitochondrial respiratory complexes (CI to IV) are responsible for the oxidation of the reducing equivalents, in the form of NADH or FADH₂, originating from different metabolic pathways (glycolysis, fatty acid oxidation or the Krebs cycle). Oxidation of NADH and FADH₂ is coupled with the pumping of protons into the IMS, and the resulting proton gradient is used by the ATPase (complex V) to generate utilizable energy in the form of ATP molecules. NADH reducing equivalents enter the mitochondrial electron transport chain (mtETC) through complex I, whereas FADH₂ through complex II or other dehydrogenases. The electrons are then delivered to coenzyme (CoQ), and subsequently to complex III, cytochrome c, and complex IV, where the final acceptor oxygen is reduced to water (Acin-Perez and Enriquez, 2014). Altogether this processes is called respiration (Mitchell, 1961). Respiratory complexes are not present within the IMM as single entities but are organized in supercomplexes or respirasomes. Studies on isolated bovine heart mitochondria revealed a supercomplex consisting of one copy of complex I, one complex III dimer, and one or more complex IV monomer (Lapiente-Brun, 2013). This drives the path of electrons from NADH via the iron-sulfur clusters of complex I to ubiquinol, then to the prosthetic groups of complex III, and finally to molecular oxygen at complex IV. Genetic evidence provides strong support for the existence of respirasomes in vivo (Mileykovskaya, 2012; Koopman, 2013). The OXPHOS pathway is integrally coupled to the creation of reactive oxygen species (ROS). Under standard conditions, both cytosolic and mitochondrial ROS amounts are controlled by mitochondrial and cytosolic antioxidant systems and utilize a signalling function. Still, in case the ROS levels exceed the harmless limits, bypassing the antioxidant systems, DNA, proteins and lipid molecules are exposed to being damaged. If this exposure takes place over the years it leads to the slow decline of mitochondrial and overall cellular integrity and function (Koopman, 2013).

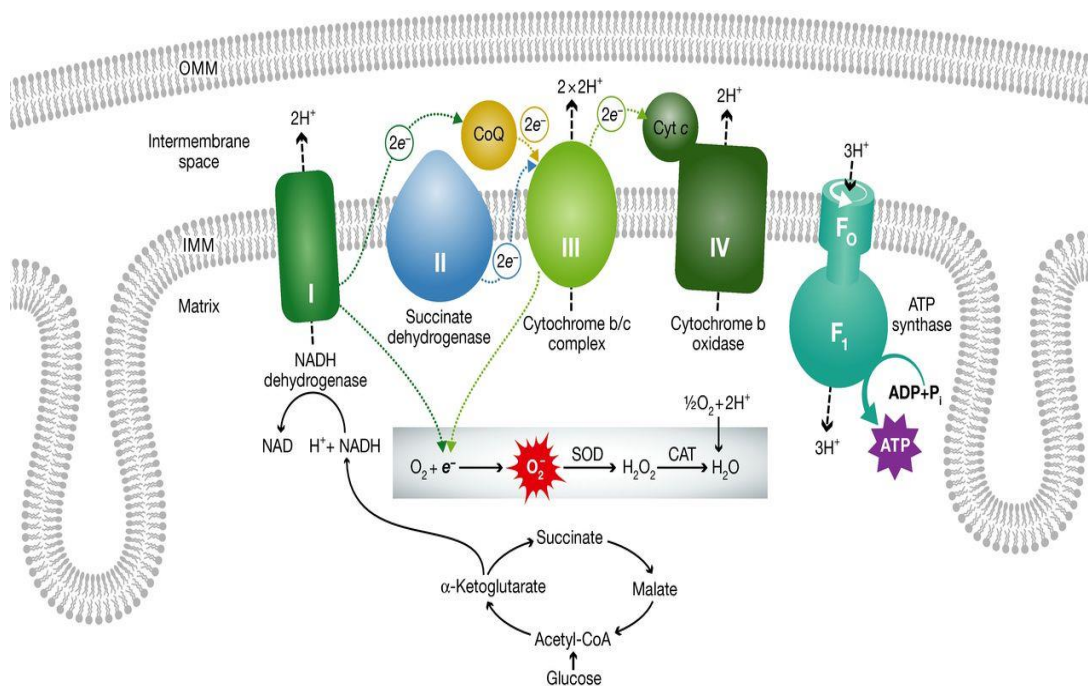


Figure 2. The mitochondrial electron transport chain and its association to ROS production. All respiratory complexes are coloured and specified with roman numbers (I-V). Transfer of electrons along the complexes (dotted arrows), proton (H^+) transport (dashed arrows) in direction from the matrix to the IMS. Proton flow through ATP synthase (complex V) converts ADP to ATP. In normal conditions oxygen is the final electron acceptor from complex IV. However, damaged mitochondria may have electron leak from complexes I or III which produces toxic reactive oxygen species (ROS) (from Dorn G.W., 2015).

2. MITOCHONDRIAL GENETICS

2.1 STRUCTURE OF MITOCHONDRIAL DNA: THE MAGIC CIRCLE

Whenever one thinks of mitochondria it must be kept in mind their bacterial origin, which helps to understand many distinguishing features of these organelles. Main characteristic, granting mitochondria to follow their own rules, is the existence of mtDNA. This little genome is maternally inherited and nowadays is just a 16.659 base pair long, circular, double stranded molecule that underwent various changes during evolution. Still, unorthodox, it remains as extra DNA in the eukaryotic cells (Carelli and Chan, 2014).

The mtDNA contains 37 genes. Each mitochondrion contains several copies of this genome (Fig. 3) and this number varies between individuals and tissue types. The mtDNA codes for the 13 most important

OXPHOS polypeptides. These include seven from nearly 45 polypeptides composing the respiratory complex I (ND1-3, ND4L, ND4-6), one of the 11 polypeptides of complex III (cytochrome b, cyt_b), three of the 13 polypeptides of complex IV, and two of the 15 polypeptides of complex V (ATP6 and 8). Complex II (succinate dehydrogenase) is the only complex that has no polypeptides coded by mtDNA. Additionally, the mtDNA encodes the mitochondrial 16S and 18S rRNAs, and 22 tRNAs for mitochondrial protein synthesis (Wallace, 2013). mtDNA has two strands, denoted as 'heavy' (H) and 'light' (L) strand, based upon their distinct base compositions, H strand is guanine rich while L strand is cytosine rich. Both strands of mtDNA are transcribed as long, polycistronic molecules, with transcription initiated from the heavy-strand promoters (HSPs) and light-strand promoter (LSP), respectively (Wallace, 2007). The mechanism of mtDNA replication is still unresolved and has been lively debated in the past twenty years. Presently, three mechanisms for replication are proposed and will be discussed later on. Compactness of mtDNA is one more extraordinary characteristic, with no introns, two pairs of protein coding regions overlapping and only two non-coding regions. The first 1kb long non-coding region (NCR) of mtDNA is also a control region (CR), containing the origin for replication of H (OH) strand, as well as promoters for transcription of both strands HSP and LSP. A very enigmatic structure, residing in the control region, is the so-called D-loop (Displacement loop) structure. In this region there is incorporated a third linear DNA strand referred as 7S DNA due to its sedimentation properties (Fig.3). The nomenclature of 7S DNA often induces confusion, since this is not one molecule but a group of molecules slightly different in size and with 5' end that may start at various positions. The exact function of this region is still unknown; however it has been speculated that because it encompasses the origin of heavy strand replication and is positioned in the control region of mtDNA, is possibly involved in mtDNA maintenance, by control of dNTP pool and/or anchoring the mtDNA molecule (Nicholls and Minczuk, 2014).

The second non-coding region is substantially smaller and contains the origin of L-strand replication (OL). It is located in a cluster of five tRNA genes approximately two thirds of the mtDNA length from the OH. The two origins divide the genome into roughly two-thirds and one-third sections, with the larger portion

denoted as the 'major arc', and the smaller portion called the 'minor arc' (Anderson et al., 1981; Fernandez-Silva et al., 2003).

The circular molecule of mtDNA has a contour length of $\sim 5 \mu\text{m}$ and each mitochondrion, wide approximately $\sim 0.5 \mu\text{m}$, contains numerous mtDNA circular molecules. Therefore, mtDNA has to be arranged to fit within a mitochondrion. This is accomplished by shaping the mtDNA in ellipsoidal structures termed nucleoids that present basic organizational units of mtDNA not wider than few hundred nanometers (Kukat, 2011; Kukat, 2015).

Taking advantage of new stimulated emission depletion (STED) nanoscopy, electron microscopy and electron cryo-tomography (cryo-ET), it has been elucidated that most mammalian mitochondrial nucleoids contain a single mtDNA copy compacted by mitochondrial transcription factor A (TFAM) aggregation and cross-strand binding. TFAM is very abundant, present at approximately thousand copies per mtDNA molecule and besides being responsible for compacting mtDNA it has essential role in mtDNA replication as well as in transcription (Kukat, 2015). Expression of TFAM also governs the mtDNA copy number in cells, therefore this protein is irreplaceable for mtDNA maintenance. However, TFAM is not the only protein that affects the morphology and the organization of the nucleoids (Bogenhagen, 2012). Other proteins crucial for mtDNA maintenance are additional components of nucleoids: mitochondrial polymerase gamma (Poly), mitochondrial single-stranded DNA binding protein, replicative helicase TWINKLE, mitochondrial transcription factors B1 and B2 (TFB1M and TFB2M), mitochondrial transcription termination factor (mTERF), along with others (Bogenhagen, 2008; Kolesnikov, 2016).

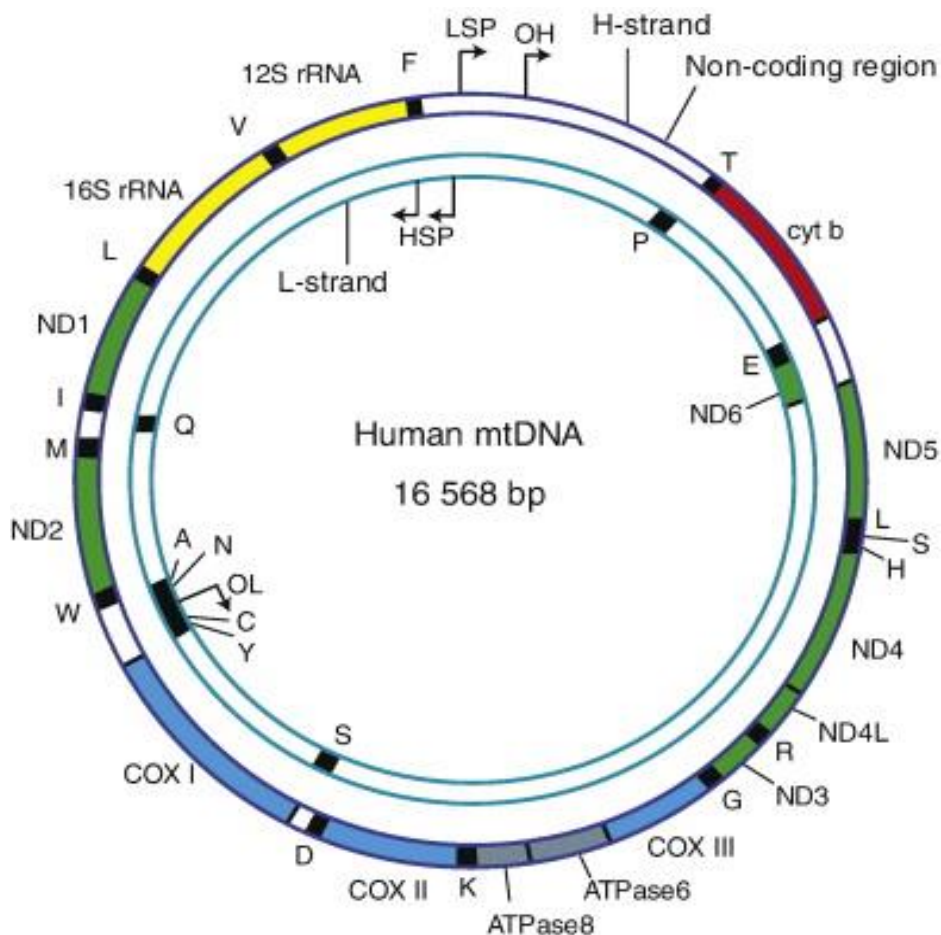


Figure 3. The human mitochondrial genome. The human mitochondrial genome consists of 16569 base pairs and contains a heavy (H-strand) and light-strand (L-strand). Complex I NADH dehydrogenase (ND) genes are presented in green; Complex III cytochrome b (Cytb) gene is presented in red; Complex IV cytochrome c oxidase (COX) genes are presented in light blue; Complex V ATP synthase (ATPase) genes are presented in grey. Transfer RNA genes are in black and ribosomal RNA genes (rRNA) are in yellow (from Wanrooij and Falkenberg, 2010).

2.2 MITOCHONDRIAL REPLICATION, TRANSCRIPTION AND TRANSLATION

All components needed for mtDNA transcription and replication are encoded in the nuclear genome, same as the mitochondrial translation machinery (Peralta S., 2012).

2.2.1 MODELS FOR MITOCHONDRIAL DNA REPLICATION

Strand displacement model

Replication and turnover of mtDNA occurs independently from the cell cycle. The molecule of mtDNA is small and replicates within few hours. In the early 1980's an extensive body of work has been done to define the rules of mtDNA replication (Bogenhagen, 1979; Nass, 1969; Tapper and Clayton, 1981). From

these studies the mtDNA replication model generated was denominated as strand-displacement model. This model implies that mtDNA replication starts with synthesis of the H strand near to the origin of heavy strand replication. Replication of heavy strand would then proceed and parental strand will be displaced. At about two thirds of genomic distance is the origin of light strand replication and when replication fork exposes this region the replication of the lagging strand may begin. This operational asynchrony of the two origins of mtDNA replication results in segregation of two different progeny circles, one of them requires single-strand gap filling before closure (Clayton, 1982). Strand-displacement model assumes that replication is unidirectional, without formation of Okazaki fragments, asynchronous and asymmetrical (McKinney and Oliveira, 2013)

RITOLS (RNA Incorporated Through Out the Lagging Strand) model

In the early 2000's new replicative intermediates have been discovered with use of two-dimensional agarose gel electrophoresis (2DAGE). These new intermediates are essentially wide segments of RNA that are incorporated into the lagging strand hybridized to leading strand (Yang, 2002; Yasukawa, 2006). With use of antibodies specific to RNA-DNA hybrids it was shown that replicating mtDNA's are duplexes, with RNA being present in long tracts, and these findings were confirmed with transmission electron microscopy (Pohjoismaki, 2010).

The strand-coupled model

This model was proposed from Holt et al. in the 2000. Essentially it assumes that mtDNA replication is more like to the one seen in bacteria, due to existence of *theta* like structures, double DNA replication intermediates found after artificially induced mtDNA depletion. By this model, replication starts from the broad zone and proceeds bidirectional (Bowmaker, 2003). It would be necessary, in this model, that Okazaki fragments are present and that two polymerases function simultaneously, and to date these are still not found. However, there are indications within the field that both RITOLS and strand-coupled model could represent alternative modes of mtDNA replication (Brown and Clayton, 2006).

2.2.2 MTDNA REPLICATION- REPLIOSOM

Mitochondria contain enzymatic systems responsible for mtDNA replication, diverse from those in the nucleus, however all these proteins are encoded by nuclear genes (Figure 4). To date, just three of these proteins have been identified operating at the mtDNA replication fork. Ahead of the fork, the replicative helicase Twinkle translocate on one DNA strand in 5' to 3' direction, unwinding double-stranded DNA into single-stranded DNA that now may serve as a template for DNA polymerase performing DNA synthesis. For the protection from nucleolysis, mtDNA binds to the mitochondrial single-stranded DNA-binding protein (mtSSB). Replication is primed by extension of processed RNA transcripts laid down by the mitochondrial RNA polymerase (Reyes, 2013). Part of replication enzymes, POLRMT, the catalytic subunit of mtDNA polymerase (POL γ A), and the replicative mitochondrial helicase (TWINKLE) are similar to proteins encoded by the T-odd lineage of bacteriophages and not related to eubacteria (Shutt and Gray, 2006).

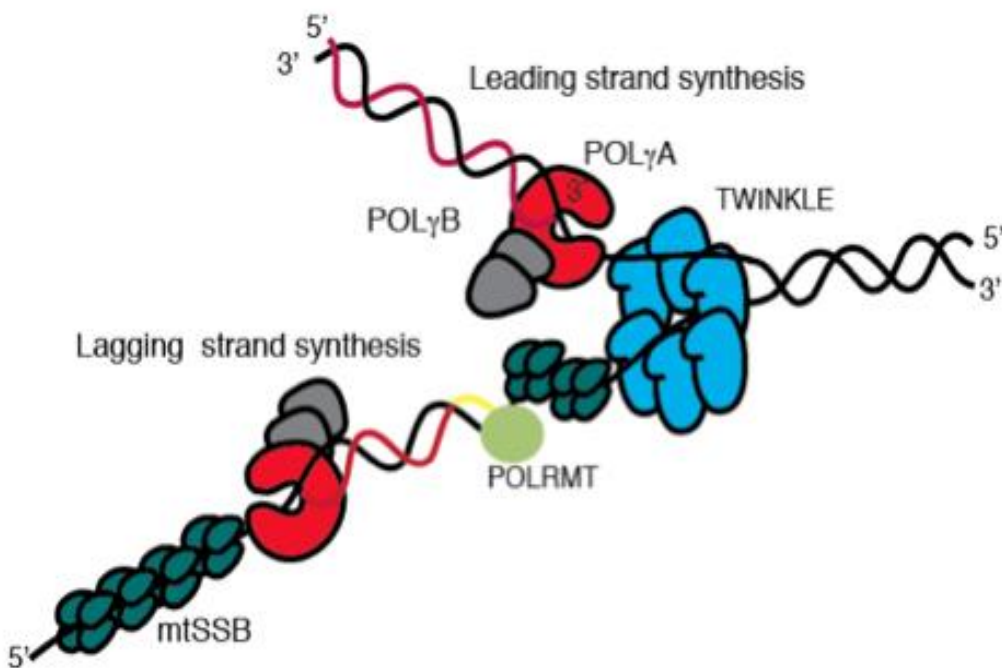


Figure 4. The mtDNA replication machinery. The TWINKLE helicase (blue) moves in a 5' to 3' direction while unwinding dsDNA. The mtSSB protein (dark green) stabilizes the single stranded conformation and

stimulates the DNA synthesis by the POLy (red (A) and gray (B)). POLRMT (light green) synthesizes the RNA primer (yellow line) needed for lagging strand DNA synthesis (from Wanrooij and Falkenberg, 2010).

Mitochondrial DNA polymerase γ

The only DNA polymerase found in mammalian mitochondria is the POLy or POLG1 the enzyme promoting mtDNA replication and repair (Kaguni, 2004).

The enzyme belongs to the family A group of DNA polymerases and human catalytic subunit POLyA has a molecular mass of 140 kDa. The catalytic subunit POLyA is associated with a smaller protein, the mtDNA polymerase γ accessory subunit (POLyB), which has molecular mass of 55 kDa (Gray and Wong, 1992). POLyA and POLyB form a heterotrimer (POLyAB₂) in mammalian cells (Yakubovskaya, 2006); for sake of simplicity, later on the holoenzyme will be denoted simply as POLG. POLyB subunit significantly enhances the catalytic activity and the processivity of main subunit POLyA. To some extent this may be explained with enhanced binding of POLyA to mtDNA in the holoenzyme formation and also with increased nucleotide binding. Altogether this suggests that the accessory subunit has fundamental influence on the function of the catalytic subunit and allows for the most efficient binding of substrate (Falkenberg, 2007). POLyA subunit possess the enzyme's 5'-3' polymerase, 3'-5' exonuclease and 5' deoxyribose-5 phosphate lyase activities, and is probably the most studied polypeptide of the mtDNA replisome at the clinical, biochemical and structural levels (Stumpf and Copeland, 2011). Given that it is the only mtDNA polymerase, which functions in both mtDNA replication and repair, it is not surprising that research has been focused to disease-associated POLG mutations. Since the first POLG mutations were found to be associated with progressive external ophthalmoplegia (PEO) (Van Goethem, 2001), over 200 mutations in the POLG1 and POLG2 genes have been detected in association with various mitochondrial diseases (Akhmedov and Marin-Garcia, 2015).

TWINKLE

Mutations in the human Twinkle gene (C10orf2) were for the first time reported as a cause of autosomal dominant PEO, associated with multiple mtDNA deletions (Spelbrink, 2001). Later, biochemical studies showed the NTPase, 5'-3' ssDNA translocase and dsDNA unwinding activities of the enzyme, identifying Twinkle as the replicative mtDNA helicase (Korhonen, 2004).

Mitochondrial single-stranded DNA binding (mtSSB)

This protein resembles *Escherichia coli* SSB and is the only protein of three replication-fork associated proteins that has no similarities with phage proteins (Tiranti, 1993). MtSSB binds to single-stranded DNA as a tetramer composed of four 16 kDa subunits (Yang, 1997). The protein stimulates synthesis of mtDNA by facilitating POLG primer recognition and enhancing POLG processivity (Genuario and Wong, 1993). MtSSB also stimulates the dsDNA unwinding activity of TWINKLE (Korhonen, 2003).

Recent study of mtSSB protein showed this protein is highly abundant being present at more than two thousand units per mtDNA. It was demonstrated that mtSSB is actively recruited to nucleoids during mtDNA replication in vivo. MtSSB covers displaced single strands of replicative intermediates (Van Tuyle and Pavco, 1985). It was found that mtSSB is not evenly distributed over the genome, and that it associates exclusively with the H strand. Highest levels of mtSSB are downstream of the D-loop region, at the 3' end of 7S DNA, and mtSSB levels gradually reduce towards OriL. A second, minor, peak of mtSSB take place just after OriL, but it weakens away going towards the D-loop region (Fuste, 2014). All these findings strongly favour strand displacement mode as primary mtDNA replication mechanism.

2.2.3 TRANSCRIPTION

In human cells, transcription initiation depends from promotor regions, and each strand has its own promoters: the light-strand promoter (LSP) and the two heavy-strand promoters (HSP). Transcription

from these promoters finally results in polycistronic precursor RNAs. These primary transcripts are processed to produce the individual mRNA, rRNA, and tRNA molecules (Montoya, 1981; Ojala, 1981; Clayton, 1991).

Two heavy strand promoters HSP1 and HSP2 have been identified at the H strand (Micol, 1997). The HSP1 and HSP2 promoters are located very close, spaced by about 100 bp in the D-loop region and transcribed in the same direction (Martin, 2005). Transcription from the HSP1 promoter is prematurely terminated downstream of the 16S rRNA, transcribing only for the tRNA^{Val}, tRNA^{Phe} and the 2 rRNAs. Premature termination is result of a site-specific binding of the mitochondrial termination factor MTERF1 (Roberti M, 2009). Transcription initiated from the HSP2 promoter produces a full-length polycistronic transcript covering the 2rRNAs (12S rRNA and 16S rRNA), 12mRNAs and 13 tRNAs. All the protein-coding and rRNA genes are flanked by tRNA genes, which need to be excised in order to have mature mRNA and rRNA molecules (Falkenberg, 2007).

Transcription from the LSP produces the RNA primers required for initiation of mtDNA replication at the origin of H-strand DNA replication (OH) (Clayton, 1991; Chang and Clayton, 1985). The molecular mechanism stopping the transcription and allowing the switch to primer formation is still not completely explained. However, very recent research showed that transcription and replication of mtDNA cannot go in parallel without interfering with each other. It was proposed that in presence of human transcription elongation TEFM, mitochondrial RNA polymerase (mtRNAP) efficiently transcribes through termination sites of transcription (Agaronyan, 2015).

As mentioned above, within the control region there are three conserved sequence blocks (CSBI- III) downstream of LSP (Walberg and Clayton, 1983). CSB II increases the stability of an RNA-DNA hybrid, and transitions from the RNA primer to the newly synthesized DNA have been mapped near CSBII (Falkenberg, 2007). Termination of transcription is still under investigation, since it is known just one exact termination site. This termination site is located at the end of the 16S rRNA gene, when

transcription starts from the HSP1 end (Christianson and Clayton, 1988). Transcription termination at this site is determined by the mitochondrial transcription termination factor (mTERF).

The mitochondrial ribosome is shaped when mitochondrial ribosomes, 12SrRNA and 16S, form a complex with the mitochondrial ribosomal proteins (Pietromonaco, 1991). It is still unclear if 5S rRNA, which is imported within mitochondria, also assembles with mitochondrial ribosomes (Smirnov, 2011).

2.2.4 TRANSLATION

The components of mitochondrial translation are different from the cytosolic counterparts and, at the same time, there are also differences with the bacterial translation machinery. These differences concern not only the structure of the mitoribosome, which is more similar to the bacterial one, but in particular the number of associated proteins that is higher when compared to both the cytosolic and bacterial ribosomes. The role of most of these proteins is not assigned, but it is thought they may serve as a protection of rRNA from ROS insults (Lightowers, 2014). Translation of the mtDNA-encoded protein transcripts results in nascent polypeptides key for OXPHOS, while the other polypeptides of this system are translated in the cytosol. Not surprisingly the two translation systems are synchronized during mitochondrial biogenesis in yeast (Couvillion, 2016). Mito-translation takes place through the following major steps: formation of initiation complex, elongation of the rising polypeptide chain, and termination, and recycling of the mitoribosome is considered as the final step of the process (Boczonadi and Horvath, 2014). The initiation complex consists from: 28S small subunit, mRNA, fMET-tRNA and IF2/3mt. When this complex is formed the mRNA enters into the IF3mt:28S subunit complex. The supposed role for IF3mt is to provide the right position of mRNA in binding the small subunit at the peptidyl (P) site of the mitoribosome. When the suitable start codon is matched, the formylmethionin -tRNA can bind to the first codon with the assistance of IF2mt. The assembly of the mitoribosome signals for release of initiation factors and the elongation proceeds on the 55S ribosome (Boczonadi and Horvath, 2014).

The mitochondrial elongation factor (EF-Tu^{mt}-GTP) and an amino-acylated tRNA occupy the A-site of the mitoribosome where truthful codon anticodon pairing takes place. If codon-anticodon pairing is correct then the elongation factor leaves the mitoribosome while the aminoacyl-tRNA moves to the P position where formation of peptide bond is catalysed leading to extension of the growing polypeptide chain. When the stop codon (UAA, UAG, AGA or AGG) comes across at the A-site, elongation stop is terminated (Boczonadi and Horvath, 2014). Stop codon is recognized, by the mitochondrial release factor (mtRF1a), which binds to the mitoribosome, inducing hydrolysis of the peptidyl-tRNA bond in the A-site, thus releasing the mature protein from the site (Richter, 2010).

2.3 INHERITANCE OF MITOCHONDRIAL DNA

Among many peculiarities of mtDNA, inheritance is maybe the most intriguing. The mtDNA is inherited in a uniparental fashion, meaning that all the copies of mtDNA are passed to next generation solely from the mother (Giles, 1980). This implies that recombination of mitochondrial genetic material, if occurring, involves identical mtDNA molecules, raising the question why is there uniparental inheritance and how is this accomplished (Lane, 2012)? This question is still a matter of scientific debate, and a few recent studies may shed some light. First, the mtDNA sequence is highly variable even amongst individuals of the same mammalian specie and certain sequence polymorphisms can have influence even on acidity of the mitochondrial matrix (Gómez-Durán, 2010; Kazuno, 2006). As a consequence, mixing two distinct sequences, with different influences on certain physiological conditions, and with different variants in the same OXPHOS polypeptides may have harmful effects (Wallace, 2007). Indeed, a recent study showed that if two normal, but different mtDNA haplotypes are artificially mixed in the same mice model, an incompatibility manifests as the heteroplasmic state is unstable, resulting in a pathological phenotype with behavioural abnormalities (Sharpley, 2012). Second, different mtDNA haplotypes support equal

rates of ATP synthesis but differ in reactive oxygen-species (ROS) leak and mtDNA copy number. ROS leak seems to optimize ATP synthesis by stimulating mtDNA copy increase (Moreno-Loshuertos, 2006). Thus, for various possible reasons, the uniparental transmission of mtDNA is evolutionary conserved and favoured (Lane, 2011). But, how human paternal DNA gets eliminated? Two models are considered in the field: passive and active elimination (Carelli, 2015). First, the passive or “dilution” model reasons that paternal mtDNA, much inferior in copy number, is basically watered down away by the excess of oocyte mtDNA and consequently it is hardly detectable in the offspring (Sato and Sato, 2012). In accordance to this model, study done on mice showed paternal mtDNA elimination prior to fertilization, while infrequent not eliminated paternal mtDNA enters in the egg and could be found in newborn mice (Luo, 2013). However, when this model was tested in humans, by examining heteroplasmy in buccal derived DNA from the children, confirmation for paternal mtDNA transmission was not found (Pyle, 2015). Second, the active elimination model predicts that paternal mtDNA is selectively eliminated, by ubiquitination or other still elusive mechanisms, in order to prevent its transmission to offspring. Mechanisms involved in this elimination are diverse, and may act at different pre- or post-fertilization levels (Carelli, 2015).

2.4 MITOCHONDRIAL GENETICS AND HUMAN DISEASE

Mitochondrial dysfunction underlies a large and diverse array of human diseases. The list of diseases in which mitochondrial dysfunction is recognized as a cause or a contributor to the pathogenic mechanism has been constantly growing in the past decade (Wallace and Chalkia, 2013). Many of the functions that mitochondria carry out in eukaryotic cell are key to survival, and have implications far beyond the energy supply. Independently from the energy production capacity, mitochondria affect a number of other cellular processes interfering with the expression of several thousands of genes linked to diverse cellular functions (Elstner and Turnbull, 2012; Latorre-Pellicer, 2016). The mtDNA has 100-1000 higher mutation

rate than nDNA and each cell variably contains 100-1000 copies of mtDNA. A subset of mtDNA molecules may carry pathogenic mutations, leading to the condition of intracellular heteroplasmy. Nuclear genes implicated in mitochondrial functions are estimated to range from 1000 to 2000 (Pitchard, 2016). Thus, mitochondrial function may be of relevance for any complex disease. Individuals can accumulate different mtDNA mutations over time, impinging on the energetic capacity of the cell, and such clusters of mtDNA mutations are relevant for aging and cancer. Epidemiological surveys estimated that incidence of the most common pathogenic mtDNA mutations is one in 5000 (Schaefer, 2008). A second study of newborn cord bloods revealed that one in 200 infants harbour one of the 10 most common pathogenic mtDNA mutations (Chinnery, 2012). In general, mitochondrial diseases can be defined as a clinically heterogeneous group of disorders related with OXPHOS dysfunction. Mitochondrial disorders typically affect postmitotic and energy-demanding tissues, such as brain, heart or muscle, can appear sporadically or be maternally inherited (Schon, 2012). There is no cure for mitochondrial disease and therapy is mostly limited to manage symptoms. Despite the fact that it is now well established that overall mitochondrial disorders cannot be considered rare, our understanding of the pathogenic mechanisms remains limited.

3. MITOCHONDRIAL DNA DELETIONS

The first pathogenic mtDNA mutations, deletions and point mutations, were discovered nearly three decades ago (Holt, 1988; Wallace, 1988). Both large-scale rearrangements (deletions or duplications) and point missense mutations of mtDNA have been linked to a vast array of clinical phenotypes. MtDNA deletions are pathogenic mutations that remove various portions of mitochondrial genome thus resulting in shorter molecules of mtDNA. Circular deleted mtDNA is smaller than wild-type, due to the missing section of the genome, but it remains in a closed circular structure. The mtDNA deleted molecules are transcribed, but there is no evidence that the "fusion" transcript crossing the deletion breakpoint is translated into a chimeric protein. On the other hand, mtDNA deletions remove a certain

number, depending on size and position of the deletion, of indispensable tRNA genes consequently disrupting the translation of key mtDNA-encoded respiratory chain polypeptides (Nakase, 1990). Thus, the deleterious effect of mtDNA deletions is out of any doubt. The phenotypic heterogeneity observed in patients carrying mtDNA deletions, imply however further elements to be considered, specifically the heteroplasmy and clonal expansion. In patients, we may distinguish two classes of mtDNA deletions: single and multiple deletions. These classes are based on inheritance pattern and the variety of deletions present. Furthermore, mtDNA sequence surrounding the deletion breakpoints may be used for classification of the mtDNA deletions. In fact, deletions may occur flanked by two direct repeats with identical sequences (class I deletions), flanked by imperfect repeats (class II deletions) and those that have no direct repeats (class III deletions). The deletions may vary in size from in the range from 2 kb to 10 kb and may cover any mtDNA gene. Regardless of that, distribution of mtDNA deletions is not random; the mtDNA deletions are prevalent in the major arc of mtDNA, between two origins of the replication. Only 1.4% of all deleted regions, published and described in largest database of mtDNA deletions- Mitobreak (www.mitobreak.portugene.com), is located within the minor arc of mtDNA (Damas, 2014). In single deletions the size of the deletion is associated with the severity of clinical phenotype, because larger the deletion is more mtDNA genes are removed, and consequently OXPHOS is more compromised (Grady, 2014). The location for the majority of deletions within the major arc explains the length constraint; the length of the major arc (11,230 nt) creates an upper limit for the size of the deletions. The central region of the major arc is often deleted, with the one ranging from positions 7,946 to 15,158 being missed in more than half of cases and that ranging from positions 10,936 to 12,893, including tRNA-His (TRNH) and tRNA-Ser (TRNS2) genes, being missed in 90% of cases (Damas, 2014). A few studies identified a significant number of minor arc mtDNA deletions in sporadic inclusion body myositis patients (sIBM) and in elder people studied in ageing research (Rygiel, 2015; Bank, 2000). The two regions that cannot be deleted are the origin of heavy-strand replication and the light-strand promoter, as these regions are necessary for replication of both the deleted and wild-type mtDNA molecules (Moraes,

2003). The predominant deletion in the patient's population is a 4977-bp deletion ("common deletion"), surrounding several mitochondrial genes encoding for structural proteins and tRNAs, and bordered with a long 13-bp direct repeat on both breakpoints (Schon, 1989).

3.1 MITOCHONDRIAL DNA DELETIONS HETEROPLASMY AND CLONAL EXPANSION

Every deleted mtDNA molecule exists mixed with wild type mtDNA molecules in an intracellular pool of mitochondrial genomes, making this pool non homogenous, and defined as heteroplasmic. When a new mtDNA mutation, in this case a deletion, arises it is just one mutant mtDNA molecule coexisting amongst thousands of non-mutant mtDNA molecules. Under these circumstances, the wild-type mtDNA easily compensates for the few mutant mtDNA molecules. Thus, low levels of mtDNA deletions can be easily tolerated, but once the mutant mtDNA molecules overcome a critical threshold level, a biochemical defect arises. This threshold level significantly varies between tissues and is distinct for different mutations. In the case of mtDNA deletions, the threshold level is proposed to be around 80%. In rapidly dividing cells such as hair or blood cells heteroplasmy of rearranged mtDNA is markedly shifted in favour of wild-type mtDNA (Moraes, 2003). A genetic drift during the germ-line bottleneck, characterized by a drastic drop in the number of mtDNA segregating units during oogenesis, can remarkably change the heteroplasmy levels between generations (Rebolledo-Jaramillo, 2014).

Over time, the pathogenic mtDNA mutations (i.e. deletions) may become prevalent in certain cells, due to their clonal expansion, which may take place in both the germline and somatic cells. The mechanism beyond the clonal expansion is still poorly understood. Three major hypothesis deal with potential forces leading to clonal expansion of mtDNA deletions: replicative advantage of a smaller molecule, lower levels of ROS production and random genetic drift.

The replicative advantage mechanism argues that deleted mtDNA molecules, due to being smaller size, are replicated faster than wild-type mtDNA, thus allowing for the mtDNA deletion to accumulate

(Wallace, 1992; Corral-Debrinski, 1992). This mechanism would provide a plausible explanation if two prerequisites are fulfilled. First, mtDNA replication needs to take significant amount of time in compared with time needed for mtDNA turnover, thus allowing for smaller molecules to accumulate. Second, this would imply that replicative advantage would favour larger deletions (Campbell, 2014). Indeed, in agreement with this second prerequisite, two studies found that larger deletions accumulate in greater extent (Diaz, 2002; Fukui and Moraes, 2008, 2009), but this accumulation is observed only under relaxed copy number conditions and when no biochemical defect was observed, respectively. Another valuable study performed on patient tissues reported that there is no preferential accumulation of larger deletions over smaller deletions, under normal copy-number control. Given that mtDNA replication takes from one to two hours and time of mitochondrial half-life is estimated to be from one to three weeks, replication can hardly be rate limiting the turnover (Campbell, 2014). However, mtDNA point mutations are also accumulated by clonal expansion, and they cannot have any influence on the size of mtDNA molecule, thus replicative advantage of shorter molecules cannot be interpretation for the clonal expansion (Elson, 2001).

Survival of the slowest hypothesis argues that because of decline in respiratory chain function, provoked by mtDNA damage, free radical production is also reduced. This way the compromised mitochondria manage to be spared from mytophagy and apoptosis as they are not considered as producers of toxic free radicals. Consequently the deleted mitochondria will predominate within a cell (De Grey, 1997). This hypothesis has not been supported by experimental evidence.

The random genetic drift hypothesis implies there is no selective advantage for deleted molecules (Elson, 2001). Random genetic drift model is established on validated rules of mtDNA replicative dynamics, which assume a relaxed mtDNA replication unrelated to the cell cycle, and is based on the mathematical models (Elson, 2001). On the other hand, evidences for significant levels of mtDNA deletions in the most of dopaminergic neurons of substantia nigra from older persons (Kraytsberg, 2006) contrasts with the predicted low levels of age-related COX-deficient cells, which should be less than 5% if only age driven.

Furthermore, this model does not explain the preferential accumulation of mtDNA deletions in certain tissues, under the assumption of a replicative turnover under relaxed replication and copy number control (Campbell, 2014).

None of the proposed mechanisms fully explains the prevalent accumulation of mtDNA deletions in certain tissues and the consequent occurrence of a clinical phenotype.

In muscle fibres, clonally expanded mtDNA genomes are found in specific, more or less restricted domains. These domains presumably represent areas with extended expansion process. Segmental nature of mtDNA clonal expansion is suggesting that mitochondrial fusion is restricted to some extent, and this is visible in elongated cells like muscle fibres. It seems likely and has been proposed that the dynamic processes of fusion and fission would affect the dimensions of segmental domains where deleted mtDNA expanded, becoming prevalent (Carelli and Chan, 2015).

No matter the mechanism for arise of clonal expansion, it leads to local shifts in heteroplasmy rates, within cells or even within cell domains as in the case of skeletal muscle. Such heteroplasmy can vary between cells and tissues, making the phenotypic expression of a mitochondrial disorders difficult to predict. Thus, clonal expansion is the driving force leading to prevalent populations of deleted mtDNAs, ultimately causing the deleterious effect on mitochondrial OXPHOS and other metabolic pathways. Waiting to understand the mechanisms of clonal expansion, the distribution pattern of mtDNA heteroplasmy remains an unpredictable aspect of mitochondrial genetics (Wallace, 2013; Carelli, 2015).

3.2 SINGLE MITOCHONDRIAL DNA DELETIONS

Clinical features

The first mtDNA mutations discovered in 1988, were in fact single mtDNA deletions and the Leber's hereditary optic neuropathy point mutation, proving for the first time that mtDNA mutations cause human disease (Holt, 1988; Wallace, 1988). In patients with single mtDNA deletions, there is one prevalent deletion species exhibiting a wide tissue distribution. Single, large scale, deletions often cause a sporadic disease, which may be present from early childhood such as Pearson and Kearns-Sayre

syndromes or, later in life with chronic progressive external ophthalmoplegia (CPEO). As stated above, KSS, CPEO, and PS are sporadic disorders meaning that detectable mtDNA deletions are not found in other family members (mothers and maternal siblings) do not have detectable mtDNA deletions. Opposed to the single mtDNA deletions, large-scale mtDNA duplications are often maternally transmitted (Ballinger, 1992, 1994; Manfredi, 1997). Single deletions account for about a third of all patients with mtDNA-related disease (Mancuso M, 2015).

Pearson's bone marrow-pancreas syndrome is a severe disorder, with high incidence of mortality. It involves the hematopoietic system, kidneys, exocrine pancreas and liver. The hallmark feature is sideroblastic anaemia, not typical for other mitochondrial diseases. The single type of mtDNA deletion is consistently found in all tissues, but in the blood it seems to be even more abundant and in neonatal period certain symptoms may differ from classical presentation (Manea, 2009). Pearson syndrome is often fatal in infancy. Individuals with Pearson syndrome who survive beyond infancy later on develop the neurological symptoms of Kearns-Sayre syndrome (Lee, 2007).

Kearns-Sayre Syndrome (KSS) is a multisystem disorder affecting predominantly the central nervous system, skeletal muscle, and heart. Onset is usually in childhood, with ptosis, ophthalmoplegia, or both. Exercise intolerance and impaired night vision due to retinal dystrophy may be early symptoms (Auré, 2007). A single mtDNA deletion is again found in all tissues. The disease usually progresses to death in young adulthood.

Progressive external ophthalmoplegia (PEO) is a mitochondrial myopathy with drooping of the eyelids (ptosis), paralysis of the extraocular muscles (ophthalmoplegia), and variably severe proximal limb weakness. A few individuals with PEO have other manifestations of KSS and this situation is termed PEO plus. The disorder is quite benign, not affecting a normal life span. The single deletion occurrence is mostly restricted to skeletal muscle (Zeviani and Carelli, 2003).

3.3 INHERITANCE OF SINGLE MTDNA DELETIONS

Single, large-scale mtDNA deletions are in most cases considered sporadic events occurring in the early stages of embryonic development of an individual (Zeviani and Carelli, 2003). However, there are studies showing that mtDNA deleted molecules may be present in the oocyte where mtDNA is sustained for long time up until fertilization. A few studies reported evidence of low levels (no more than 0.1%) mtDNA deletions in human oocytes (Chen, 1995; Brenner, 1998). If an oocyte containing a certain amount of mtDNA deletion is fertilized, the deleted molecules most probably will be lost by negative selection or purifying selection during the early stages of embryonic development. However, the genetic drift potentially occurring during the germ-line bottleneck may occasionally lead to prevalent mtDNA deletion, as result of the severe reduction in mtDNA copy number during oogenesis (Rebolledo-Jaramillo, 2014). After fertilization, mtDNA variants are distributed among cells according to mitotic segregation, taking place upon fertilization, and it is assumed this process is leading to random distribution of mitochondria and mtDNAs during cell divisions (Poulton, 2010). Even if most times single mtDNA deletions are believed to be sporadic *De Novo* events, it cannot be excluded that they may in fact result from mtDNA bottleneck. The mtDNA germ-line bottleneck may provide a plausible explanation in the case of maternally inherited single mtDNA deletions, as the mother and maternal siblings of affected individual are healthy. It is possible that a low-level mtDNA deletion segregates through the bottleneck and gets the opportunity of high expansion, eventually populating the primary oocyte (Krishnan, 2008) (Fig.5). In support of the bottleneck-derived germline transmission of deleted mtDNA there are a few cases of maternal inheritance in single mtDNA deletions that have been reported (Blakely, 2004; Shanske, 2002; Bernes, 1993). A good example is the case of a woman with sporadic CPEO who harboured a single large-scale mtDNA deletion, which was transmitted to her infant son, affected with PS. The single deletion of 5,355-bp in mtDNA, without flanking direct repeats, was the only abnormal species of mtDNA identified in both patients (Shanske, 2002). In another case reported, a woman, again with CPEO, and her son who also had a Pearson-like syndrome, both harboured the 4,977-bp “common”

mtDNA deletion. Although this case was similar to the previous one, the experimental analysis did not rule out the presence of duplicated mtDNA, which could have explained the transmission from mother to child (Bernes, 1993). In a third reported case, a woman and her daughter both had CPEO, but mother and daughter harboured different single mtDNA deletions (Ozawa, 1989).

It is important to point out that these few cases with documented maternal inheritance of a single mtDNA deletion cannot be considered as definitive proof for the not sporadic nature of these mutations. In order to confirm maternal transmission, more cases should be thoroughly investigated. An important feature of mtDNA deletions is that they are usually not detectable in blood, except in the cases of Pearson syndrome, and muscle biopsy sampling of clinically unaffected mothers are ethically problematic. Therefore the development of highly sensitive approaches for detection of mtDNA deletions would be of utmost importance for understanding potential transmission of these deleterious mutations, and consequently would help in genetic counselling.

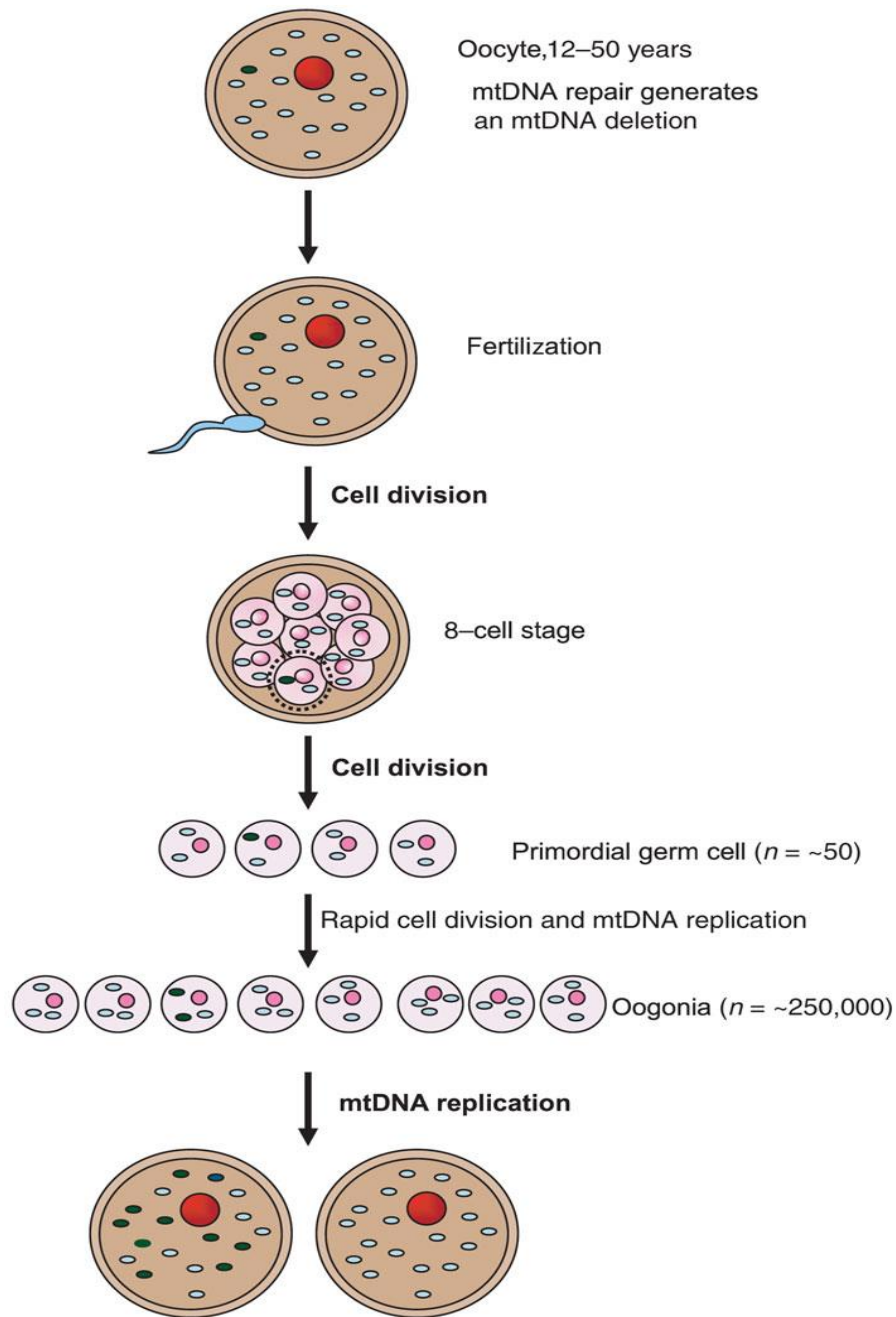


Figure 5. Illustration of a model for existence of sporadic mtDNA deletions in the oocyte. Formation of mtDNA deletion due to repair of oocyte mtDNA. The segregation of mtDNA deletion after fertilization and cell division. If the segregation was at the level of primordial cell than extensive synthesis of mtDNA could lead to the prevalence of mtDNA deletion in the oocyte. If this oocyte is fertilized in future, a child born would be at risk of being born with high levels of an mtDNA deletion (from Kirshnan, 2008).

3.4 MULTIPLE MITOCHONDRIAL DNA DELETIONS

Shortly after the discovery of single, sporadic mtDNA deletions, the accumulation of multiple mtDNA-deleted species was observed in families with recurrent cases of CPEO transmitted as an autosomal

dominant trait (Zeviani, 1989). Mendelian inheritance of mtDNA mutations appeared puzzling, since this genome is transmitted in a strictly maternal fashion. However, this observation was explained as the consequence of a dominant mutation in a nuclear gene leading to altered structural integrity of mtDNA (Zeviani, 1990). This hypothesis proved to be correct, as it led to the discovery that many genes responsible for familial CPEO were associated with multiple mtDNA deletions. Later on, it was determined that multiple mtDNA deletions may arise secondarily from mutations in nuclear genes involved in mtDNA maintenance. The list of genes involved in mtDNA maintenance, and thereby associated with multiple deletion formation, is constantly growing. Thus, the inheritance of these mtDNA deletions follows the classic Mendelian rules.

These genes can be involved directly in mtDNA replication (POLG, POLG2, TWINKLE, RNASEH1, MGME1, and DNA2), but also in nucleotide pool balance (TYMP, SLC25A4, TK2, DGUOK, RRM2B, and MPV17) and, quite surprisingly, in mitochondrial dynamics (OPA1 and MFN2) (Sommerwille, 2014; Copeland, 2012). Also, mutations in genes difficult to categorize in aforementioned groups, are being correlated with multiple deletions like SPG7- paraplegin mutations and its partner protein AFG3L2, previously associated with dominant spinocerebellar ataxia type 28 disease (Gorman, 2015). Most recently, the CHCHD10 gene of unknown function was also found mutated in a few families with accumulation of mtDNA multiple deletions in muscle (Bannwarth, 2014). Thus, it is important to emphasize that these are not all mtDNA maintenance genes (Fig.6). Mutations in the nuclear encoded mitochondrial maintenance genes may cause two molecular phenotypes: mtDNA multiple deletions (“mtDNA multiple deletion disorders”) and reduction of mtDNA copy number (“mtDNA depletion syndromes”, MDS). The two molecular phenotypes may co-exist and are known collectively as mtDNA maintenance disorders (Kornblum, 2013). They can be either autosomal-recessive or -dominant mitochondrial disorders, in most cases with CPEO as the common clinical feature (Reyes, 2015).

To complicate the scenario, mtDNA multiple deletions arise and accumulate also spontaneously as age-dependent by-product of mtDNA replication in post-mitotic tissues. This somatic accumulation of mtDNA

multiple deletions characterizes certain subpopulations of neurons in neurodegenerative disorders, such as the dopaminergic neurons of substantia nigra in Parkinson disease (PD), as well as in elderly subjects (Carelli, 2015; Chan, 2015). Questions that still remain open are why in PD the accumulation of mtDNA deletions leads to detrimental consequences when the levels of deletion loads are similar in aged individuals? A very recent study reported that in elderly subjects the mtDNA copy number increased significantly with age and correlates with level of mtDNA deletions, whereas this compensatory affect fails in PD patients (Dolle, 2016).

3.5 MITOCHONDRIAL DNA MAINTENANCE GENES AND MULTIPLE MTDNA DELETIONS

Mutations in the DNA polymerase- γ (*POLG*) gene are a major cause of clinically heterogeneous mitochondrial diseases, associated with mtDNA depletion and multiple deletions.

POLG is the only polymerase responsible for mtDNA replication, and knockout mouse for *POLG* show embryonic lethality (Hance, 2005). *POLG*-related disorders are currently defined by at least five major neurological phenotypes, that include: childhood myocerebrohepatopathy spectrum (MCHS), myoclonic epilepsy myopathy sensory ataxia (MEMSA), Alpers-Huttenlocher syndrome (AHS), the ataxia neuropathy spectrum (ANS), and chronic progressive external ophthalmoplegia (CPEO), some of them being fatal in early childhood (Wong, 2008). In individuals presenting with CPEO and multiple mtDNA deletions most likely the laboratory tests will find pathogenic mutations in *POLG*. Psychiatric symptoms together with Parkinsonism are particularly prevalent in patients harbouring mutations of *POLG*. Other clinical manifestations include *POLG*-related encephalopathy and lactic acidosis and stroke-like episodes syndrome (MELAS)-like phenotype (Sommerwille, 2014; Hudson, 2006). In summary, both mtDNA depletion and accumulation of mtDNA deletions are important consequences of *POLG* mutations, but their reciprocal impact is variable among patients (Carelli, 2015).

C10orf2 (*twinkle*) encodes the mitochondrial protein *twinkle*, as mentioned above, this protein is DNA helicase that unwinds double stranded mtDNA in the 5' to 3' direction. This process is dependent on ATP and essential for mtDNA replication (Spelbrink, 2001). Two *Twinkle* mutations have been expressed in mice, dup352–364 and A359T, associated with CPEO in patients. The accumulation of mtDNA deletions was observed in the mouse muscle and brain tissues. The number of deleted molecules increased with age, along with the progressive respiratory chain dysfunction and myopathy (Tyynismaa, 2005). Dominant and recessive forms of PEO were reported in patients with *C10orf2* mutations. Phenotypic spectrum seen in patients with *Twinkle* mutations is very diverse, including gait disturbance, exercise intolerance, diabetes mellitus, visual impairment, diplopia, hearing loss, ataxia, and seizures. Psychiatric symptoms are particularly common in these patients and may be any of the following, or combination of more symptoms, like: more or less severe depression and dementia, Alzheimer's disease, avoidant personalities and other. Presence of mtDNA deletions is a hallmark of these mutations (Spelbrink, 2001; Van Hove, 2009; Sommerwille, 2014).

Recently *RNASEH1* was identified as another gene crucial for mtDNA maintenance. *RNASEH1*, encoding ribonuclease H1 (RNase H1), is an endonuclease that is present in both the nucleus and mitochondria and digests the RNA component of RNA-DNA. Patients first present with CPEO and exercise intolerance followed by muscle weakness, dysphagia, and spino-cerebellar signs with impaired gait coordination, dysmetria, and dysarthria (Reyes, 2015). Mouse knockout of *RNASEH1* shows embryonic lethality due to failure to synthesize mtDNA (Carittelli, 2003). Deleterious *RNASEH1* mutations slow down and stall mtDNA replication, causing both mtDNA depletion and deletions and ultimately leading to mitochondrial disease (Reyes, 2015).

MGME1 (mitochondrial genome maintenance exonuclease 1), encodes a mitochondrial RecB-type exonuclease belonging to the PD-(D/E) XK nuclease superfamily. *MGME1* cleaves single-stranded DNA and processes DNA flap substrates, also necessary for maintaining mitochondrial 7SDNA levels. By date only homozygous mutations in the gene are causing clinical phenotype characterized by ptosis in

childhood, followed by CPEO, diffuse skeletal muscle wasting and weakness, profound emaciation, and respiratory distress. Interestingly, mtDNA deletions from patients with *MGME1* mutations were unusually large and detectable in DNA derived from blood (Kornblum, 2013).

The molecular pathway responsible for the involvement of DNA2 in mtDNA is still under investigation. However, DNA2 encodes a helicase/nuclease family member that is most likely involved in mtDNA replication, as well as in the long-patch base-excision repair (LP-BER) pathway. Patients present with lower limb weakness, ophthalmoplegia, diplopia, myalgia and progressive myopathy. Multiple mtDNA deletions were reported in muscle (Ronchi, 2013).

TYMP encodes thymidine phosphorylase which catalyses the conversion of thymidine to thymine and deoxyuridine to uracil (El-Hattab, 2017). Depletion of thymidine phosphorylase disturbs dNTP supply affecting mtDNA replication. Mutations of the *TYMP* cause mitochondrial neurogastrointestinal encephalopathy (MNGIE). This is a multisystem disorder and gastrointestinal dysmotility is the main symptom. Other common symptoms are CPEO, cachexia, muscle weakness, muscle atrophy and hearing loss. One of the hallmarks of MNGIE is somatic alteration of mtDNA, namely, depletion, multiple deletions, and site-specific point mutations (Valentino, 2007).

SLC25A4 (ANT1) encodes ADP/ATP translocase1, as the name of this protein suggests it is necessary in the exchange of ATP generated within mitochondria and ADP present in the cytoplasm. Phenotype manifestation is associated to adCPEO and Senger's syndrome. Patients often have ptosis and neuromuscular symptoms, if present, are usually restricted to the facial muscles, mostly extra ocular. There were reports with psychiatric symptoms in patients (Sommerwille, 2014).

TK2 encodes thymidine kinase 2, which phosphorylates thymidine, deoxycytidine, and deoxyuridine and is essential for dNTP generation for mtDNA replication. Thus, TK2 is an enzyme of the mitochondrial nucleotide salvage pathway and its loss-of-function mutations have shown to underlie the early-infantile myopathic form of mtDNA depletion syndrome (MDS). Heterozygous mutations lead to arCPEO, with

multiple deletions. Clinical presentation is with mild late-onset CPEO together with myopathy and central nervous system involvement (Tynismaa, 2012).

DGUOK encodes deoxyguanosine kinase, enzyme necessary for the first step of salvage of deoxyribonucleotides in the mitochondria. This function is essential for mtDNA maintenance. Heterozygous mutations with very late onset CPEO and ptosis were described to have multiple mtDNA deletions (Ronchi, 2012). Interestingly, the same mutations were found in in early onset mitochondrial disease patients with mtDNA depletion (Sommerwille, 2014).

RRM2B encodes ribonucleoside-diphosphate reductase subunit M2 B (p53R2), protein that has essential role for dNTP supply for mtDNA replication, and consequently to its role it is involved in both mtDNA maintenance and repair. Mutations in *RRM2B*, after *POLG* and *TWINKLE*, represent the third major number of adult-onset CPEO patients, and patients may have a broad spectrum of symptoms including milder CPEO, ptosis may occur but not necessary, exercise intolerance, muscle weakness, muscle atrophy, fatigue and hearing loss. Multiple mtDNA deletions are a common molecular finding in these patients (Sommerwille, 2014).

MPV17 is a mitochondrial inner membrane protein, and its absence or dysfunction may cause OXPHOS failure and mtDNA depletion in affected individuals and in the *Mpv17* knockout mice. Severe mtDNA depletion manifests as early childhood-onset failure to thrive, hypoglycemia, encephalopathy, and hepatopathy progressing to liver failure (Spinazzola, 2006). Homozygous mutation in *MPV17* was found in Navajo Indian patients with infantile-, childhood-, or juvenile-onset neurohepatopathy (Spinazzola, 2008). Heterozygous mutation was reported only in one patient, initially diagnosed with Charcot-Marie-Tooth disease. Later in life patient developed other symptoms: progressive proximal limb weakness, exercise intolerance, diabetes mellitus, ptosis, ophthalmoparesis, hearing loss, gastrointestinal dysmotility and depression. MtDNA deletions are found only in one patient, thus *MPV17* mutations manifest preferentially as mtDNA depletion disorders (Garone, 2012).

As discussed previously, *OPA1* encodes the mitochondrial dynamin-like GTPase, inserted within the IMM and crucial for regulation of mitochondrial fusion and morphology. In 2008, both our and another group reported the occurrence of a multisystem disorder, named dominant optic atrophy plus (DOA-plus), characterized by severe optic atrophy, visual loss, sensorineural deafness and associated with accumulation of mtDNA multiple deletions in skeletal muscles (Amati- Bonneau, 2008; Hudson, 2008). Mutations in *MFN2* gene are the most commonly identified cause of Charcot-Marie-Tooth type 2 (CMT2), a dominantly inherited disease characterized by degeneration of peripheral sensory and motor axons (Zuchner, 2004). Dominant *MFN2* missense mutations may also lead to an optic atrophy plus phenotype. Importantly, both *OPA1* and *MFN2* are involved in mitochondrial fusion machinery. Deletions of mtDNA were also found in patients with *MFN2* mutations, providing further evidence that mitochondrial fusion/fission is necessary for mtDNA maintenance (Rouzier, 2012).

CHCHD10 encodes a coiled-coil helix protein whose function is still unknown. It belongs to a family of mitochondrial proteins located in the IMS, some of which interact with *OPA1* and are involved in cristae integrity and mitochondrial fusion (An, 2012). Families reported to have mutation in *CHCHD10* had motor neuron disease, cognitive decline resembling frontotemporal dementia, non-CPEO myopathy, and accumulation of mtDNA multiple deletions in skeletal muscle (Bannwarth, 2014).

SPG7 encodes paraplegin, which localises to the mitochondrial inner membrane. Typical presentation of symptoms is onset of either CPEO/ptosis and spastic ataxia, or a progressive ataxia disorder.

AFG3L2 encodes AFG3-like protein 2, which forms a homo-oligomer, an m-AAA protease, with paraplegin in the mitochondrial inner membrane. Patients present with late-onset, slowly progressive ptosis and ophthalmoparesis with slurred speech and lower limb muscle weakness. So far, only two patients were reported with *AFG3L2* mutations and CPEO with mtDNA multiple deletions (Gorman, 2015).

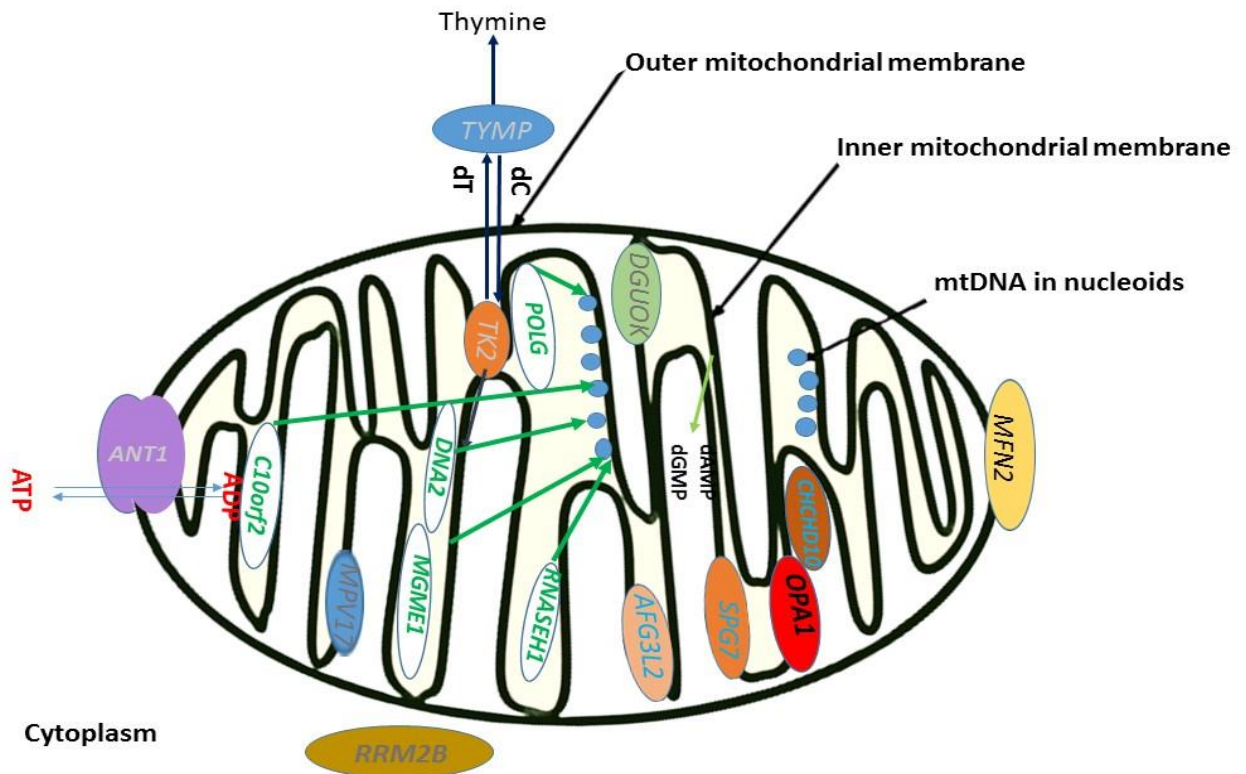


Figure 6. Mendelian disorders of mtDNA maintenance associated with multiple mtDNA deletions. A cartoon identifying the major genes which have been associated with disorders of mtDNA maintenance including multiple mtDNA deletion syndromes. Genes involved directly in mtDNA replication (italicised in green); involved in nucleotide pool balance (italicised in grey); involved in mitochondrial dynamics (italicised in black); with still not well defined function (italicised in light blue) and the sub-mitochondrial localisation of the proteins encoded by these genes (Trifunov, unpublished figure).

3.6 MECHANISMS OF MTDNA DELETIONS FORMATION

Many qualitative studies gathered a significant knowledge on the general characteristics of mtDNA-deletions. Single and multiple mtDNA deletions are similar in size, may be flanked or not by repeat sequences and length of this repeats is similar between the two groups. These common features between single and multiple mtDNA deletions suggest that the same mechanism underlies their formation in different clinical settings (Krishnan, 2008).

As discussed previously, the most reported mtDNA deletions occur in the major arc of mtDNA, between the two origins of mtDNA replication. This preferential location for mtDNA deletions is principal to the

hypothesis that mtDNA deletions arise by slipped-strand mispairing among direct homologous base-pairs during replication, if the replication is of strand displacement type. This is possible because this replication model implies presence of long single stranded DNA (Shoffner, 1989). While replication is ongoing, the repeat of the H-strand, which is now single-stranded, may misanneal with the recently exposed L-strand repeat. This occurrence results with formation of a loop downstream of single-stranded parental H-strand that is later degraded with ligation of the free H-strands. After this event, replication is continued and results in formation of one wild type and one deleted mtDNA molecule (Fig. 7) (Pitceathly, 2012).

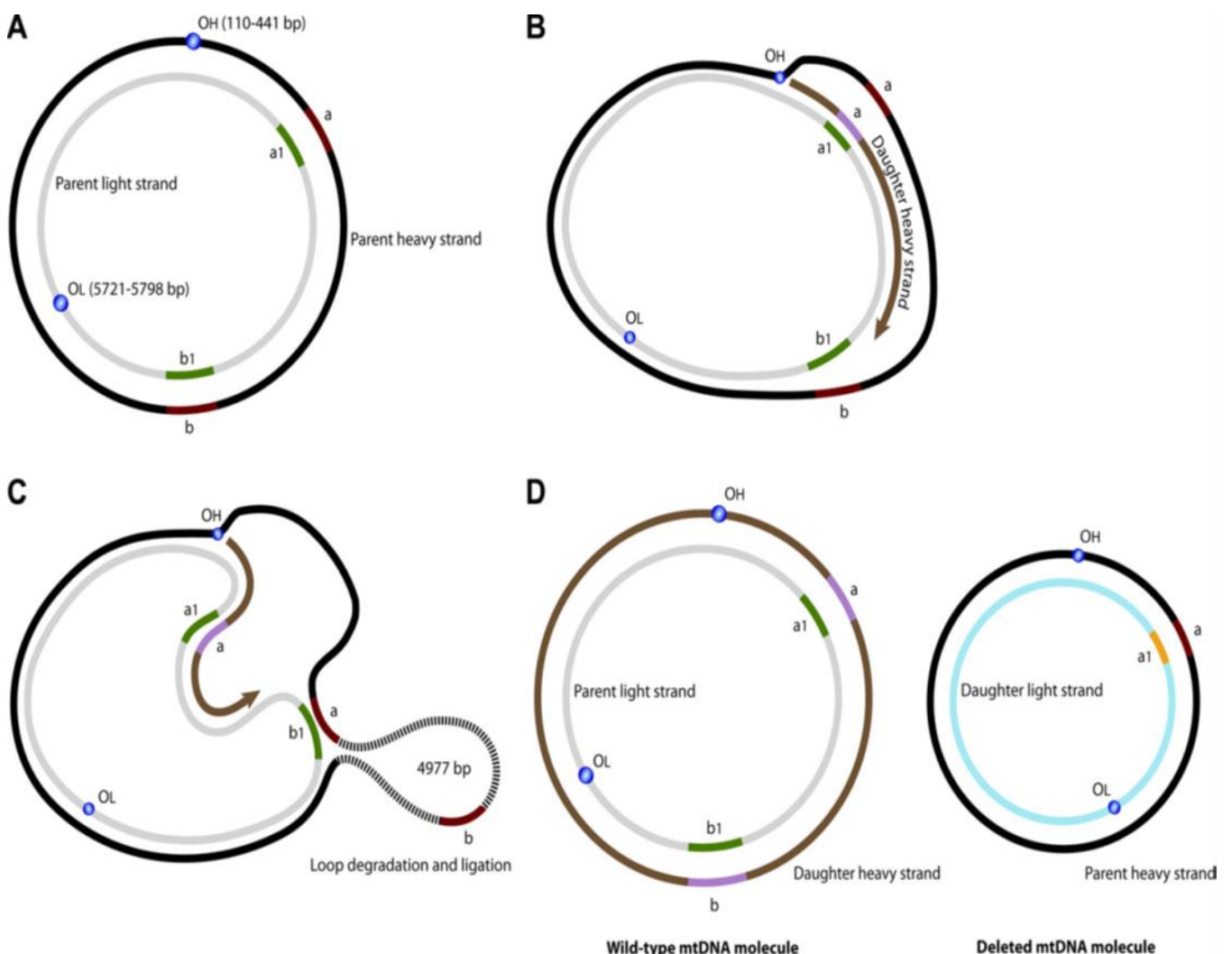


Figure 7. Illustration of mitochondrial DNA deletion formation by slipped-strand model. (A) MtDNA molecule before replication with two direct homologous repeats (a/a1 and b/b1). The OH and OL are shown. (B) Initiation of mtDNA replication starting at OH. The daughter heavy strand (indicated with brown arrow) uses as a template the parental light strand simultaneously displacing the parent heavy stand. (C) Misannealing of direct bp repeat from the parent heavy strand (a) and the newly exposed

direct bp repeat on the parent light strand (b1), which results in formation of a loop downstream of heavy strand. The single-stranded loop is degraded until double-stranded DNA is reached, and this results with loss of the second parent heavy strand bp repeat (b). Ligation of the free ends of the parent heavy strand and continual replication of the daughter heavy strand. Replication of the daughter light strand starts when OL in the heavy strand is exposed; the parent heavy strand is used as template, in the opposite direction. (D) Result is the synthesis one deleted and one wild type mtDNA molecule (from Pitceathly, 2012).

A different hypothesis suggests deletion formation during the repair of mtDNA at double-strand breaks (DSB), and not during the replication (Krishnan, 2008; Fukui and Moraes, 2009). This model proposes that mtDNA deletions are initiated by single-stranded regions of mtDNA generated through exonuclease activity at DSBs. This process takes place with nuclear single stranded DNA, allowing microhomologous sequences to anneal. Eukaryotic cells have alert systems for DSB that alert for start of repair process (Pardo, 2009). In mtDNA, by the proposed model, DSB would provoke repair leading to subsequent ligation and finally degradation of the single strands (Fig.8). Altogether this may lead to rise of mtDNA deletion, as it was observed in mouse model that, due to induced restriction endonuclease with mitochondrial targeting, generates substantial amounts of mtDNA deletions (Fukui and Moraes, 2009). This model argues that if deletion formation would only occur during replication, higher levels of deleted molecules should be present in mitotic rather than post-mitotic cells (Krishnan, 2008). As discussed previously, in patients with different pathologies characterized by accumulation of mtDNA deletions occurs the opposite, since these are accumulated preferentially in post mitotic tissues.

It is possible that the two models are not mutually exclusive. In different time points and dependant on the cell status, both mechanisms could occur and this issue still need to be fully elucidated.

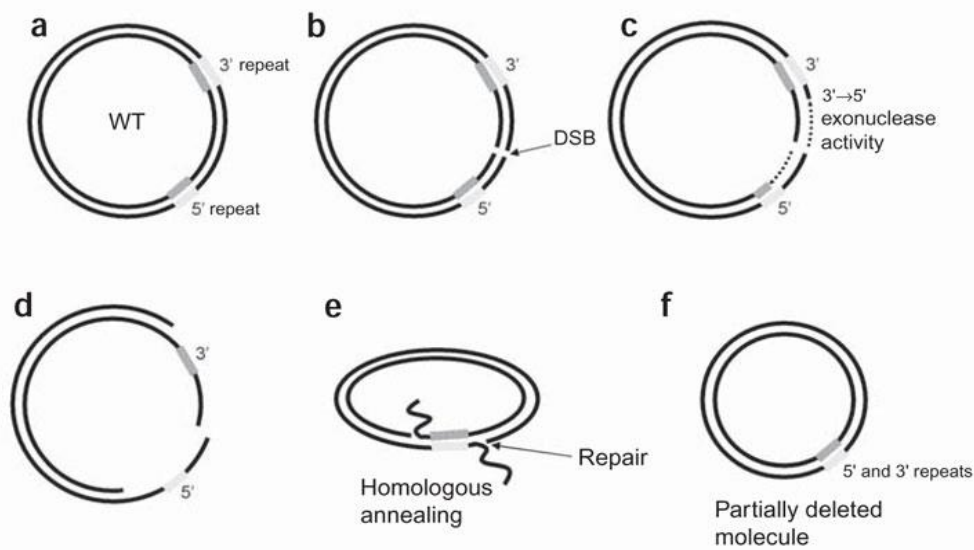


Figure 8. Illustration of suggested model for generation of mtDNA deletions during the process of mtDNA repair. (a) Two direct repeats in mtDNA marked 3' and 5'; (b) The DSB is generated. (c,d) The DSB is vulnerable to 3'→5' exonuclease activity, further leading to the creation of single strands (d). (e) The 5'- and 3'-repeats may misanneal, which leads to degradation of the released single strands and ligation of the double strands. (f) Results is the creation of a deleted mtDNA, containing copies of both the 5' and 3' repeats (from Krishnan, 2008).

3.7 METHODS FOR QUANTITATIVE ANALYSIS OF HETEROPLASMY

Quantification of deleted mtDNA is a difficult task, due to the fact that these molecules are always mixed with wild type mtDNA, thus requiring a highly sensitive approach. It becomes even more complex when quantification involves low abundance mtDNA deletions, because of technical limitations in sensitivity that usually require previous enrichment. Another important feature to be considered is the source of DNA to be used. Total DNA should be purified from a not fast replicative cell type, ideally from the muscle. If fast dividing cells, like hair or blood cells, are used as a source of mtDNA, the results may lead to wrong conclusions because heteroplasmy of mtDNA in these tissues is markedly shifted toward wild-type mtDNA (Moraes, 2003).

Southern blotting is the gold standard technique for the detection and quantification of most mtDNA rearrangements. This is not possible for single cells due to the quantity of DNA required and the limited sensitivity of the technique (He, 2002). The identification of deleted molecules is also possible using techniques such as long-range PCR, but this technique is not quantitative and has only the value of detection of a deletion (Reynier and Malthiery, 1995). This is the case also for the Southern blot, as for assessment of deletion heteroplasmy, densitometric analysis of the resulting band/s is used for heteroplasmy assessment. Another widely used technique for quantitative assessment of mtDNA deletions heteroplasmy is quantitative PCR. Assays for qPCR measuring mtDNA deletion level and mtDNA copy numbers (mtDNA CN) are abundant in the literature (He, 2002; Rygel, 2015; Philips, 2014). Quantitative PCR requires use of external standards, often in form of plasmid DNA, for quantification of mtDNA deletions. The size and breakpoint positions of many mtDNA deletions have been mapped in a large number of patients with single and multiple deletions (Damas, 2014). Generally, in quantitative PCR, two regions within mtDNA are detected at the same time: first region lays within the minor arc of mtDNA, where deletions hardly ever occur and a second region lays within the major arc where most mtDNA deletions span. By comparison of the target quantities the percentage of the deletion is calculated (He, 2002).

Recently, a new and powerful technique, digital PCR (dPCR) was used for quantification of deleted mtDNA and was shown to be more precise, in comparison to more traditional qPCR (Belmonte, 2016). Droplet digital PCR is a variation of digital PCR offered by Bio-Rad (Hindson, 2011). Digital PCR can amplify a number of DNA copies, wherein the reaction simultaneously proceeds inside several thousands of nanoliter microspheres, thereby allowing higher data reliability. The quantitative real-time PCR is commonly done in triplicate reactions, and the data are presented as arithmetic mean. However, in digital droplet PCR, numerous reactions happen simultaneously, which extensively decreases inaccuracy (Sofronova, 2016). An additional, prominent, benefit of ddPCR in heteroplasmy quantification is that it doesn't require the usage of external standards, and also therefore results in lower error rates.

Partitioning of samples brings enhanced sensitivity and the final reaction is visualised using fluorescence rather than gel analysis (Belmonte, 2016; Manoj, 2016). New methods to increase the sensitivity of measuring mtDNA deletions are key to the diagnosis of primary mitochondrial disease.

AIMS

Mitochondrial DNA deletions are pathogenic mutations removing various portions of this genome, thus resulting in shorter molecules. In patients, there are two classes of mtDNA deletions: single and multiple deletions (Holt, 1988; Zeviani, 1988). Single mtDNA deletions are in most cases sporadic and not transmitted, probably because they arise de novo somatically during early stages of embryogenesis. Multiple mtDNA deletions are generated secondarily to mutations in nuclear genes involved in mtDNA maintenance, thus they are inherited as Mendelian traits.

The mtDNA deletions have been qualitatively investigated since they were first reported as causative human diseases. Quantitative investigation of mtDNA deletions has remained a demanding task, requiring highly sensitive technical approaches, due to the multicopy nature of mtDNA implying a heterogeneous population of deleted and wild-type molecules (Belmonte, 2016).

The first aim of this study is to set more reliable quantification strategies for assessment of mtDNA deletions, which will be applied to determine heteroplasmy levels in muscle biopsy samples originating from different single and multiple deletion patients. To this end a new technique, the droplet digital PCR (ddPCR), is applied and compared with other, more traditional, methods such as Southern blot and quantitative real-time PCR.

The second and final aim of this study is to investigate the clonal expansion as driving force leading toward prevalence of mtDNA deletions in certain cells. The mechanisms and dynamics of clonal expansion are still elusive and the distribution of mtDNA heteroplasmy remains an unpredictable aspect of mitochondrial genetics. Clonal expansion acts at the single cell level, and for this reason droplet digital PCR (ddPCR) will be applied for the first time to quantitatively assess mtDNA deletions heteroplasmy and mitochondrial DNA copy number in single muscle fibres laser captured from patient's muscle biopsies.

Overall, dissecting the dynamics of clonal expansion may also lead to better understanding of germline transmission of mtDNA deletions, which is certainly necessary for preventing diseases due to these pathogenic mutations.

MATERIALS AND METHODS

1. Patients

We selected 7 patients presenting with three different pathologies associated with mtDNA deletions: 2 patients with dominant mutation in the OPA1 gene and a DOA “plus” syndrome, 2 patients with recessive mutations in the POLG gene and the SANDO syndrome (sensory ataxic neuropathy, dysphagia, ophthalmoplegia), and 3 sporadic patients with single mtDNA deletion and CPEO. This choice was done to represent three different categories of mitochondrial disorders: the patients with OPA1 mutations may accumulate mtDNA multiple deletions because of defective mitochondrial dynamics, the patients with POLG mutations present with pathological mtDNA maintenance due to defective mtDNA replication, and finally the patients with single mtDNA deletion are the paradigm of sporadic occurrence of mtDNA deletions.

We also used 3 healthy, age-matched individuals as controls for this study.

Patient 1:

A 76-year-old man presented since he was young with the main symptoms of muscle weakness, gait unsteadiness, chronic and bilateral ptosis. Psychiatric symptoms included anxiety, panic attacks and depression. All these symptoms progressed and later in time he developed peripheral neuropathy, deafness, optic atrophy and Parkinsonism. At the time of biopsy he was 66 years old, and biopsy revealed cytochrome c oxidase (COX) negative fibres. The mtDNA analysis revealed the presence of multiple mtDNA deletions by long-range PCR. The patient belonged to a large family with dominant transmission of the same phenotype. Screening of candidate genes involved with multiple mtDNA deletions revealed heterozygous missense mutation in OPA1, affecting nucleotide c.1462G>A. This mutation affects conserved amino acid p.G488R in the GTPase domain of OPA1. This family has been previously reported (Carelli, 2015).

Patient 2:

This is a 49 year old man who had poor vision since he was 4-year-old that progressed to complete blindness later in life. Since 9 years of age he also suffered a progressive hearing loss needing acoustic

prosthesis. At 30 years of age he developed gait difficulties with frequent falls due to peripheral neuropathy. At the time of muscle biopsy he was 42, and biopsy was positive for COX negative fibres. Electron microscopy of skeletal muscle showed mitochondria with morphologically abnormal cristae and accumulation of lipid droplets. Long-range PCR analysis of mtDNA revealed the presence of mtDNA multiple deletions. Screening of candidate genes was positive for the mutation c.1316 G4T affecting a conserved amino acid p.G439V in the GTPase domain of OPA1. The patient daughter developed the same phenotype and this case has been previously reported (Amati-Bonneau, 2008).

Patient 3:

This is a 63-year-old man with a multisystemic syndrome known with the acronym of SANDO. He suffered with ptosis and ophthalmoplegia by the age of 30; ten years later he started to develop a progressive skeletal muscle weakness and a sensitive polyneuropathy causing an ataxic gait. By the age of 50 he had dysarthria. His muscle biopsy showed a mitochondrial myopathy with Ragged Red Fibres and COX negative fibres. He carried two heterozygous mutations in the POLG1 gene (a missense mutation c.934T>C causing the amino acid change W312R and an insertion, 3629insA, causing a stop codon Y1210X). MtDNA multiple deletions were evident at long range PCR of muscle DNA.

Patient 4:

This 67-year-old woman suffered from ptosis and ophthalmoplegia from the age of 30 years. By the age of 56 years she clinically presented with ptosis, ophthalmoplegia, skeletal muscle weakness, peripheral polyneuropathy. A few years later she also developed dysphagia and a Parkinsonian syndrome with hypomimia, hypophonia, camptocormia and bradykinesia. Her muscle biopsy showed a mitochondrial myopathy with Ragged Red Fibres and COX negative fibres. She carried a homozygous missense mutation c.1943C>G in POLG1 gene leading to the amino acid change p.P648R. Multiple mtDNA deletions were evident with long range PCR.

Patient 5:

This 50-year-old man started to develop a progressive bilateral ptosis and ophthalmoplegia by the age of 17 years. By the age of 45 years he suffered from diabetes mellitus, cardiomyopathy and skeletal muscle weakness. His muscle biopsy revealed numerous COX negative fibres. He carried a single mtDNA deletion of 4977 base pairs (nt. 8469-nt.13447).

Patient 6:

This 23-year-old girl suffered of monolateral ptosis by the age of 15 years without ophthalmoparesis. Her neurological examination was negative except for monolateral ptosis and electromyography didn't show signs of myopathy and/or polyneuropathy. Audiometry was normal. She had lactic acidosis after aerobic effort and muscle biopsy showed a mitochondrial myopathy with COX negative fibres. She carried a single mtDNA deletion of 4977 base pairs (nt. 8469-nt.13447).

Patient 7: This 55-year-old man developed by the age of 18 ophthalmoparesis and later, at 40 years, a bilateral progressive ptosis; he also presented with a mild peripheral polyneuropathy and neurosensorial hearing loss. His muscle biopsy showed a mitochondrial myopathy with COX negative fibres, without Ragged Red fibres. He carried a single mitochondrial DNA deletion of 5992 base pairs (breakpoint nt.9431-nt.15423). At the time of the biopsy he was 50 years old.

Control 1: 37 year old female

Control 2: 20 year old female

Control 3: 41 year old female

Control 4: 38 year old male

Table 1: Characteristics of samples used in this study

<i>Case</i>	<i>Patient or control</i>	<i>Age at the time of biopsy</i>	<i>Age</i>	<i>Sex</i>	<i>Tissue sampled</i>
P1	OPA1	66	76	M	<i>Vastus L</i>
P2	OPA1	42	49	M	<i>Vastus L</i>
P3	POLG	53	63	M	<i>Vastus L</i>
P4	POLG	57	67	F	<i>Vastus L</i>
P5	SINGLE DELETION (Common)	49	50	M	<i>Vastus L</i>
P6	SINGLE DELETION (Common)	18	23	F	<i>Vastus L</i>
P7	SINGLE DELETION	50	55	M	<i>Vastus L</i>
C1	Control 1	37	NA	F	<i>Vastus L</i>
C2	Control 2	20	NA	F	<i>Vastus L</i>
C3	Control 3	41	NA	F	<i>Vastus L</i>
C4	Control 4	38	NA	M	<i>Blood DNA</i>

2. Southern Blot

Labelling of the probe

As probe we used the whole mtDNA amplified by PCR in 11 products. The DIG DNA labelling and detection kit (Roche) was used to label the DNA with Digoxigenin-dUTP using random oligonucleotides as primers. In this method, the complementary DNA strand of denatured DNA is synthesized by Klenow polymerase using the 3'-OH end of the random oligonucleotides as primers. The labelling reaction was carried out according to manufacturer's instructions. Briefly, 1ug of probe was diluted in 15ul of distilled water, boiled to denature for 10 minutes and cooled down in ice. To the denatured probe was added: 10x hexanucleotide mix, dNTP labeling mix and Klenow enzyme in appropriate volumes. Mixture was incubated at 37°C over-night and reaction was stopped the following morning by heating at 65°C. Hybridization mixture was stored at -20°C until hybridization.

Restriction enzyme digestion and agarose gel electrophoresis

Total genomic DNA was directly extracted from portions of frozen muscle biopsy tissues or from blood, with phenol-chloroform standard protocol. One microgram (ug) of DNA was digested with restriction enzyme BamHI (Thermo Fisher Scientific), following the manufacturer's instruction. Restriction enzyme digestion was performed at 37°C and overnight. BamHI is restriction enzyme which cuts mtDNA just once at nucleotide position 14258, linearizing the mtDNA molecule. Digestions were separated on 0.8% agarose gel with Marker X (Rosche) by electrophoresis at 50V for 8h.

DNA transfer to the membrane

Following the digestion, filter paper and Mini Trans Blot filter paper (Biorad) were cut to the dimensions of gel as well as the positively charged nylon membrane (Boehringer Mannheim) and marked for recognising. Gel with digestions was placed in a dish with 50ml of 0.25M HCl for 15 min on shaker, for depurination and rinsed in distilled water. Then soaked twice in 50ml of NaOH for 20min on shaker for denaturation of DNA. After denaturation, gel was rinsed in distilled water, and placed in a container with

50ml of neutralization buffer (1M Tris, pH 7.4; 1.5M NaCl) for 10min on shaker. In the meantime, plastic tray with two plastic hubs upside down and glass square was prepared. The glass was covered with filter paper, in a way that the ends of filter paper are touching plastic tray. In plastic tray and over the filter paper was poured 10X SSC buffer (prepared from stock solution 3M NaCl; 300mM $\text{Na}_3\text{C}_6\text{H}_5\text{O}_7$; pH 7). The gel was placed on filter paper upside down. On the upper side of gel was placed positively charged membrane in 2X SSC buffer. Membrane was covered with the membrane Mini Blot (BioRad) filter paper, and regular filter paper and paper towels until 10cm high. Second glass square was positioned on top together with 1kg of weight. The transfer from gel to membrane was overnight.

DIG EASY HYB buffer (Roche) was preheated to hybridization temperature. The membrane was placed in a plastic tray and incubated with preheated buffer for 30 minutes at 42°C. The DIG-labelled DNA probe, prepared as described above, was denatured by boiling for 5min and rapidly cooling in ice. The denatured probe was added to pre-heated DIG Easy HYB buffer, and the membrane was incubated overnight incubation at 42°C.

Washing the membrane, detection of luminescence and densitometry analysis

Upon hybridization, membrane was washed in stringency buffers, two times for 30 minutes in each buffer (Buffer I- 0.02M Na_2HPO_4 with 5% SDS; Buffer II- 0.02M Na_2HPO_4 with 1% SDS; Buffer III- 0.02M Na_2HPO_4 with 0.5% SDS). Membranes were then incubated in blocking solution (Roche) diluted in maleic acid, to decrease the background in nonradioactive filter hybridization and the detection of nucleic acid hybrids. After blocking, membranes were incubated in Anti-Digoxigenin-AP Conjugate antibody (Roche) diluted 1:5000 in blocking solution, and washed two times in Washing solution (Roche). After washing the membrane was immersed in CSPD ready to use (Roche) for 5 minutes in dark. CSPD is a chemiluminescent substrate for alkaline phosphatase that enables fast and sensitive detection of biomolecules by producing visible light. Light emission was recorded on luminescence imager system (Li-Core) and densitometry analysis was performed with Image Studio TM (Li-Core).

3. Preparation of recombinant plasmid for standard curve

Total genomic DNA was extracted from blood of healthy controls. PCR primers were designed to amplify regions inside the ND1 and ND4 genes, a fragment of DNA in the NCR (noncoding region), and a fragment encompassing the common deletion breakpoints. PCR products were analysed on agarose gel, and DNA fragments were cut out and purified using QIAquick Gel Extraction kit (Quiagen). DNA was quantified by NanoDrop™ spectrophotometer. PCR products were cloned into vector TOPO® TA cloning (Thermo Scientific). Competent cells were grown in Luria–Bertani (LB) medium at 37°C containing, 50ug/ml of ampicillin and 25ug/ml of kanamycin, for the selection of recombinant clones. Positive clones were inoculated overnight in liquid Luria-Bertani medium at 37°C and plasmid DNA was isolated with GeneElute Plasmid Miniprep kit (Sigma-Aldrich).

4. Quantitative real-time PCR

PCR primers and fluorogenic probes (Integrated DNA Technologies) for all regions amplified are shown in Table 2. The absolute quantification method was achieved by standard curve generation. Serial dilutions of the recombinant plasmid were used for a standard curve for qPCR. Region within minor arc, within ND1 gene was compared with region in the major arc the ND4 gene (Kirshnan, 2007, Philips, 2014). One microliter of DNA extracted from muscle biopsy homogenate was amplified separately with the ND1/ ND4 and D-loop/ND4 primer and probe combinations. To each sample 4.22 µl nanopure water and 12.5 µl LightCycler® TaqMan® Master Mix were added. The concentration of all PCR primers was 300 nM and the fluorogenic probes 100 nM. PCR and fluorescence analysis was performed using the Roche LightCycler® 480 Instrument and detection system (Roche Molecular Biochemicals, Germany). Amplification conditions were: 2 min at 50°C, 10 min at 95°C then 40 cycles of 15 s at 95°C and 1 min at 62°C (for probe/primer hybridisation and DNA synthesis).

5. Transversal and longitudinal muscle biopsy sectioning

Quadriceps muscle biopsies, were taken under local anaesthetic from all patients as well as from healthy controls. All muscle biopsies (all from vastus lateralis) were frozen in liquid nitrogen-cooled isopentane and stored at -80°C until processed. Adjacent 10-mm sections were cut using a cryostat microtome and fixed on PEN membrane glass slides (Thermofisher). In this study we used both transversal and longitudinal sections of the muscle biopsy. We were successful in obtaining the longitudinal sections from three muscle biopsies (patient 1, patient 4 and patient 5), it is very challenging to cut sections over long segments of an individual muscle fibre. This is in part because of the characteristics of tissue orientation, and also from a propensity of fresh muscle tissue to coil along the longitudinal axis

6. Histochemical analysis and classification of individual muscle fibres

To discriminate COX positive and COX negative muscle fibres, sequential COX/succinate dehydrogenase (SDH) histochemistry was performed on every section in the same incubation bath in parallel. COX activity was verified histochemically in a medium containing 4 mM 3, 3'- diaminobenzidine tetrahydrochloride (DAB) and 100 mM cytochrome c (Sigma) in 0.1 M phosphate buffer, pH 7.0 at 37°C . SDH activity was assayed by using 1.5 mM nitrobluetetrazolium, 130mM sodium succinate, 0.2 mM phenazine methosulfate, and 1.0 mM sodium azide in 0.1 M phosphate, pH 7.0 at 37°C . A 40-min incubation for COX activity was used, this allows detection of all histochemically demonstrable COX activity. The SDH reaction was incubated for 30 min, permitting the SDH in COX negative/SDH positive fibres to be demonstrated (Old, 1989).

Upon COX/SDH staining, percentage of COX negative and intermediate fibres was determined (Table 3).

According to COX/SDH staining fibres were classified as COX positive, COX negative, ragged red fibres RRB and intermediate. Intermediate fibres have grey colour due to brown/blue mixed reaction product in COX/SDH staining (Figure 12).

7. Laser Capture Microdissection

The Leica laser capture microdissection (LCM) system (Leica Biosystems) was used, as described by the manufacturer's instructions to isolate 12-mm thick COX negative, COX positive and intermediate regions of single fibres at both transversal and longitudinal sections. Prior to collection, each fibre was assigned a number and the total surface of the fibre was measured. This system uses UV laser and gravity collection. Presence of the single fibre in the collection tubes was always verified. Before microdissection, the tissue sections were subjected to an ethanol and dehydration series for 10–15 min at each step.

8. Lysis of the single cells

Muscle biopsies from seven patients and 3 healthy controls, prepared as described above, provided a source for individual laser microdissected muscle fibres. They were previously stained for COX/SDH activity. Individual COX negative (n= 70), COX positive (n=265) and intermediate fibres (n=98) were collected. Cells were lysed in 2.5ul of lysis buffer containing: 50mM Tris-HCl pH 8.5, 200ng/ml of Proteinase K (Invitrogen) and 1% Tween (Sigma). Cells were incubated for 16 hours at 55°C and then 10 minutes at 95°C for denaturation of Proteinase K. After lysis, cells were digested for 1hour at 37°C with enzyme *PvuII* (Thermo Fisher Scientific) following the manufacturer's instruction.

9. Digital droplet PCR (ddPCR) assay

The 20ul reactions consisted of 1X digital PCR supermix for probes (Bio-Rad Laboratories), 375nM of ND1 probe, 900 nM of ND1 primers, 125nM of ND4 probe, 450nM ND4 primers and nuclease-free water. Reactions were transferred to 96well plates (Eppendorf) and droplet generation was carried out in an Automated Droplet Generator with DG32 cartridges (Bio-Rad Laboratories). Automated Droplet generator partitions samples into around 20,000 nanoliter-sized droplets, adding to each sample the 70 µl of Droplet Generation Oil for Probes (Bio-Rad Laboratories). Droplets are automatically transferred to 96-well plates and sealed ready for further amplification. PCR reactions were carried on C1000 Touch

thermal cycler (Bio-Rad Laboratories) using standard cycling conditions as follows: 95°C- 10 minutes, 40 cycles of 94°C-30 s, 40 cycles of 60°C-1min and 98°C- 10 minutes.

Following PCR amplification of the nucleic acid target, droplets were analysed on QX200 Droplet Digital PCR (ddPCR™). Each droplet was analysed individually using a two-colour detection system (set to detect FAM and HEX); PCR-positive and PCR-negative droplets are counted to provide absolute quantification of target DNA in digital form using QuantaSoft™Pro software (Bio-Rad). Results are collected and visually examined in 1D and 2D plots (Fig 16). The levels of mtDNA wild type molecules is calculated by dividing the absolute number of MTND4 positive droplets with the absolute number of MTND1 positive droplets, and the percentage of mtDNA deletion is 1-wt molecules (He, 2002). The mtDNA copy number density was measured at the single fibre level and presents the total number of mtDNA molecules in a muscle fibre section, divided by the fiber's cross-sectional area (Yu- Wai-Man, 2010). Each sample was assessed in triplicate.

Table 2. Primers and probes used in qPCR and ddPCR experiments

ND1 forward	5'CCCTAAAACCCGCCACATCT-3'
ND1 reverse	5'-GAGCGATGGTGAGAGCTAAGGT-3'
ND1 probe	5'-FAM/CCATCACCTCTACATCACCGCCC/BHQ1-3'
ND4 forward	5'-CCATTCTCCTCCTATCCCTCAAC-3'
ND4 reverse	5'-CACAATCTGATGTTTTGGTTAAACTATATTT-3'
ND4 probe	5'-HEX/CCGACATCATTACCGGGTTTTCTCTTG/BHQ2-3'

10. Single cell long range PCR

Long range PCR was carried out using PrimeSTAR GXL DNA polymerase (TaKaRa, Clontech) on available DNA samples extracted from individual muscle fibres. Briefly, single muscle fibres were laser dissected,

lysed and digested as described earlier. Due to limited amounts of DNA quantification prior to PCR was not possible. Primer pairs were: forward 6222-6240 and reverse 16133-16153. Reaction was prepared as follows: 1× buffer, 0.2 uMdNTP mix, 0.4 uM forward and reverse primers, 0.625 unit polymerase and 3ul DNA. Cycling conditions were: 94°C-1 min; 35 cycles of 94°C-10 s, 60°C-15 s and 68°C-10 min; 72°C-10 min. Amplified PCR products were electrophoresed on 0.8% agarose gels. Smaller bands, suggesting the presence of mtDNA deletions were cut out of gels. DNA was extracted according to manufacturer's protocol with QIAquick Gel Extraction Kit (Quiagen) and sequenced.

11. Statistical analysis

For the purpose of group evaluations, statistical investigation was done using GraphPad™ v.5.03 statistical software (GraphPad Software). Group comparisons were considered to be statistically non-significant (ns) if the calculated P-value was greater than 0.05, significant (*) with P = 0.01 to 0.05, very significant (**) with P = 0.001 to 0.01 and extremely significant (***) when the P-value was less than 0.001.

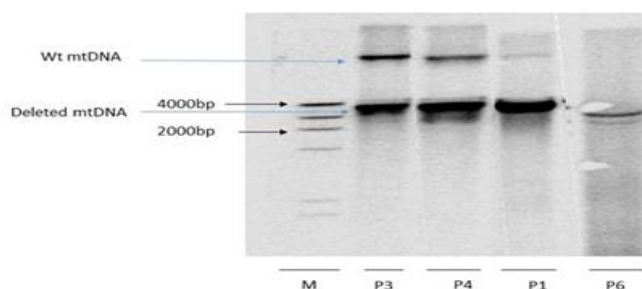
RESULTS

1. Validation of Digital Droplet PCR (ddPCR)

To quantitatively assess mtDNA deletions heteroplasmy in single cells, a ddPCR method was validated first on the total DNA extracted from homogenate of muscle biopsies. The results obtained were thus compared to the quantitative real-time PCR from the same samples and with Southern blot densitometric estimation of linearized mtDNA. Southern blot analysis and quantitative PCR methods are well-established methods for determining the amount of deleted mtDNA. For both quantitative real-time PCR and ddPCR, we analysed each sample in triplicate. For this validation we selected four patients (patients 2, 3, 4 and 6) from which the bioptic material was more abundant and we took care to include at least one patient per group. The mean values of deleted mtDNA load for patient 2 were 28.62% (SD=4.6) when assessed by qPCR, 37% by Southern blot densitometry and 9.06% (SD=0.75) by ddPCR. Similarly, in patients 3 and 4 the mean values with qPCR were respectively 50.58% (SD=2.4) and 73.10% (SD=2.3), 62% and 76% by Southern blot, and 44.39% (SD=3.1) and 70.50% (SD=2.6) by ddPCR. In patient 6, harbouring a single mtDNA deletion, qPCR mean was 33.9% (SD=5), Southern blot was 74%, and ddPCR was 53% (SD=4). These results are summarized in Figure 9. Overall, by correlating the values obtained by each technique for each case there was a stronger correlation of the deletion load detected by ddPCR and Southern blotting (Fig.10A), as compared with qPCR (Fig.10B). Southern blot is considered a reference, being the only technique that does not imply a DNA amplification step, as it relies on the existing total DNA extracted from the sample. The highest discrepancies between Southern blot and ddPCR results were observed in patient 2 and patient 6. The most probable explanation for these differences can be in the probe used; in Southern blot, we probed the entire mtDNA while in ddPCR probes are located within *MTND1* and *MTND4* genes. Patient 2, where this difference was greater (37% by Southern blot densitometry and 9.06% of mtDNA deletions by ddPCR), suffers from multiple mtDNA deletions and it is possible that part of the deleted molecules encompass regions different than *MTND1* and *MTND4* genes and/or are smaller and thus undetectable with our ddPCR assay. On the other hand, patient 6 with single deletion detectable by ddPCR, difference between Southern blot and ddPCR was

74% and 53%, respectively. In this case the possible explanation could be that Southern blot detects any mtDNA deletion potentially co-existing in the background of the prevalent single deletion.

A



B

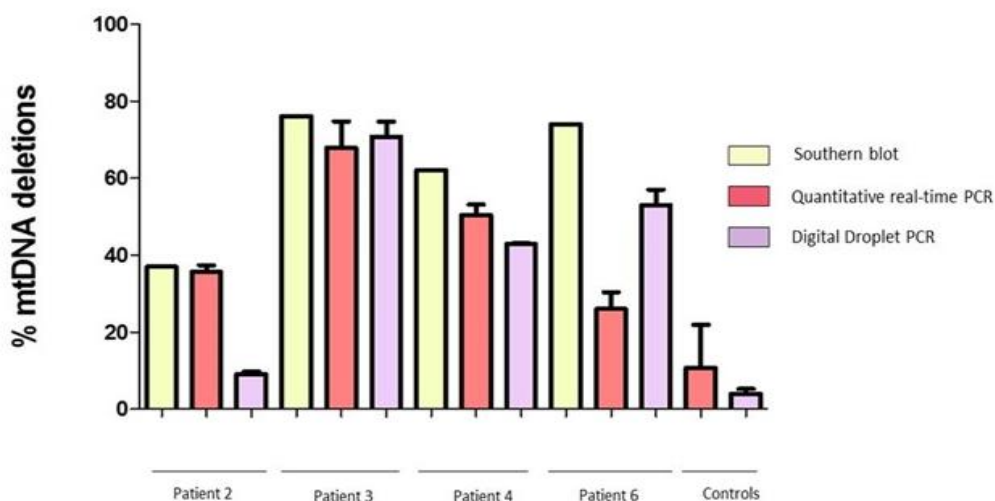
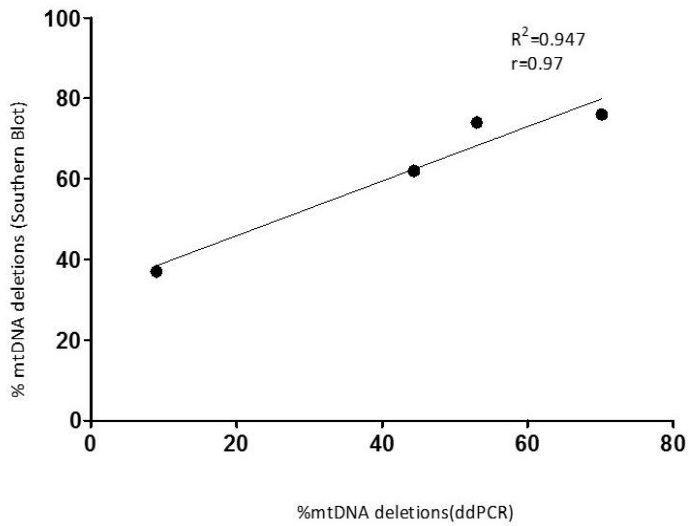


Figure 9. MtDNA deletions heteroplasmy levels. (A) Representative image for Southern blot. The positions of deleted and wild type (wt) mtDNA are indicated by blue arrows. (B) Comparison of heteroplasmy levels obtained with qPCR, ddPCR and Southern blot. Graph presenting mean values of qPCR measurements (red), ddPCR measurements (violet) and Southern blot densitometry (light yellow). Data for qPCR and ddPCR are means \pm SEM of three independent experiments.

A



B

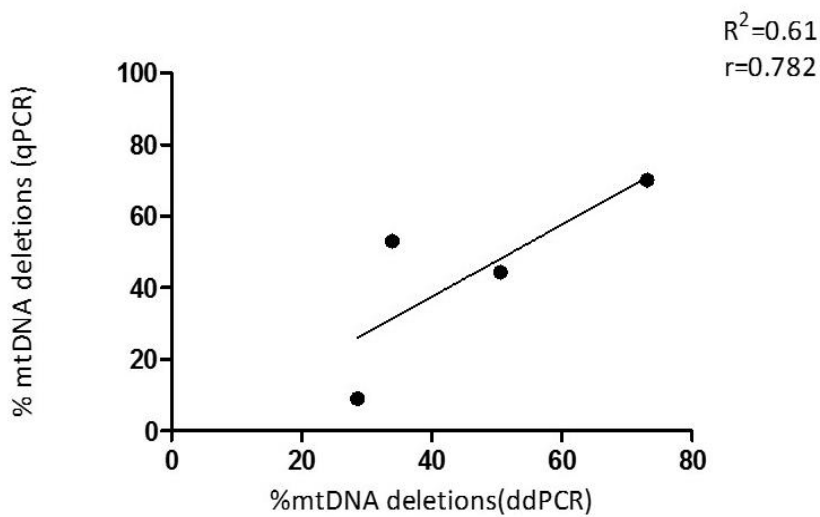


Figure 10. A- Correlation between mean values obtained for each patient with Southern Blot and ddPCR
B- Correlation between mean values obtained for each patient with qPCR and ddPCR; r values present correlation coefficient; R^2 values present coefficient of determination.

2. Proportion of COX negative and intermediate fibres throughout different patient groups

The standard histoenzymatic diagnostic staining performed on muscle biopsies includes the COX (cytochrome c oxidase, complex IV) and SDH (succinate dehydrogenase, complex II) stainings, performed simultaneously. COX has 3 subunits encoded by mtDNA and classically becomes deficient when the mutational load of heteroplasmic mtDNA deleted molecules crosses a certain threshold. On the contrary, SDH is completely encoded by nDNA, thus the staining is not affected by deleted mtDNA or is even increased when compensatory mitochondrial biogenesis is activated. The overlapping of COX (yellow staining) and SDH (blue) results in brownish staining, with SDH/blue emerging when COX/yellow is reduced.

Thus, the percentage of COX negative fibres for each biopsy used in this study (n=10) was visually determined. In healthy controls, as expected, COX negative fibres were absent. The lowest percentage, 2.53% of COX negative fibres, was found in the biopsy from patient 1, with an OPA1 mutation, followed by 5% of COX negative fibres in patient 2 with a similar pathology. The highest values, 28.5% of COX negative fibres, was found in patient 5 with single “common” deletion, and 28.3% in patient 3 with mutations in POLG. We observed a modest correlation between age of the patients and the levels of COX negative fibres found in the biopsy (Fig.11). The percentage of intermediate fibres was lowest for the patients 1 and 2, 2% and 4.3% of intermediate fibres respectively. The highest load of intermediate fibres 20.7%, was found in the biopsy from patient 3, whereas the second highest load, 18.5% of intermediate fibres, was found in patient 6, another patient with the single “common” deletion pathology. These results are summarized in Table 3. Representative images for biopsies are presented in figure 12.

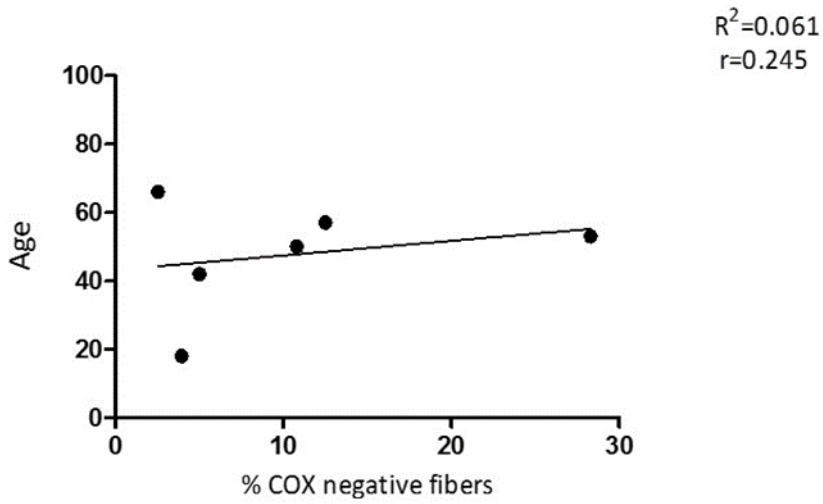


Figure 11. Correlation between patients age at the time of biopsy with levels of COX negative fibres; r values present correlation coefficient; R^2 values present coefficient of determination.

Table 3. Proportion of COX negative and intermediate samples

Pathology	Number of patient	%COX negative	%COX intermediate
OPA1	Patient 1	2.53	2
OPA1	Patient 2	5	4.3
POLG	Patient 3	28.3	20.7
POLG	Patient 4	12.5	16
SINGLE DELETION	Patient 5	28.5	16.5
SINGLE DELETION	Patient 6	3.94	18.5
SINGLE DELETION	Patient 7	10.8	20

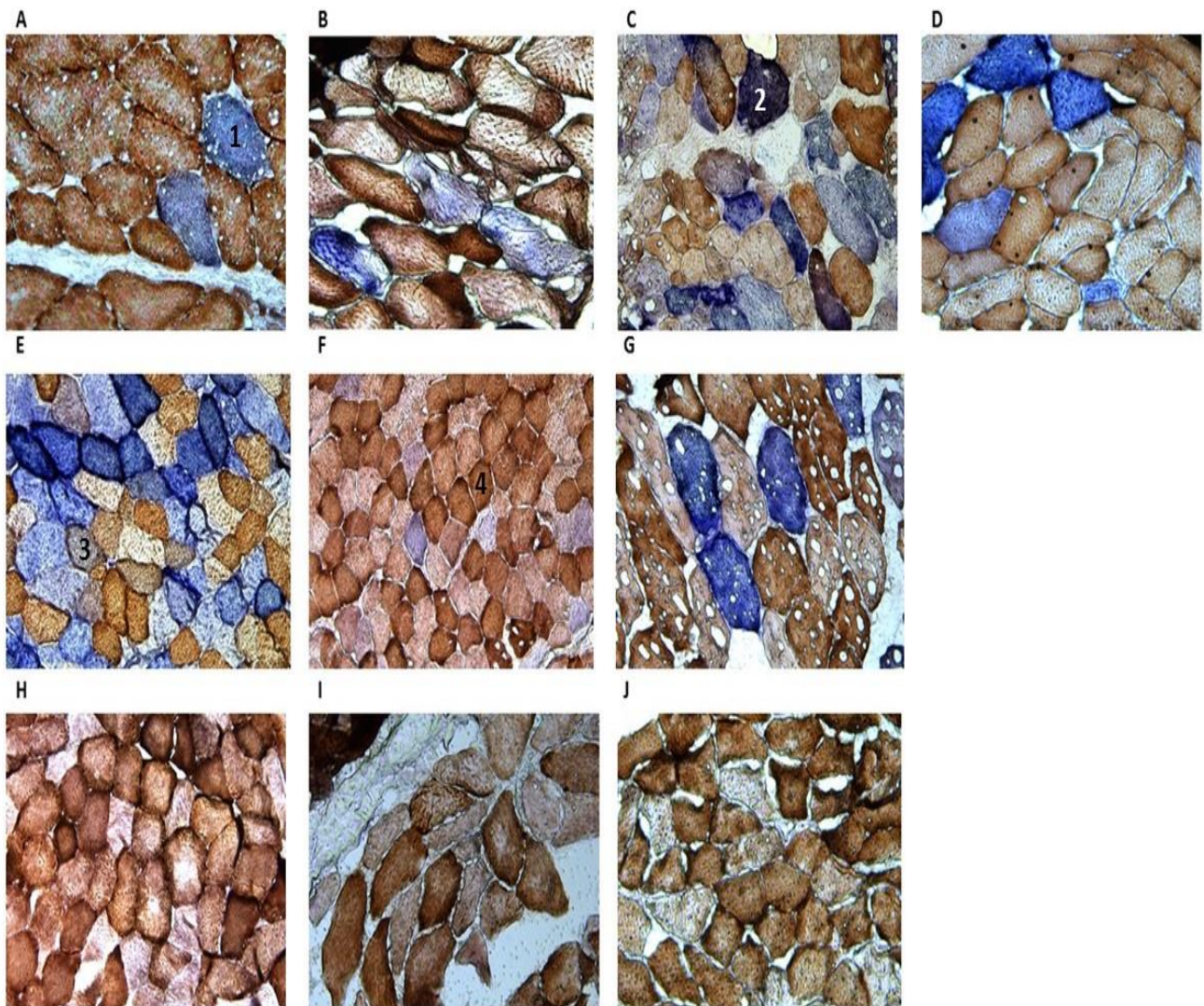


Figure 12. Biopsy COX/SDH stain. A-Patient 1, COX negative fibre marked with number 1; B-Patient 2; C-Patient 3, RRB fibre marked with number 2; D-Patient 4; E-Patient 5, COX intermediate fibre marked with 3; F-Patient 6, COX positive fibre marked with 4; G-Patient 7; H-Control 1; I-Control 2;J-Control 3.

3. Levels of mtDNA deletions in patients with OPA1 mutations

We have assessed the deletion load by ddPCR in COX negative fibres (n=17), intermediate fibres (n=17) and COX positive fibres (n=27) from patients 1 and 2, both with mutations in OPA1 (Figure 13). Deletions were absent in two COX negative fibres from patient 1. The mean value of deletion load in COX negative fibres was 78.54% (SD=30.83). In intermediate fibres deletion load had lower values with a mean value of 29.22% (SD=39). COX positive fibres from OPA1 group did not harbour mtDNA deletions, with a mean value of deletion load of 0.2473% (SD=0.75). This value is not significantly different from values found in COX positive fibres from controls (n=105) with a mean of 0.5234% (SD=1.3).

4. Levels of mtDNA deletions in patients with POLG mutations

Patients 3 and 4 harboured mutations in POLG. We assessed deletion load in COX negative fibres (n=15) from these patients and found mean values of 81% (SD=13.3) (Figure 13). Among the COX negative fibres we also analysed the subcategory of ragged blue fibres (n=29). These fibres express the characteristic pattern of accumulation of abnormal mitochondria (massive proliferation and enlargement of mitochondria) that visually distinguishes them among the COX negative cells (Figure 12). The SDH reaction product is deep blue, with apparent dark blue fibre edges. These fibres usually express the highest levels of mtDNA deletions, as confirmed by our findings, being the mtDNA deletions mean value of 94.06% (Figure 14). Intermediate fibres (n=35) had deletion loads with mean values of 65.04% (SD=27.07). COX positive fibres from the POLG group (n=69) did not harbour mtDNA deletions, having a mean value for deletion load of 2.09% (SD=4) with no significant difference compared to controls.

5. Levels of mtDNA deletions in patients with single deletions

Patients 5, 6, and 7 had sporadic single deletion pathology. COX negative fibres (n=37) accumulate mtDNA deletions with a mean value of 93.08% (SD=5.38), while RRBs (n=23) have a mean value of 96.79% (SD=1.43). Intermediate cells bear mtDNA deletions with a mean value of 80.52% (SD=12.5). Surprisingly, more than 50%, 27 of 55 COX positive fibres, in the single deletion patient group harbour mtDNA deletions at variable percentages (Mean= 15.8% SD=25).

6. Comparison of mtDNA deletion accumulation in all patient groups

We observed that deletion levels in COX negative fibres from single deletion patients are significantly higher ($P<0.05^*$) than in OPA1 and POLG patients, with a mean value of 93.08% of deletions respect to

78.5% and 81%. There were no significant differences between deletion levels of COX negative cells in OPA1 and POLG patients. Considering the RRB subcategory of COX negative fibres, that we found only in POLG and single deletion groups, there was a significant difference between the two groups ($P < 0.05^*$), with higher percentages of deletion loads in the single deletion patients (Fig.14).

The intermediate fibres still have COX activity, but they are close to passing the threshold level for becoming COX negative. It is known that threshold levels are variable between the different tissue types. Interestingly, we have observed that threshold levels are different at the single fibre level as well. Load of mtDNA deletions in single fibres varies in each phenotype group from a mean value of 29.2% in the OPA1 patients, 65.04% in POLG patients and 80.5% in single deletion patients. Again, the accumulation patterns of mtDNA deletions were significantly different ($p < 0.0001^{***}$) when the three groups are compared.

As COX positive fibres are considered to be healthy and have unchanged OXPHOS activity, these cells are not usually analysed. However, there are few valuable studies that have sampled COX positive fibres, and described the presence of low levels of mtDNA deletions (Yu-Wai Man, 2010). Since all these studies were done with qPCR and used external standards in the form of plasmids, these low levels of mtDNA deletions were often assigned to qPCR error. We applied the ddPCR to a significant number of COX positive fibres collected from patients and healthy controls. In total we examined 265 COX positive cells from healthy controls and patients. We found that in COX positive cells from single deletion patients there was a significant accumulation of mtDNA deletions when compared with both POLG and OPA1 patients and the healthy control group ($P < 0.0001^{***}$)(Fig. 13). Remarkably, more than 50% of all examined COX positive cells from single deletion patients, harboured the mtDNA deletions in various amounts.

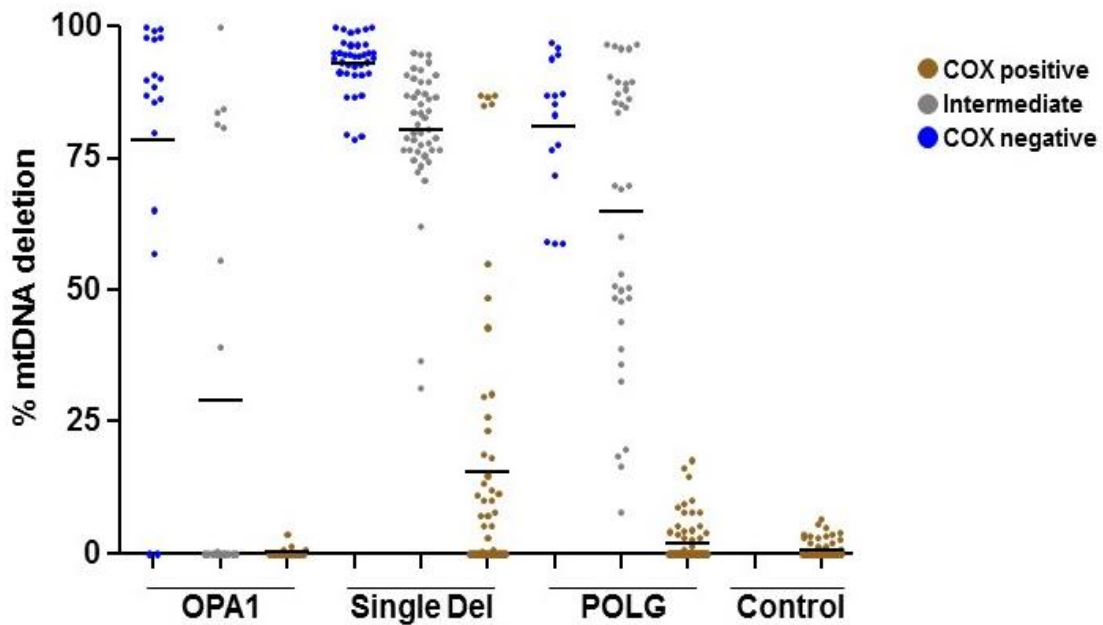


Figure 13. Percentages of mtDNA deletions obtained with ddPCR in COX positive, COX negative and intermediate fibres across all patient groups and controls. Highest levels of mtDNA deletions in COX positive (brown dots), COX negative (blue dots) and intermediate fibres (grey dots) are observed in single deletion group. All measurements are in triplicate. Mean values per each group of fibres are presented with black horizontal lines.

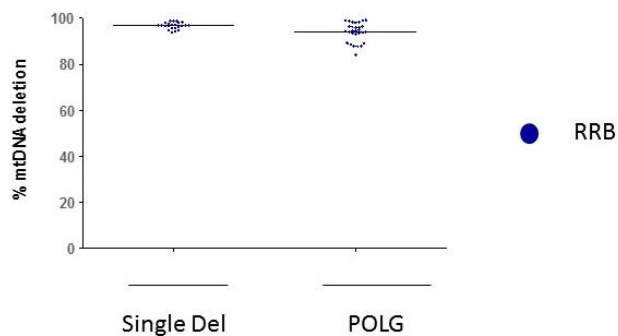


Figure 14. Percentages of mtDNA deletions obtained with ddPCR in RRB fibres. RRB type of fibres was present only in single deletion and POLG group. RRB fibres from single deletion group express the highest level of mtDNA deletions. All measurements are in triplicate. Mean values per each group of fibres are presented with black horizontal lines.

7. Deletion levels in longitudinal biopsy sections

As discussed earlier, we successfully obtained longitudinal sections from three muscle biopsies (patient 1, patient 4 and patient 5), representing one patient per group. This is due to difficulties in cutting single sections from end to end of the extensive segments of an individual muscle fibre, thus requiring a larger biopsy that was frozen and kept under optimal conditions.

In our study, the longitudinal fibres analysis strengthened the results previously observed with cross-sectioned fibres. Again, the single deletions group had the highest total levels of deletions in COX negative parts of fibres (mean=87.32%) as compared with POLG (mean=56.34%) and OPA1 (mean=76.88%). Similar results were found in COX positive parts (Single deletion mean=42.78%, POLG=16.19% and OPA1=1.5%). The results are summarized in figure 15.

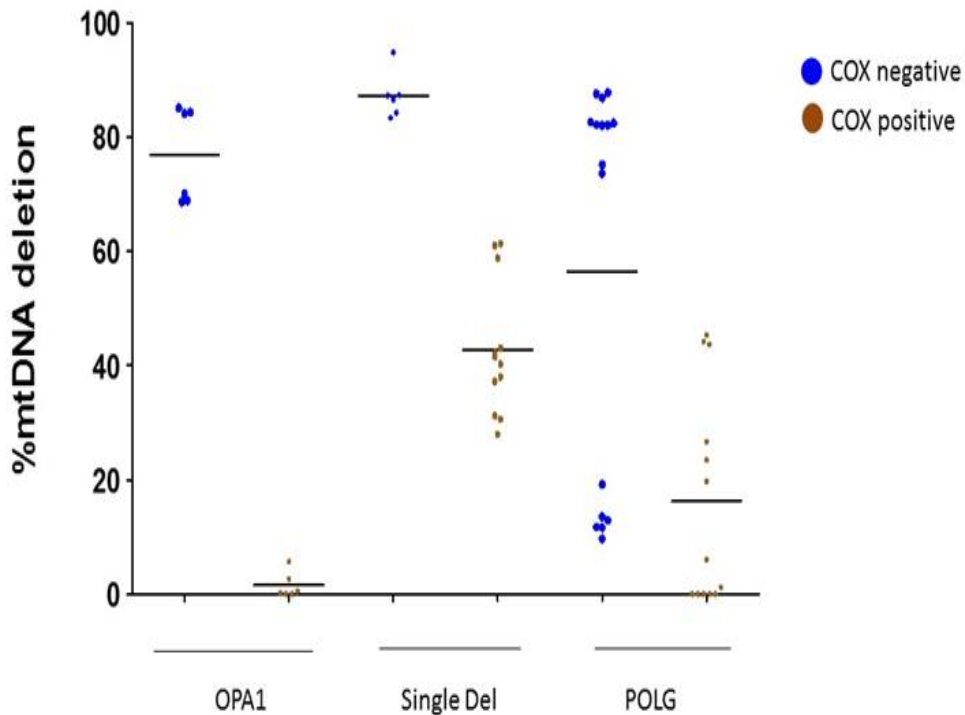


Figure 15. Percentages of mtDNA deletions in longitudinal fibres obtained by ddPCR. Highest load of mtDNA deletions is in COX negative parts of fibre (blue dots) from single deletion group. All measurements are in triplicate. Mean values per each group of fibres are presented with black horizontal lines.

In the case of POLG and OPA1 the areas of COX negativity were more localized, whereas in single deletion longitudinal fibres we noticed a wider dispersion of the COX negative domain (Fig.16). It was challenging to select fibres that contained both COX negative and COX positive zones and, at the same time, did not show blue staining across the entire fibre. To be sure that we collected truly COX positive zones in single deletion biopsy, we sampled the entire COX positive fibres that had no COX negative parts. We found a significant amount of mtDNA deletions in two entirely different COX positive longitudinal fibres (fibre 1: mean 29.96 %; fiber2: mean 60.38% mtDNA deletion).

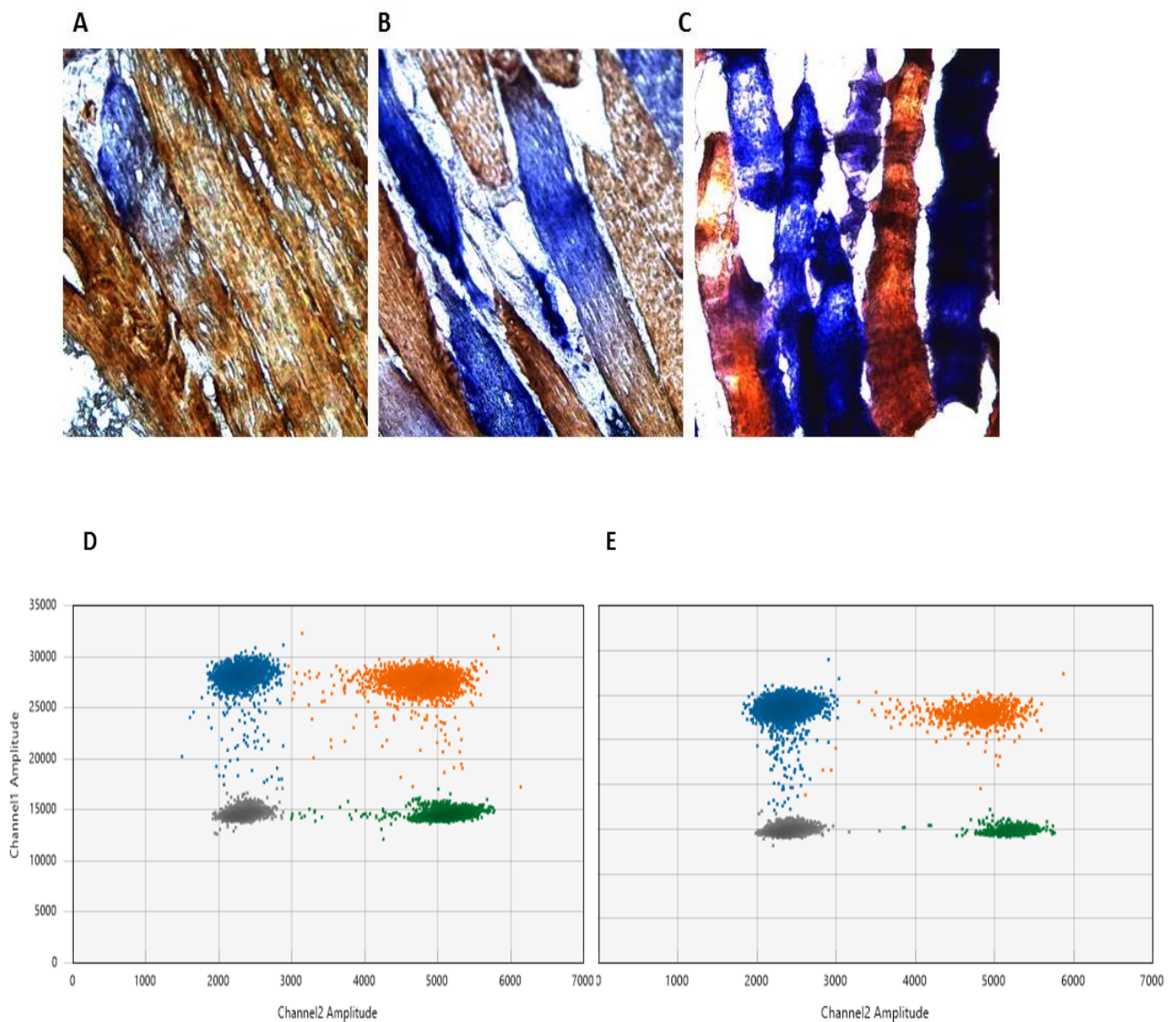


Figure 16. Representative images of longitudinal biopsy sectioning and 2D ddPCR plots. (A) Longitudinal biopsy section from patient 1 with OPA1 mutation. (B) Longitudinal biopsy section from patient 3 with

POLG mutation. (C) Longitudinal biopsy section from patient 5 with single deletion. (D) 2D ddPCR plot of COX negative part of fibre from patient 1. (E) 2D ddPCR plot of COX positive part of fibre from patient 1; blue dots represent ND1 positive droplets; green dots represent ND4 positive droplets; orange dots represent double positive droplets; grey dots represent empty droplets.

8. MtDNA copy number levels show mtDNA proliferation in certain fibre types

We compared total mtDNA copy per μm^2 between different fibre types and control fibres. MtDNA copy number was variable in the control group, ranging from 0.36 to 3.59 copies copies/ μm^2 with mean values 1.71. This variability was also observed between our patients from all groups. This variability can be due to differences in metabolic activity, as it is well established that skeletal muscle is a highly adaptable tissue and that mtDNA density can be increased as a consequence of physical activity (Adhihetty, 2007). However, our results indicate that COX negative, RRB and intermediate fibres from the single deletion group showed significant increase in mtDNA density compared to healthy controls, similar to what we observed in RRB fibres from the POLG group. COX positive fibres from all groups as well as COX negative and intermediate fibres from POLG and OPA1 groups, did show increased values compared to controls, but not in the extent to achieve statistical significance (Fig. 17).

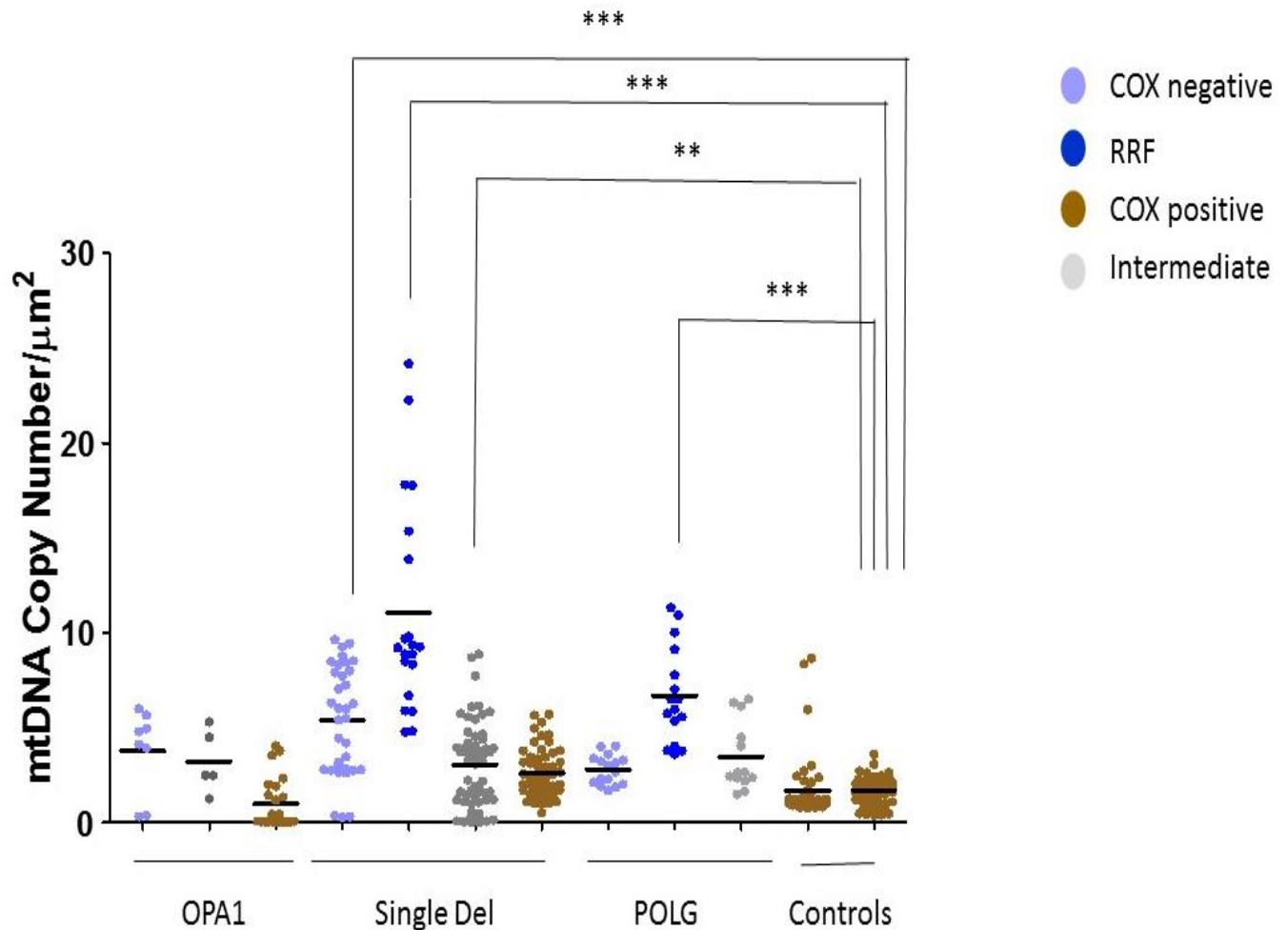


Figure 17. MtDNA copy number density per μm^2 , assessed by ddPCR. All measurements are in triplicate. Mean values per each group are presented with black horizontal lines. The calculated P-value is denoted as very significant (**) with $P = 0.001$ to 0.01 and extremely significant (***) when the P-value is less than 0.001 , when compared with the controls group.

9. Single cell long range PCR confirms presence of mtDNA deletions

To verify our findings in COX positive fibres from single deletion patients obtained with ddPCR, we used long-range PCR to amplify DNA extracted from longitudinal fibres. As discussed previously, long range PCR is not a quantitative method because of the preferential amplification of smaller mtDNA molecules. However, it was confirmatory to show the presence or absence of mtDNA deletions, especially considering the ddPCR results from COX positive cells in single deletion samples. Long range PCR analysis confirmed the presence of mtDNA deletions in single deletion COX positive cells (Fig. 18).

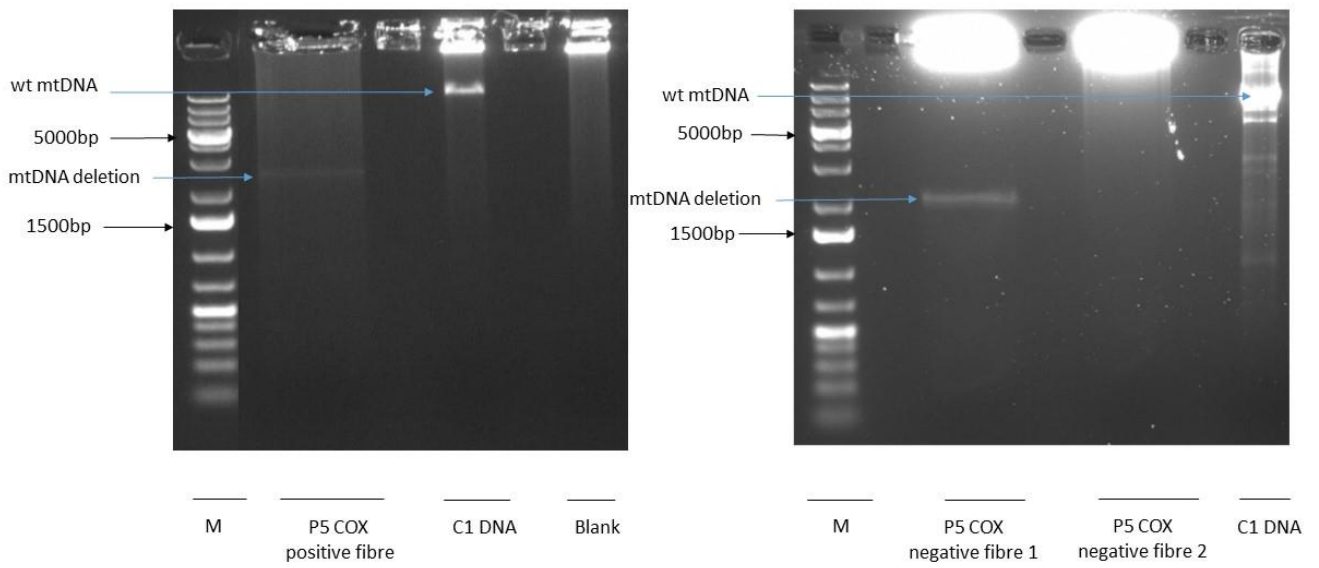


Figure 18. Single cell long range PCR. Representative images for detection of deleted mtDNA in single fibres from a single deletion P5 and DNA from muscle of control 1 by long range PCR. The positions of deleted and wild type (wt) mtDNA are indicated by blue arrows.

DISCUSSION

The single, large-scale mtDNA deletions were the first mutations of the mtDNA linked with human disease (Holt, 1988). However, almost 30 years upon their discovery many questions remain to be answered. Beside the mechanisms that lead to the formation and expansion of both multiple and single mtDNA deletions, the nature of the single mtDNA deletions inheritance remains “*terra incognita*” (DiMauro, 2013). Considering the few documented cases of maternal transmission and the large majority of cases described as sporadic, it remains difficult to conclude if these mtDNA mutations are early *de novo* somatic events occurring at any post-fertilization stage during embryogenesis, or they are inherited through the maternal germline, undergoing occasional expansion in single primary oocytes (Carelli and Chan, 2014). If they are *de novo* events, at which time point in embryonic development do they arise and what are the determining factors for their later clonal expansion? However, if they were transmitted through the maternal germline, than the bottleneck theory would explain why mothers and maternal relatives of affected children are healthy. Absence or very low loads of mtDNA deletions in fast dividing cells like blood cells, in conjunction with technical limitations and lack of highly sensitive approaches for their quantification, all contributed to the limited understanding we still have (Zeviani and Carelli, 2003). We designed our study to tackle the question of clonal expansion in single cells either of single or multiple deletions generated by different mechanisms. In particular besides patients with single deletions, we considered the two main causes of multiple deletions, i.e. defective mitochondrial dynamics as in the case of *OPA1* mutations and impaired fusion, or defective mtDNA maintenance as in the case of *POLG1* mutations with increased replicative errors. We first validated the novel ddPCR technique applied to quantitatively assess mtDNA deletions and then adapted this approach to be used in the setting of single cell quantification. The ddPCR quantification turned to be reliable and accurate, due to the partitioning of the mtDNA molecules to thousands of nanoliter sized droplets, with the PCR reaction taking place in each of them, ideally starting from a single mtDNA molecule per droplet. We then combined ddPCR with laser capturing microdissection on single muscle cells, to explore the dynamics of clonal expansion at the

single cell level, and in different domains of the same muscle fibre as revealed by the histoenzymatic staining defining where OXPHOS was deficient and where not. Our results introduce novel findings on the clonal expansion of deleted mtDNA molecules in single cells, highlighting different patterns of mtDNA deletions accumulation according to the different pathomechanisms assumed: single deletions, defective fusion (*OPA1* mutation) and defective mtDNA replication (*POLG* mutations). In particular, we observed that in single deletions patients the deleted mtDNA is present at variable heteroplasmic loads across all fibre types (COX positive, COX negative, RRBs and intermediate), at amounts significantly higher than in patients with multiple deletions (*OPA1* and *POLG*). This substantiates that the original deletion event occurred at a very early stage of embryonic development or even that is maternally transmitted via the germline. The distinctive feature of this study is that we have investigated the cell populations graded by histoenzymatic staining, both from patients and from control muscles. In this context we emphasize that the COX positive cells by definition do not suffer OXPHOS impairment. Consequently, the most remarkable result of this study is that in COX positive fibres from single deletion patients there is a substantial load of mtDNA deleted molecules, in some fibres reaching even high levels. This result was further confirmed when we analysed longitudinal fibres from the same patients, with high levels of mtDNA deletion even in the same COX positive fibres along its entire length. We also emphasize that this is the first study to investigate COX positive fibres from healthy controls. Earlier valuable studies on single muscle fibres investigated mtDNA deletions by quantitative PCR, in muscles from patients suffering single and multiple mtDNA deletions (He, 2002; Krishnan, 2007; Yu-Wai-Man, 2010; Rygel, 2014). Coming to our results on patients with mtDNA multiple deletions we have shown that COX positive fibres from *OPA1* patients did not accumulate mtDNA deletions being remarkably similar to controls. This is different from an earlier report on COX positive fibres from *OPA1* patients, which observed that the majority of COX positive fibres harboured low deletion levels, less than 30% (Yu-Wai-Man, 2010). The difference between the latter study and ours could be attributed to the different quantification methods, as with qPCR on blood from healthy controls we also observed the same low

values for mtDNA deletions, possibly artefacts. These artefacts may be explained with the necessity for external standards in quantitative PCR, resulting in false positive results. For validation of ddPCR we have tested a wide range of control DNA from blood and muscle (homogenate and single cells), and in all measurements the deletion levels were from 0-5%, indicating that ddPCR is a precise method for quantification of mtDNA deletions.

As part of mitochondrial biogenesis and turnover, mitochondria can undergo fission and fusion events, enabling the regulation of mtDNA copy number (Carelli, 2015). Mitochondrial inner membrane fusion is orchestrated by *OPA1* and pathogenic mutations in this gene are responsible for the majority of cases with autosomal dominant optic atrophy (DOA). Furthermore, *OPA1* plays a role in apoptosis, maintenance of crista junctions and was shown to be necessary for the stability of respiratory chain complexes (Cogliati, 2013). Discovery of mtDNA deletions in patients with *OPA1* mutations was an unexpected finding at the time, refocusing research toward the role of *OPA1* in mtDNA stability; the role of *OPA1* in nucleoid stabilization has been proposed. There is a substantial clinical heterogeneity in patients harbouring missense *OPA1* mutations affecting the GTPase domain of the protein, reflecting the deleterious effects of impaired fusion not only for the optic nerve, but also for the brain, peripheral nerves and skeletal muscle (Burte, 2015; Hudson 2008, Yu Wai Man, 2010; Elachouri, 2011).

Interestingly, our current results in the *OPA1* group of patients showed localised clonal expansion of mtDNA multiple deletions. In this case, the fusion defect seems to favour the clonal expansion of pre-existing deletions in single unfused mitochondria. On the other hand, these deletions seem to be insufficiently eliminated by mitophagy, when fusion is impaired. Our findings in the *OPA1* group of patients (Figure 13), especially the results from our longitudinal fibres analysis (Figure 15), substantially support the recently identified existence of mitochondrial domains in the skeletal muscle (Mishra, 2015). These domains are regulated by OXPHOS capacity and the length of these domains is controlled by fusion proteins, clearly pointing to involvement of fusion in the dynamics of clonal expansion (Mishra, 2015). This study observed that, as response to lower OXPHOS capacity caused by genetically-driven

dysfunction or due to ageing, mitochondrial fusion rates become reduced and these mitochondrial domains displaying the OXPHOS deficiency become longer in length, thus spreading in distinct areas that end up as COX-negative domains (Figure 19). Our study confirms this model for the first time in humans, as highlighted by our patients with *OPA1* mutation, where the fusion rates are lower, leading to COX-negative segments where the mtDNA deleted molecules expand, in contrast with the adjacent COX-positive domains where the amount of mtDNA deleted molecules is similar to controls. Thus, under this interpretation, in *OPA1* patients the fusion defect increases the probability of clonally expand pre-existing age-related mtDNA deletion, possibly in the absence of increased rate of mtDNA mutagenesis.

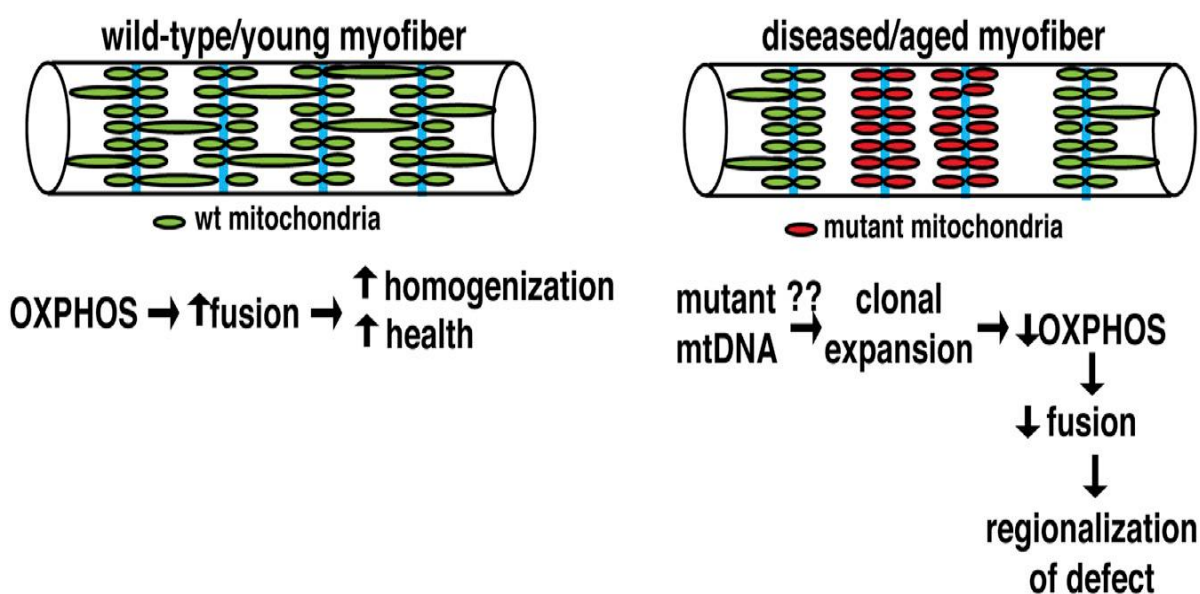


Figure 19. Model connecting the OXPHOS activity and mitochondrial fusion in promoting health and limiting the spread of mtDNA defects in myofibers (Left). In healthy myofiber, oxidative activity promotes fusion of mitochondria across the sarcomere, leading to partial homogenization of the organelle population along the longitudinal axis. Z-lines are depicted in blue. (Right) Clonal expansion of the mutated mtDNA outcomes in decreased OXPHOS activity. This decrease leads to lower local fusion rates, promoting compartmentalization and restraining the spread of the mutant mtDNA genome throughout the fibre (from Mishra, 2015).

POLG mutations cause a remarkable spectrum of clinical phenotypes. This is because *POLG* is the key enzyme involved in mtDNA replication and its mutations may lead to different molecular damage of mtDNA, including mtDNA base substitutions, deletions and depletion. The final result of these different mutations is a dysfunctional OXPHOS system. *POLG*-related disorders include both adult-onset mitochondrial diseases and childhood neurological disorders. (Horvath, 2006; Carelli and Chan, 2014).

In our study, patients with *POLG* mutation, due to the faulty mtDNA replication, which increases over time the pool of somatic deleted molecules, showed a tendency to clonally expand mtDNA deletions. This expansion is present at low levels also in the COX positive single muscle fibres, being at higher rate compared with control and *OPA1* groups, but significantly less than observed within single deletion patients (Figure 13). Obviously, the compensatory mtDNA biogenesis becomes particularly activated in the COX-negative and RRB fibres of both single deletion patients and *POLG* cases with the SANDO recessive syndrome, as revealed by our assessment of mtDNA copy number (Figure 17).

Altogether, our results lead to propose a model based on the hypothesis that efficiency of fusion is the key determining factor for regulating the dynamics and ultimately the final pattern of clonal expansion of deleted mtDNA. The difference between our model and the one proposed by Mishra in 2015, is that in the latter model the authors assumed that the OXPHOS defect reduces the levels of fusion that further lead to localized expansion of the mtDNA mutation. We may agree with the proposition that defective OXPHOS lowers the fusion rates. However, we do not know the exact threshold for defective OXPHOS after which the fusion activity becomes impaired. We propose that in patients that have mutations in the fusion *OPA1* gene, fusion is disrupted and expansion of pre-existing age-related mtDNA deletions is promoted, explaining the overall modest accumulation of mtDNA multiple deletions, with essentially similar load of mtDNA deletions as controls in the COX-positive domains of individual muscle fibres. Furthermore, because of the fusion defect, fusion rates are lower and this promotes also a compartmentalization and limits the spread of the mutant mtDNA genome. We propose that the patients with *POLG* mutations may have less severe downregulation in fusion. This may be because the OXPHOS dysfunction again lowers the fusion as proposed earlier (Mishra, 2015). Differently, the single deletion patients, in our study, show the widest dispersion of the mtDNA mutation across the muscle fibre, opposite to the patients with *OPA1* and *POLG* mutations. Consequently, it would be logical that fusion may become upregulated at some point in embryonic development. Under these, hypothetical, circumstances the upregulation of fusion would promote wider dispersion of the deleted mtDNA

molecules along the muscle fibers, overcoming the compartmentalization. Indeed, research of OPA1 protein levels during zebrafish embryonic development pointed out that certain isoforms of OPA1 are highly abundant while others may be markedly reduced at specific stages of embryonic development. The same research identified, by gene expression analysis, a 50% up-regulation of genes involved in regulating mitochondrial biogenesis (including *OPA1*) at specific time point during embryonic development (Rahn, 2013). Unfortunately, similar observations are not available for human embryos, as well as the information about possible fluctuations of fusion levels during oocyte maturation and in mature oocyte.

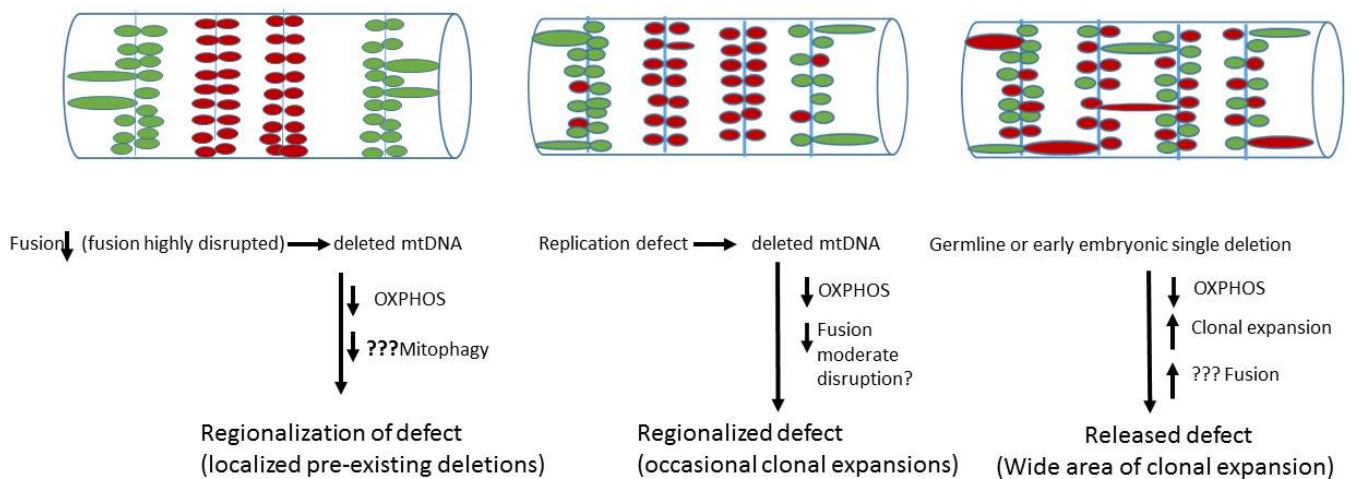


Figure 20. Model: clonal expansion patterns of mutated mtDNA. (Right) Myofibre appearance in patients with mutation in *OPA1* (fusion); due to mutations in fusion gene fusion is severely disrupted, this results in low fusion rates along longitudinal axis. Pre-existing mtDNA deletion remain localized. Due to presence of mtDNA deletion OXPHOS rates are lower. (Middle) Myofibre appearance in patients with mutations in *POLG* (disrupted replication and repair); Replication defect leads to significant accumulation of mtDNA deletions, lowering OXPHOS rates, fusion rates along longitudinal axis are less severe affected compared to when mutation in genes involved directly in fusion is present. Occasional fusion between wt mtDNA and deleted mtDNA along longitudinal axis may occur. (Left) Myofibre appearance in patients with single deletion; Clonal expansion in myofibre shows wide dispersion of mutated(deleted) mtDNA implying that fusion rates were high; promotion of fusion during certain stages of embryonic development may be the

reason why clonal expansion via fusion shows wide dispersion (Trifunov, unpublished figure, partially adapted from Mishra, 2015).

Thus, bearing in mind that clonal expansion plays a crucial role in spreading the mtDNA deletions and acts at the single cell level, it is of outmost importance to elaborate on strategies to counteract this mechanism. This study identified droplet digital PCR as a reliable method for heteroplasmy determination within single muscle cells. However, more experiments are needed prior to introduce this quantification strategy as a diagnostic procedure. Analysis of longitudinal muscle fibres is an elegant way to visualize and sample segments with clonally expanded mtDNA deletion fitting with the cell domain displaying the COX defect, and we believe it could have wider application to study the patterns of mtDNA deletion accumulation in different tissues, at the single cell level.

Finally, many questions regarding mtDNA deletions formation and subsequent clonal expansion wait to be further tackled. This study highlighted different patterns of mtDNA deletions accumulation by using for the first time the ddPCR on single muscle fibres. We are confident that new and more sensitive methods, like ddPCR, will ultimately provide answers in quantitative mitochondrial genetics, especially when it will be applied at the germline level, in primary oocytes, finally solving the origin of single mtDNA deletions.

REFERENCES

- Acin-Perez R, Enriquez JA. The function of the respiratory supercomplexes: The plasticity model. *Biochim Biophys Acta*. 2014; 1837:444-50.
- Adihetty PJ, Taivassalo T, Haller RG, Walkinshaw DR and Hood DA. The effect of training on the expression of mitochondrial biogenesis- and apoptosis-related proteins in skeletal muscle of patients with mtDNA defects. *Am. J. Physiol. Endocrinol. Metab.* 2007; 293, E672–E680.
- Agaronyan K, Morozov IY, Anikin M, Temiakov D. Replication-transcription switch in human mitochondria. *Science*. 2015; 548-551.
- Akhmedov AT, Marín-García J. Mitochondrial DNA maintenance: an appraisal. *Mol Cell Biochem*. 2015; 409:283-305.
- Altmann, R. *Die Elementarorganismen und ihre Beziehungen zu den Zellen*. Verlag Von Veit & Comp. 1890.
- Amati-Bonneau P, Valentino ML, Reynier P, Gallardo ME, Bornstein B, Boissiere A, Campos Y, Rivera H, de la Aleja JG, Carroccia R, Iommarini L, Labauge P, Figarella-Branger D, Marcorelles P, Furby A, Beauvais K, Letournel F, Liguori R, La Morgia C, Montagna P, Liguori M, Zanna C, Rugolo M, Cossarizza A, Wissinger B, Verny C, Schwarzenbacher R, Martín MA, Arenas J, Ayuso C, Garesse R, Lenaers G, Bonneau D, Carelli V. OPA1 mutations induce mitochondrial DNA instability and optic atrophy plus phenotypes. *Brain*. 2008; 131, 338–351.
- An J, Shi J, He Q, Lui K, Liu Y, Huang Y, Sheikh MS. CHM1/CHCHD6, a novel mitochondrial protein linked to regulation of mitofilin and mitochondrial cristae morphology. *J Biol Chem*. 2012; 287:7411-26.
- Anderson S, Bankier AT, Barrell BG, de Bruijn MH, Coulson AR, Drouin J, Eperon IC, Nierlich DP, Roe BA, Sanger F, Schreier PH, Smith AJ, Staden R, Young IG. Sequence and organization of the human mitochondrial genome. *Nature*. 1981; 290:457-65.

Ballinger SW, Shoffner JM, Hedaya EV, Trounce I, Polak MA, Koontz DA, Wallace DC. Maternally transmitted diabetes and deafness associated with a 10.4 kb mitochondrial DNA deletion. *Nat Genet.* 1992; 11-5.

Ballinger SW, Shoffner JM, Gebhart S, Koontz DA, Wallace DC. Mitochondrial diabetes revisited. *Nat Genet.* 1994; 458-9.

Bank C, Soulimane T, Schroder JM, Buse G, Zanssen S. Multiple deletions of mtDNA remove the light strand origin of replication. *Biochem. Biophys. Res. Commun.* 2000; 595–601.

Bannwarth S, Ait-El-Mkadem S, Chausseot A, Genin EC, Lacas-Gervais S, Fragaki K, Berg-Alonso L, Kageyama Y, Serre V, Moore DG, Verschueren A, Rouzier C, Le Ber I, Augé G, Cochaud C, Lespinasse F, N'Guyen K, de Septenville A, Brice A, Yu-Wai-Man P, Sesaki H, Pouget J, Paquis-Flucklinger V. A mitochondrial origin for frontotemporal dementia and amyotrophic lateral sclerosis through CHCHD10 involvement. *Brain.* 2014; 2329-45.

Belmonte FR, Martin JL, Frescura K, Damas J, Pereira F, Tarnopolsky MA, Kaufman BA. Digital PCR methods improve detection sensitivity and measurement precision of low abundance mtDNA deletions. *Sci Rep.* 2016; 6:25186.

Bernes SM, Bacino C, Prezant TR, Pearson MA, Wood TS, Fournier P, Fischel-Ghodsian N. Identical mitochondrial DNA deletion in mother with progressive external ophthalmoplegia and son with Pearson marrow-pancreas syndrome. *J Pediatr.* 1993; 123:598.

Blakely EL, He L, Taylor RW, Chinnery PF, Lightowlers RN, Schaefer AM, Turnbull DM. Mitochondrial DNA deletion in "identical" twin brothers. *J Med Genet.* 2004 Feb; 41(2):e19.

Boczonadi V, Horvath R. Mitochondria: impaired mitochondrial translation in human disease. *Int J Biochem Cell Biol.* 2014; 77-84.

Bogenhagen DF, Sakonju S, Brown DD. A control region in the center of the 5S RNA gene directs specific initiation of transcription: II. The 3' border of the region. *Cell.* 1980; 27-35.

Bogehagen DF, Rousseau D, Burke S. The layered structure of human mitochondrial DNA nucleoids. *J Biol Chem.* 2008; 283:3665-75.

Bogehagen DF. Mitochondrial DNA nucleoid structure. *Biochim Biophys Acta.* 2012; 1819: 914-20.

Bowmaker M, Yang MY, Yasukawa T, Reyes A, Jacobs HT, Huberman JA, Holt IJ. Mammalian mitochondrial DNA replicates bidirectionally from an initiation zone. *J Biol Chem.* 2003; 278:50961-9.

Brenner CA, Wolny YM, Barritt JA, Matt DW, Munné S, Cohen J. Mitochondrial DNA deletion in human oocytes and embryos. *Mol Hum Reprod.* 1998;4:887-92.

Brown, R. On the organs and mode of fecundation in Orchideae and Asclepiadeae. *Trans. Linn. Soc. Lond.* 1833; 16:685-745.

Brown TA, Clayton DA. Genesis and wanderings: origins and migrations in asymmetrically replicating mitochondrial DNA. *Cell Cycle.* 2006; 5:917-21.

Burke N, Hall AR, Hausenloy DJ. OPA1 in Cardiovascular Health and Disease. *Curr Drug Targets.* 2015; 912-20.

Burté F, Carelli V, Chinnery PF, Yu-Wai-Man P. Disturbed mitochondrial dynamics and neurodegenerative disorders. *Nat Rev Neurol.* 2015; 11-24.

Campbell G, Krishnan KJ, Deschauer M, Taylor RW, Turnbull DM. Dissecting the mechanisms underlying the accumulation of mitochondrial DNA deletions in human skeletal muscle. *Hum Mol Genet.* 2014; 23:4612-20.

Carelli V, Maresca A, Caporali L, Trifunov S, Zanna C, Rugolo M. Mitochondria: Biogenesis and mitophagy balance in segregation and clonal expansion of mitochondrial DNA mutations. *Int J Biochem Cell Biol.* 2015; 63:21-4.

Carelli V, Musumeci O, Caporali L, Zanna C, La Morgia C, Del Dotto V, Porcelli AM, Rugolo M, Valentino ML, Iommarini L, Maresca A, Barboni P, Carbonelli M, Trombetta C, Valente EM, Patergnani S, Giorgi C, Pinton P, Rizzo G, Tonon C, Lodi R, Avoni P, Liguori R, Baruzzi A, Toscano A, Zeviani M.

Carelli V. Keeping in shape the dogma of mitochondrial DNA maternal inheritance. *PLoS Genet.* 2015; 11(5):e1005179.

Carelli V, Chan DC. Mitochondrial DNA: impacting central and peripheral nervous systems. *Neuron.* 2014; 84:1126-42.

Cerritelli SM, Frolova EG, Feng C, Grinberg A, Love PE, Crouch RJ. Failure to produce mitochondrial DNA results in embryonic lethality in *Rnaseh1* null mice. *Mol Cell.* 2003; 11:807-15.

Chan DC. Fusion and fission: interlinked processes critical for mitochondrial health. *Annu Rev Genet.* 2012; 46:265–287

Chang DD, Clayton DA. Priming of human mitochondrial DNA replication occurs at the light-strand promoter. *Proc Natl Acad Sci U S A.* 1985; 82:351-5.

Chen X, Prosser R, Simonetti S, Sadlock J, Jagiello G, Schon EA. Rearranged mitochondrial genomes are present in human oocytes. *Am J Hum Genet.* 1995;57:239-47.

Chen H, Detmer SA, Ewald AJ, Griffin EE, Fraser SE, Chan DC. Mitofusins Mfn1 and Mfn2 coordinately regulate mitochondrial fusion and are essential for embryonic development. *J Cell Biol.* 2003; 160:189-200.

Chen H, Vermulst M, Wang YE, Chomyn A, Prolla TA, McCaffery JM, Chan DC. Mitochondrial fusion is required for mtDNA stability in skeletal muscle and tolerance of mtDNA mutations. *Cell.* 2010; 141:280-9.

Chinnery PF, Elliott HR, Hudson G, Samuels DC, Relton CL. Epigenetics, epidemiology and mitochondrial DNA diseases. *Int J Epidemiol.* 2012; 41:177-87.

Christianson TW, Clayton DA. A tridecamer DNA sequence supports human mitochondrial RNA 3'-end formation in vitro. *Mol Cell Biol.* 1988; 4502-9.

Cipolat S, Martins de Brito O, Dal Zilio B, Scorrano L. OPA1 requires mitofusin 1 to promote mitochondrial fusion. *Proc Natl Acad Sci USA.* 2004; 101:15927-32.

Clayton DA. Replication of animal mitochondrial DNA. *Cell.* 1982; 28:693-705.

- Clayton DA. Replication and transcription of vertebrate mitochondrial DNA. *Annu Rev Cell Biol.* 1991; 7:453-78.
- Cogliati S, Frezza C, Soriano ME, Varanita T, Quintana-Cabrera R, Corrado M, Cipolat S, Costa V, Casarin A, Gomes LC, Perales-Clemente E, Salviati L, Fernandez-Silva P, Enriquez JA, Scorrano L. Mitochondrial cristae shape determines respiratory chain supercomplexes assembly and respiratory efficiency. *Cell.* 2013; 155:160-71.
- Cogliati S, Enriquez JA, Scorrano L. Mitochondrial Cristae: Where Beauty Meets Functionality. *Trends Biochem Sci.* 2016; 261-73.
- Couvillion MT, Soto IC, Shipkovenska G, Churchman LS. Synchronized mitochondrial and cytosolic translation programs. *Nature.* 2016; 533(7604):499-503.
- Copeland WC. Defects in mitochondrial DNA replication and human disease. *Crit Rev Biochem Mol Biol.* 2012; 47:64-74.
- Corral-Debrinski M, Horton T, Lott MT, Shoffner, JM, Beal, MF and Wallace, DC. Mitochondrial DNA deletions in human brain: regional variability and increase with advanced age. *Nature Genet.* 1992; 2, 324–329.
- Damas J, Samuels DC, Carneiro J, Amorim A, Pereira F. Mitochondrial DNA rearrangements in health and disease—a comprehensive study. *Hum Mutat.* 2014; 35:1-14.
- Damas J, Carneiro J, Amorim A, Pereira F. MitoBreak: the mitochondrial DNA breakpoints database. *Nucleic Acids Res.* 2014 Jan; 42(Database issue):D1261-8.
- De Grey AD. A proposed refinement of the mitochondrial free radical theory of aging. *Bioessays.* 1997; 19:161-6.
- Diaz, F., Bayona-Bafaluy, M. P., Rana, M., Mora, M., Hao, H., & Moraes, C. T. Human mitochondrial DNA with large deletions repopulates organelles faster than full-length genomes under relaxed copy number control. *Nucleic Acids Research.* 2002; 4626–4633.

- DiMauro S, Schon EA, Carelli V, Hirano M. The clinical maze of mitochondrial neurology. *Nat Rev Neurol*. 2013; 9(8):429-44.
- Dölle C, Flønes I, Nido, GS, Miletic, H, Osuagwu, N, Kristoffersen, S, Lilleng PK, Petter Larsen J, Ole-Bjørn T, Haugarvoll K, Bindoff L, Tzoulis C. Defective mitochondrial DNA homeostasis in the substantia nigra in Parkinson disease. *Nat Commun*. 2016; 7: 13548.
- Dorn II GW. Mitochondrial dynamism and heart disease: changing shape and shaping change. *EMBO Mol Med*. 2015; 7: 865–877.
- Dorn GW, Kitsis RN. The mitochondrial dynamism-mitophagy-cell death interactome: multiple roles performed by members of a mitochondrial molecular ensemble. *Circ Res*. 2015; 116:167-82.
- Elachouri G, Vidoni S, Zanna C, Pattyn A, Boukhaddaoui H, Gaget K, Yu-Wai-Man P, Gasparre G, Sarzi E, Delettre C, Olichon A, Loiseau D, Reynier P, Chinnery PF, Rotig A, Carelli V, Hamel CP, Rugolo M, Lenaers G. OPA1 links human mitochondrial genome maintenance to mtDNA replication and distribution. *Genome Res*. 2011; 21:12-20.
- El-Hattab AW, Craigen WJ, Scaglia F. Mitochondrial DNA maintenance defects. *Biochim Biophys Acta*. 2017; S0925-4439(17)30058-3.
- Elson JL, Samuels DC, Johnson MA, Turnbull DM, Chinnery PF. The length of cytochrome c oxidase-negative segments in muscle fibres in patients with mtDNA myopathy. *Neuromuscul Disord*. 2002 Nov; 12(9):858-64.
- Elson JL, Samuels DC, Turnbull DM, Chinnery PF. Random intracellular drift explains the clonal expansion of mitochondrial DNA mutations with age. *Am J Hum Genet*. 2001; 68(3):802-6.
- Elstner M, Turnbull DM. Transcriptome analysis in mitochondrial disorders. *Brain Res Bull*. 2012; 88(4):285-93.
- Ernster L, Schatz G. Mitochondria: a historical review. *J Cell Biol*. 1981; 91(3 Pt 2):227s-255s.
- Falkenberg M, Larsson NG, Gustafsson CM. DNA replication and transcription in mammalian mitochondria. *Annu Rev Biochem*. 2007; 76:679-99.

- Fernandez-Silva P, Enriquez JA, Montoya J. Replication and transcription of mammalian mitochondrial DNA. *Exp Physiol*. 2003; 88:41-56.
- Frey TG and Mannella CA. The internal structure of mitochondria. *Trends Biochem Sci*. 2000; 25:319-324.
- Frezza C, Cipolat S, Martins de Brito O, Micaroni M, Beznoussenko GV, Rudka T, Bartoli D, Polishuck RS, Danial NN, De Strooper B, Scorrano L. OPA1 controls apoptotic cristae remodeling independently from mitochondrial fusion. *Cell*. 2006; 126(1):177-89.
- Fukui H, Moraes CT. The mitochondrial impairment, oxidative stress and neurodegeneration connection: reality or just an attractive hypothesis? *Trends Neurosci*. 2008; 31(5):251-6.
- Fukui H, Moraes CT. Mechanisms of formation and accumulation of mitochondrial DNA deletions in aging neurons. *Hum Mol Genet*. 2009; 18(6):1028-36.
- Miralles Fusté J, Shi Y, Wanrooij S, Zhu X, Jemt E, Persson Ö, Sabouri N, Gustafsson CM, Falkenberg M. In vivo occupancy of mitochondrial single-stranded DNA binding protein supports the strand displacement mode of DNA replication. *PLoS Genet*. 2014; 10(12):e1004832.
- Garone C, Rubio JC, Calvo SE, Naini A, Tanji K, Dimauro S, Mootha VK, Hirano M. MPV17 Mutations Causing Adult-Onset Multisystemic Disorder With Multiple Mitochondrial DNA Deletions. *Arch Neurol*. 2012; 69(12):1648-51.
- Genuario R, Wong TW. Stimulation of DNA polymerase gamma by a mitochondrial single-strand DNA binding protein. *Cell Mol Biol Res*. 1993; 39(7):625-34.
- Giles RE, Blanc H, Cann HM, Wallace DC. Maternal inheritance of human mitochondrial DNA. *Proc Natl Acad Sci U S A*. 1980; 77(11):6715-9.
- Gómez-Durán A, Pacheu-Grau D, López-Gallardo E, Díez-Sánchez C, Montoya J, López-Pérez MJ, Ruiz-Pesini E. Unmasking the causes of multifactorial disorders: OXPHOS differences between mitochondrial haplogroups. *Hum Mol Genet*. 2010; 19(17):3343-53.

Gorman GS, Pfeffer G, Griffin H, Blakely EL, Kurzawa-Akanbi M, Gabriel J, Sitarz K, Roberts M, Schoser B, Pyle A, Schaefer AM, McFarland R, Turnbull DM, Horvath R, Chinnery PF, Taylor RW. Clonal expansion of secondary mitochondrial DNA deletions associated with spinocerebellar ataxia type 28. *JAMA Neurol.* 2015; 72(1):106-11.

Grady JP, Campbell G, Ratnaike T, Blakely EL, Falkous G, Nesbitt V, Schaefer AM, McNally RJ, Gorman GS, Taylor RW, Turnbull DM, McFarland R. Disease progression in patients with single, large-scale mitochondrial DNA deletions. *Brain.* 2014; 137(Pt 2):323-34.

Gray H, Wong TW. Purification and identification of the human mitochondrial polymerase. *J. Biol. Chem.* 1992; 5835-5841.

Griparic L, van der Blik AM. The many shapes of mitochondrial membranes. *Traffic.* 2001; 2(4):235-44.

Hance N, Ekstrand MI, Trifunovic A. Mitochondrial DNA polymerase gamma is essential for mammalian embryogenesis. *Hum Mol Genet.* 2005; 14(13):1775-83.

He L, Chinnery PF, Durham SE, Blakely EL, Wardell TM, Borthwick GM, Taylor RW, Turnbull DM. Detection and quantification of mitochondrial DNA deletions in individual cells by real-time PCR. *Nucleic Acids Res.* 2002; 30(14):e68.

Hindson BJ, Ness KD, Masquelier DA, Belgrader P, Heredia NJ, Makarewicz AJ, Bright IJ, Lucero MY, Hiddessen AL, Legler TC, Kitano TK, Hodel MR, Petersen JF, Wyatt PW, Steenblock ER, Shah PH, Bousse LJ, Troup CB, Mellen JC, Wittmann DK, Erndt NG, Cauley TH, Koehler RT, So AP, Dube S, Rose KA, Montesclaros L, Wang S, Stumbo DP, Hodges SP, Romine S, Milanovich FP, White HE, Regan JF, Karlin-Neumann GA, Hindson CM, Saxonov S, Colston BW. High-throughput droplet digital PCR system for absolute quantitation of DNA copy number. *Anal Chem.* 2011 Nov 15; 83(22):8604-10

Holt IJ, Cooper JM, Morgan-Hughes JA, Harding AE. Deletions of muscle mitochondrial DNA. *Lancet.* 1988 Jun 25; 1(8600):1462.

Holt IJ, Lorimer HE, Jacobs HT. Coupled leading- and lagging-strand synthesis of mammalian mitochondrial DNA. *Cell.* 2000; 100(5):515-24.

- Horvath R, Hudson G, Ferrari G, Fütterer N, Ahola S, Lamantea E, Prokisch H, Lochmüller H, McFarland R, Ramesh V, Klopstock T, Freisinger P, Salvi F, Mayr JA, Santer R, Tesarova M, Zeman J, Udd B, Taylor RW, Turnbull D, Hanna M, Fialho D, Suomalainen A, Zeviani M, Chinnery PF. Phenotypic spectrum associated with mutations of the mitochondrial polymerase gamma gene. *Brain*. 2006; 129(Pt 7):1674-84.
- Hudson G, Amati-Bonneau P, Blakely EL, Stewart JD, He L, Schaefer AM, Griffiths PG, Ahlqvist K, Suomalainen A, Reynier P, McFarland R, Turnbull DM, Chinnery PF, Taylor RW. Mutation of OPA1 causes dominant optic atrophy with external ophthalmoplegia, ataxia, deafness and multiple mitochondrial DNA deletions: a novel disorder of mtDNA maintenance. *Brain*. 2008; 131(Pt 2):329-37.
- Hudson G, Chinnery PF. Mitochondrial DNA polymerase-gamma and human disease. *Hum Mol Genet*. 2006; 15 Spec No 2:R244-52.
- Kaguni LS. DNA polymerase gamma, the mitochondrial replicase. *Annu Rev Biochem*. 2004; 73:293-320.
- Kazuno AA, Munakata K, Nagai T, Shimosono S, Tanaka M, Yoneda M, Kato N, Miyawaki A, Kato T. Identification of mitochondrial DNA polymorphisms that alter mitochondrial matrix pH and intracellular calcium dynamics. *PLoS Genet*. 2006; 2(8):e128.
- Kolesnikov AA. The Mitochondrial Genome. *The Nucleoid*. *Biochemistry (Mosc)*. 2016; 81(10):1057-1065
- Korhonen JA, Gaspari M, Falkenberg M. TWINKLE Has 5' to 3' DNA helicase activity and is specifically stimulated by mitochondrial single-stranded DNA-binding protein. *J Biol Chem*. 2003; 278(49):48627-32.
- Korhonen JA, Pham XH, Pellegrini M, Falkenberg M. Reconstitution of a minimal mtDNA replisome in vitro. *EMBO J*. 2004; 23(12):2423-9.
- Koopman WJ, Distelmaier F, Smeitink JA, Willems PH. OXPHOS mutations and neurodegeneration. *EMBO J*. 2013; 32(1):9-29.
- Kornblum C, Nicholls TJ, Haack TB, Schöler S, Peeva V, Danhauser K, Hallmann K, Zsurka G, Rorbach J, Iuso A, Wieland T, Sciacco M, Ronchi D, Comi GP, Moggio M, Quinzii CM, DiMauro S, Calvo SE, Mootha VK, Klopstock

- T, Strom TM, Meitinger T, Minczuk M, Kunz WS, Prokisch H. Loss-of-function mutations in MGME1 impair mtDNA replication and cause multisystemic mitochondrial disease. *Nat Genet.* 2013; 45(2):214-9.
- Kraytsberg Y, Kudryavtseva E, McKee AC, Geula C, Kowall NW, Khrapko K. Mitochondrial DNA deletions are abundant and cause functional impairment in aged human substantia nigra neurons. *Nat Genet.* 2006; 38(5):518-20.
- Krishnan KJ1, Bender A, Taylor RW, Turnbull DM. A multiplex real-time PCR method to detect and quantify mitochondrial DNA deletions in individual cells. *Anal Biochem.* 2007; 370(1):127-9.
- Krishnan KJ, Reeve AK, Samuels DC, Chinnery PF, Blackwood JK, Taylor RW, Wanrooij S, Spelbrink JN, Lightowlers RN, Turnbull DM. What causes mitochondrial DNA deletions in human cells? *Nat Genet.* 2008; 40(3):275-9.
- Kukat C, Wurm CA, Spåhr H, Falkenberg M, Larsson NG, Jakobs S. Super-resolution microscopy reveals that mammalian mitochondrial nucleoids have a uniform size and frequently contain a single copy of mtDNA. *Proc Natl Acad Sci U S A.* 2011; 108(33):13534-9.
- Kukat C, Davies KM, Wurm CA, Spåhr H, Bonekamp NA, Kühl I, Joos F, Polosa PL, Park CB, Posse V, Falkenberg M, Jakobs S, Kühlbrandt W, Larsson NG. Cross-strand binding of TFAM to a single mtDNA molecule forms the mitochondrial nucleoid. *Proc Natl Acad Sci U S A.* 2015; 112(36):11288-93.
- Lane N. Evolution. The costs of breathing. *Science.* 2011; 334(6053):184-5.
- Lane N. The problem with mixing mitochondria. *Cell.* 2012; 151(2):246-8.
- Lane N. Bioenergetic constraints on the evolution of complex life. *Cold Spring Harb Perspect Biol.* 2014; 6(5):a015982.
- Lapuente-Brun E, Moreno-Loshuertos R, Acín-Pérez R, Latorre-Pellicer A, Colás C, Balsa E, Perales-Clemente E, Quirós PM, Calvo E, Rodríguez-Hernández MA, Navas P, Cruz R, Carracedo Á, López-Otín C, Pérez-Martos A, Fernández-Silva P, Fernández-Vizarra E, Enríquez JA. Supercomplex assembly determines electron flux in the mitochondrial electron transport chain. *Science.* 2013; 340(6140):1567-70.
- Latorre-Pellicer A, Moreno-Loshuertos R, Lechuga-Vieco AV, Sánchez-Cabo F, Torroja C, Acín-Pérez R, Calvo E, Aix E, González-Guerra A, Logan A, Bernad-Miana ML, Romanos E, Cruz R, Cogliati S, Sobrino

- B, Carracedo Á, Pérez-Martos A, Fernández-Silva P, Ruíz-Cabello J, Murphy MP, Flores I, Vázquez J, Enríquez JA. Mitochondrial and nuclear DNA matching shapes metabolism and healthy ageing. *Nature*. 2016; 535(7613):561-5.
- Lee HF, Lee HJ, Chi CS, Tsai CR, Chang TK, Wang CJ. The neurological evolution of Pearson syndrome: case report and literature review. *Eur J Paediatr Neurol*. 2007; 11(4):208-14.
- Lightowlers RN, Rozanska A, Chrzanowska-Lightowlers ZM. Mitochondrial protein synthesis: figuring the fundamentals, complexities and complications, of mammalian mitochondrial translation. *FEBS Lett*. 2014; 588(15):2496-503.
- Luo SM, Ge ZJ, Wang ZW, Jiang ZZ, Wang ZB, Ouyang YC, Hou Y, Schatten H, Sun QY. Unique insights into maternal mitochondrial inheritance in mice. *Proc Natl Acad Sci U S A*. 2013; 110(32):13038-43.
- Mancuso M, Orsucci D, Angelini C, Bertini E, Carelli V, Comi GP, Donati MA, Federico A, Minetti C, Moggio M, Mongini T, Santorelli FM, Servidei S, Tonin P, Toscano A, Bruno C, Bello L, Caldarazzo Ienco E, Cardaioli E, Catteruccia M, Da Pozzo P, Filosto M, Lamperti C, Moroni I, Musumeci O, Pegoraro E, Ronchi D, Sauchelli D, Scarpelli M, Sciacco M, Valentino ML, Vercelli L, Zeviani M, Siciliano G. Redefining phenotypes associated with mitochondrial DNA single deletion. *J Neurol*. 2015; 262(5):1301-9.
- Manea EM, Leverger G, Bellmann F, Stanescu PA, Mircea A, Lèbre AS, Rötig A, Munnich A. Pearson syndrome in the neonatal period: two case reports and review of the literature. *J Pediatr Hematol Oncol*. 2009; 31(12):947-51.
- Manfredi G, Thyagarajan D, Papadopoulou LC, Pallotti F, Schon EA. The fate of human sperm-derived mtDNA in somatic cells. *Am J Hum Genet*. 1997; 61(4):953-60.
- Manoj P. Droplet digital PCR technology promises new applications and research areas. *Mitochondrial DNA A DNA Mapp Seq Anal*. 2016; 27(1):742-6.
- Mao CC, Holt IJ. Clinical and molecular aspects of diseases of mitochondrial DNA instability. *Chang Gung Med J*. 2009; 32(4):354-69.

- Marchi S, Patergnani S, Pinton P. The endoplasmic reticulum-mitochondria connection: one touch, multiple functions. *Biochim Biophys Acta*. 2014; 1837(4):461-9.
- Margulis L. Symbiotic theory of the origin of eukaryotic organelles; criteria for proof. *Symp Soc Exp Biol*. 1975; (29):21-38.
- Martin M, Cho J, Cesare AJ, Griffith JD, Attardi G. Termination factor-mediated DNA loop between termination and initiation sites drives mitochondrial rRNA synthesis. *Cell*. 2005; 123(7):1227-40.
- Martin WF, Garg S, Zimorski V. Endosymbiotic theories for eukaryote origin. *Philos Trans R Soc Lond B Biol Sci*. 2015; 370(1678):20140330.
- McKinney EA, Oliveira MT. Replicating animal mitochondrial DNA. *Genet Mol Biol*. 2013; 36(3):308-15.
- Micol V, Fernández-Silva P, Attardi G. Functional analysis of in vivo and in organello footprinting of HeLa cell mitochondrial DNA in relationship to ATP and ethidium bromide effects on transcription. *J Biol Chem*. 1997; 272(30):18896-904.
- Mileykovskaya E, Penczek PA, Fang J, Mallampalli VK, Sparagna GC, Dowhan W. Arrangement of the respiratory chain complexes in *Saccharomyces cerevisiae* supercomplex III₂IV₂ revealed by single particle cryo-electron microscopy. *J Biol Chem*. 2012; 287(27):23095-103.
- Mishra P, Carelli V, Manfredi G, Chan DC. Proteolytic cleavage of Opa1 stimulates mitochondrial inner membrane fusion and couples fusion to oxidative phosphorylation. *Cell Metab*. 2014; 19(4):630-41.
- Mishra P, Varuzhanyan G, Pham AH, Chan DC. Mitochondrial Dynamics is a Distinguishing Feature of Skeletal Muscle Fiber Types and Regulates Organellar Compartmentalization. *Cell Metab*. 2015; 22(6):1033-44.
- Mitchell P. Coupling of phosphorylation to electron and hydrogen transfer by a chemi-osmotic type of mechanism. *Nature*. 1961; 191:144-8.
- Montoya J, Ojala D, Attardi G. Distinctive features of the 5'-terminal sequences of the human mitochondrial mRNAs. *Nature*. 1981; 290(5806):465-70.

- Moraes CT, Atencio DP, Oca-Cossio J, Diaz F. Techniques and pitfalls in the detection of pathogenic mitochondrial DNA mutations. *J Mol Diagn.* 2003; (4):197-208.
- Moreno-Loshuertos R, Acín-Pérez R, Fernández-Silva P, Movilla N, Pérez-Martos A, Rodríguez de Córdoba S, Gallardo ME, Enríquez JA. Differences in reactive oxygen species production explain the phenotypes associated with common mouse mitochondrial DNA variants. *Nat Genet.* 2006; 38(11):1261-8.
- Nakase H, Moraes CT, Rizzuto R, Lombes A, DiMauro S, Schon EA. Transcription and translation of deleted mitochondrial genomes in Kearns-Sayre syndrome: implications for pathogenesis. *Am J Hum Genet.* 1990; 46(3):418-27.
- Narendra DP, Jin SM, Tanaka A, Suen DF, Gautier CA, Shen J, Cookson MR, Youle RJ. PINK1 is selectively stabilized on impaired mitochondria to activate Parkin. *PLoS Biol.* 2010; 8(1):e1000298.
- Nass MM. Mitochondrial DNA. II. Structure and physicochemical properties of isolated DNA. *J Mol Biol.* 1969; 42(3):529-45.
- Nicholls TJ, Minczuk M. In D-loop: 40 years of mitochondrial 7S DNA. *Exp Gerontol.* 2014; 56:175-81.
- Ojala D, Montoya J, Attardi G. tRNA punctuation model of RNA processing in human mitochondria. *Nature.* 1981; 290(5806):470-4.
- Old SL, Johnson MA. Methods of microphotometric assay of succinate dehydrogenase and cytochrome c oxidase activities for use on human skeletal muscle. *Histochem J.* 1989; 21(9-10):545-55.
- Ozawa T, Yoneda M, Tanaka M, Ohno K, Sato W, Suzuki H, Nishikimi M, Yamamoto M, Nonaka I, Horai S. Maternal inheritance of deleted mitochondrial DNA in a family with mitochondrial myopathy. *Biochem Biophys Res Commun.* 1989. 154:1240–1247.
- Palade GE. The fine structure of mitochondria. *Anat Rec.* 1952; 114(3):427-51.
- Pardo B, Gómez-González B, Aguilera A. DNA repair in mammalian cells: DNA double-strand break repair: how to fix a broken relationship. *Cell Mol Life Sci.* 2009; 66(6):1039-56.
- Peralta S, Wang X, Moraes CT. Mitochondrial transcription: lessons from mouse models.

Biochim Biophys Acta. 2012; 1819(9-10):961-9.

Phillips NR, Sprouse ML, Roby RK. Simultaneous quantification of mitochondrial DNA copy number and deletion ratio: a multiplex real-time PCR assay. *Sci Rep.* 2014; 4:3887.

Picard M, McManus MJ, Csordás G, Várnai P, Dorn GW 2nd, Williams D, Hajnóczky G, Wallace DC. Trans-mitochondrial coordination of cristae at regulated membrane junctions. *Nat Commun.* 2015; 6:6259

Picard M, Wallace DC, Buelle Y. The rise of mitochondria in medicine. *Mitochondrion.* 2016; 30:105-16.

Pietromonaco SF, Denslow ND, O'Brien TW. Proteins of mammalian mitochondrial ribosomes. *Biochimie.* 1991; 73(6):827-35.

Pitceathly RD, Smith C, Fratter C, Alston CL, He L, Craig K, Blakely EL, Evans JC, Taylor J, Shabbir Z, Deschauer M, Pohl U, Roberts ME, Jackson MC, Halfpenny CA, Turnpenny PD, Lunt PW, Hanna MG, Schaefer AM, McFarland R, Horvath R, Chinnery PF, Turnbull DM, Poulton J, Taylor RW, Gorman GS. Adults with RRM2B-related mitochondrial disease have distinct clinical and molecular characteristics. *Brain.* 2012; 135(Pt 11):3392-403.

Pohjoismäki JL, Holmes JB, Wood SR, Yang MY, Yasukawa T, Reyes A, Bailey LJ, Cluett TJ, Goffart S, Willcox S, Rigby RE, Jackson AP, Spelbrink JN, Griffith JD, Crouch RJ, Jacobs HT, Holt IJ. Mammalian mitochondrial DNA replication intermediates are essentially duplex but contain extensive tracts of RNA/DNA hybrid. *J Mol Biol.* 2010; 397(5):1144-55.

Poulton J, Chiaratti MR, Meirelles FV, Kennedy S, Wells D, Holt IJ. Transmission of mitochondrial DNA diseases and ways to prevent them. *PLoS Genet.* 2010; 6(8).

Pyle A, Hudson G, Wilson IJ, Coxhead J, Smertenko T, Herbert M, Santibanez-Koref M, Chinnery PF. Extreme-Depth Re-sequencing of Mitochondrial DNA Finds No Evidence of Paternal Transmission in Humans. *PLoS Genet.* 2015; 11(5):e1005040.

Rahn JJ, Stackley KD, Chan SS. Opa1 is required for proper mitochondrial metabolism in early development. *PLoS One.* 2013; 8(3):e59218.

- Reyes A, Kazak L, Wood SR, Yasukawa T, Jacobs HT, Holt IJ. Mitochondrial DNA replication proceeds via a 'bootlace' mechanism involving the incorporation of processed transcripts. *Nucleic Acids Res.* 2013 Jun; 41(11):5837-50.
- Reyes A, Melchionda L, Nasca A, Carrara F, Lamantea E, Zanolini A, Lamperti C, Fang M, Zhang J, Ronchi D, Bonato S, Fagiolari G, Moggio M, Ghezzi D, Zeviani M. RNASEH1 Mutations Impair mtDNA Replication and Cause Adult-Onset Mitochondrial Encephalomyopathy. *Am J Hum Genet.* 2015; 97(1):186-93.
- Reynier P, Malthiery Y. Accumulation of deletions in MtDNA during tissue aging: analysis by long PCR. *Biochem Biophys Res Commun.* 1995; 217(1):59-67.
- Richter R, Rorbach J, Pajak A, Smith PM, Wessels HJ, Huynen MA, Smeitink JA, Lightowlers RN, Chrzanowska-Lightowlers ZM. A functional peptidyl-tRNA hydrolase, ICT1, has been recruited into the human mitochondrial ribosome. *EMBO J.* 2010; 29(6):1116-25.
- Roberti M, Polosa PL, Bruni F, Manzari C, Deceglie S, Gadaleta MN, Cantatore P. The MTERF family proteins: mitochondrial transcription regulators and beyond. *Biochim Biophys Acta.* 2009; 1787(5):303-11.
- Ronchi D, Garone C, Bordoni A, Gutierrez Rios P, Calvo SE, Ripolone M, Ranieri M, Rizzuti M, Villa L, Magri F, Corti S, Bresolin N, Mootha VK, Moggio M, DiMauro S, Comi GP, Sciacco M. Next-generation sequencing reveals DGUOK mutations in adult patients with mitochondrial DNA multiple deletions. *Brain.* 2012 Nov;135(Pt 11):3404-15.
- Ronchi D, Di Fonzo A, Lin W, Bordoni A, Liu C, Fassone E, Pagliarani S, Rizzuti M, Zheng L, Filosto M, Ferrò MT, Ranieri M, Magri F, Peverelli L, Li H, Yuan YC, Corti S, Sciacco M, Moggio M, Bresolin N, Shen B, Comi GP. Mutations in DNA2 link progressive myopathy to mitochondrial DNA instability. *Am J Hum Genet.* 2013; 92(2):293-300.

Rouzier C, Bannwarth S, Chausseot A, Chevrollier A, Verschueren A, Bonello-Palot N, Fragaki K, Cano A, Pouget J, Pellissier JF, Procaccio V, Chabrol B, Paquis-Flucklinger V. The MFN2 gene is responsible for mitochondrial DNA instability and optic atrophy 'plus' phenotype. *Brain*. 2012; 135(Pt 1):23-34.

Rygiel KA, Grady JP, Turnbull DM. Respiratory chain deficiency in aged spinal motor neurons. *Neurobiol Aging*. 2014; 35(10):2230-8.

Rygiel KA, Grady JP, Taylor RW, Tuppen HA, Turnbull DM. Triplex real-time PCR--an improved method to detect a wide spectrum of mitochondrial DNA deletions in single cells. *Sci Rep*. 2015; 5:9906.

Santel A, Fuller MT. Control of mitochondrial morphology by a human mitofusin. *J Cell Sci*. 2001; 114(Pt 5):867-74.

Santo-Domingo J, Giacomello M, Poburko D, Scorrano L, Demareux N. OPA1 promotes pH flashes that spread between contiguous mitochondria without matrix protein exchange. *EMBO J*. 2013; 32(13):1927-40.

Sarraf SA, Raman M, Guarani-Pereira V, Sowa ME, Huttlin EL, Gygi SP, Harper JW. Landscape of the PARKIN-dependent ubiquitylome in response to mitochondrial depolarization. *Nature*. 2013 Apr 18; 496(7445):372-6.

Sato M, Sato K. Maternal inheritance of mitochondrial DNA: degradation of paternal mitochondria by allogeneic organelle autophagy, allophagy. *Autophagy*. 2012; 8(3):424-5.

Schaefer AM, McFarland R, Blakely EL, He L, Whittaker RG, Taylor RW, Chinnery PF, Turnbull DM. Prevalence of mitochondrial DNA disease in adults. *Ann Neurol*. 2008 Jan;63(1):35-9.

Schon EA, Rizzuto R, Moraes CT, Nakase H, Zeviani M, DiMauro S. A direct repeat is a hotspot for large-scale deletion of human mitochondrial DNA. *Science*. 1989; 244(4902):346-9.

Schon EA, DiMauro S, Hirano M. Human mitochondrial DNA: roles of inherited and somatic mutations. *Nat Rev Genet*. 2012; 13(12):878-90.

Shanske S, Yingying Tang, Michio Hirano, Yutaka Nishigaki, Kurenai Tanji, Eduardo Bonilla, Carolyn Sue, Sindu Krishna, Jose R. Carlo, Judith Willner, Eric A. Schon, Salvatore DiMauro. Identical

Mitochondrial DNA Deletion in a Woman with Ocular Myopathy and in Her Son with Pearson Syndrome. *Am J Hum Genet.* 2002; 71(3): 679–683.

Sharpley MS, Marciniak C, Eckel-Mahan K, McManus M, Crimi M, Waymire K, Lin CS, Masubuchi S, Friend N, Koike M, Chalkia D, MacGregor G, Sassone-Corsi P, Wallace DC. Heteroplasmy of Mouse mtDNA is Genetically Unstable and Results in Altered Behavior and Cognition. *Cell.* 2012; 151(2): 333–343.

Shoffner JM, Lott MT, Voljavec AS, S A Soueidan, D A Costigan, Wallace DC. Spontaneous Kearns-Sayre/chronic external ophthalmoplegia plus syndrome associated with a mitochondrial DNA deletion: a slip-replication model and metabolic therapy. *Proc Natl Acad Sci U S A.* 1989; 86(20): 7952–7956.

Shutt TE, Gray MW. Twinkle, the mitochondrial replicative DNA helicase, is widespread in the eukaryotic radiation and may also be the mitochondrial DNA primase in most eukaryotes. *J Mol Evol.* 2006; 62(5):588-99.

Smirnov A, Entelis N, Martin RP, Tarassov I. Biological significance of 5S rRNA import into human mitochondria: role of ribosomal protein MRP-L18. *Genes Dev.* 2011 Jun; 25(12):1289-305.

Smirnova E, Griparic L, Shurland DL, van der Bliek AM. Dynamin-related protein Drp1 is required for mitochondrial division in mammalian cells. *Mol Biol Cell.* 2001; 12(8):2245-56.

Sofronova JK, Ilinsky YY, Orishchenko KE, Chupakhin EG, Lunev EA, Mazunin IO. Detection of Mutations in Mitochondrial DNA by Droplet Digital PCR. *Biochemistry (Mosc).* 2016; 81(10):1031-1037.

Sommerville EW, Chinnery PF, Gorman GS, Taylor RW. Adult-onset Mendelian PEO Associated with Mitochondrial Disease. *J Neuromuscul Dis.* 2014; 1(2):119-133.

Spelbrink JN, Li FY, Tiranti V, Nikali K, Yuan QP, Tariq M, Wanrooij S, Garrido N, Comi G, Morandi L, Santoro L, Toscano A, Fabrizi GM, Somer H, Croxen R, Beeson D, Poulton J, Suomalainen A, Jacobs HT, Zeviani M, Larsson C. Human mitochondrial DNA deletions associated with mutations in the gene encoding Twinkle, a phage T7 gene 4-like protein localized in mitochondria. *Nat Genet.* 2001; 28(3):223-31.

- Spinazzola A, Viscomi C, Fernandez-Vizarra E, Carrara F, D'Adamo P, Calvo S, Marsano RM, Donnini C, Weiher H, Strisciuglio P, Parini R, Sarzi E, Chan A, DiMauro S, Rötig A, Gasparini P, Ferrero I, Mootha VK, Tiranti V, Zeviani M. MPV17 encodes an inner mitochondrial membrane protein and is mutated in infantile hepatic mitochondrial DNA depletion. *Nat Genet.* 2006; 38(5):570-5.
- Spinazzola A, Santer R, Akman OH, Tsiakas K, Schaefer H, Ding X, Karadimas CL, Shanske S, Ganesh J, DiMauro S, Zeviani M. Hepatocerebral form of mitochondrial DNA depletion syndrome: novel MPV17 mutations. *Arch Neurol.* 2008; 65(8):1108-13.
- Stumpf JD, Copeland WC. Mitochondrial DNA replication and disease: insights from DNA polymerase γ mutations. *Cell Mol Life Sci.* 2011; 68(2):219-33.
- Tapper DP, Clayton DA. Mechanism of replication of human mitochondrial DNA. Localization of the 5' ends of nascent daughter strands. *J Biol Chem.* 1981; 256(10):5109-15.
- Tiranti V, Rocchi M, DiDonato S, Zeviani M. Cloning of human and rat cDNAs encoding the mitochondrial single-stranded DNA-binding protein (SSB). *Gene.* 1993; 126(2):219-25.
- Tynismaa H, Mjosund KP, Wanrooij S, Lappalainen I, Ylikallio E, Jalanko A, Spelbrink JN, Paetau A, Suomalainen A. Mutant mitochondrial helicase Twinkle causes multiple mtDNA deletions and a late-onset mitochondrial disease in mice. *Proc Natl Acad Sci U S A.* 2005; 102(49):17687-92.
- Tynismaa H, Sun R, Ahola-Erkkilä S, Almusa H, Pöyhönen R, Korpela M, Honkaniemi J, Isohanni P, Paetau A, Wang L, Suomalainen A. Thymidine kinase 2 mutations in autosomal recessive progressive external ophthalmoplegia with multiple mitochondrial DNA deletions. *Hum Mol Genet.* 2012; 21(1):66-75.
- Valentino ML, Martí R, Tadesse S, López LC, Manes JL, Lyzak J, Hahn A, Carelli V, Hirano M. Thymidine and deoxyuridine accumulate in tissues of patients with mitochondrial neurogastrointestinal encephalomyopathy (MNGIE). *FEBS Lett.* 2007; 581(18):3410-4.

- Van Goethem G, Dermaut B, Löfgren A, Martin JJ, Van Broeckhoven C. Mutation of POLG is associated with progressive external ophthalmoplegia characterized by mtDNA deletions. *Nat Genet.* 2001; 28(3):211-2.
- Van Hove JL, Cunningham V, Rice C, Ringel SP, Zhang Q, Chou PC, Truong CK, Wong LJ. Finding twinkle in the eyes of a 71-year-old lady: a case report and review of the genotypic and phenotypic spectrum of TWINKLE-related dominant disease. *Am J Med Genet A.* 2009; 149 A (5):861-7.
- Van Tuyle GC, Pavco PA. The rat liver mitochondrial DNA-protein complex: displaced single strands of replicative intermediates are protein coated. *J Cell Biol.* 1985; 100(1):251-7.
- Walberg MW, Clayton DA. In vitro transcription of human mitochondrial DNA. Identification of specific light strand transcripts from the displacement loop region. *J Biol Chem.* 1983; 258(2):1268-75.
- Wallace DC, Singh G, Lott MT, Hodge JA, Schurr TG, Lezza AM, Elsas LJ 2nd, Nikoskelainen EK. Mitochondrial DNA mutation associated with Leber's hereditary optic neuropathy. *Science.* 1988; 242(4884):1427-30.
- Wallace DC. Mitochondrial genetics: a paradigm for aging and degenerative diseases? *Science.* 1992; 256(5057):628-32.
- Wallace DC. Why do we still have a maternally inherited mitochondrial DNA? Insights from evolutionary medicine. *Annu Rev Biochem.* 2007; 76:781-821.
- Wallace DC, Chalkia D. Mitochondrial DNA genetics and the heteroplasmy conundrum in evolution and disease. *Cold Spring Harb Perspect Biol.* 2013; 5(11):a021220.
- Wanrooij S, Falkenberg M. The human mitochondrial replication fork in health and disease. *Biochim Biophys Acta.* 2010; 1797(8):1378-88.
- Wong LJ, Naviaux RK, Brunetti-Pierri N, Zhang Q, Schmitt ES, Truong C, Milone M, Cohen BH, Wical B, Ganesh J, Basinger AA, Burton BK, Swoboda K, Gilbert DL, Vanderver A, Saneto RP, Maranda B, Arnold G, Abdenur JE, Waters PJ, Copeland WC. Molecular and clinical genetics of mitochondrial diseases due to POLG mutations. *Hum Mutat.* 2008; 29(9):E150-72.

- Xu B, Clayton DA. A persistent RNA-DNA hybrid is formed during transcription at a phylogenetically conserved mitochondrial DNA sequence. *Mol Cell Biol.* 1995; 15(1):580-9.
- Yakubovskaya E, Chen Z, Carrodeguas JA, Kisker C, Bogenhagen DF. Functional human mitochondrial DNA polymerase gamma forms a heterotrimer. *J Biol Chem.* 2006; 281(1):374-82.
- Yang C, Curth U, Urbanke C, Kang C. Crystal structure of human mitochondrial single-stranded DNA binding protein at 2.4 Å resolution. *Nat Struct Biol.* 1997; 4(2):153-7.
- Yang MY, Bowmaker M, Reyes A, Vergani L, Angeli P, Gringeri E, Jacobs HT, Holt IJ. Biased incorporation of ribonucleotides on the mitochondrial L-strand accounts for apparent strand-asymmetric DNA replication. *Cell.* 2002; 111(4):495-505.
- Yasukawa T, Reyes A, Cluett TJ, Yang MY, Bowmaker M, Jacobs HT, Holt IJ. Replication of vertebrate mitochondrial DNA entails transient ribonucleotide incorporation throughout the lagging strand. *EMBO J.* 2006; 25(22):5358-71.
- Yoon Y, McNiven MA. Mitochondrial division: New partners in membrane pinching. *Curr Biol.* 2001; 11(2):R67-70.
- Youle RJ, Narendra DP. Mechanisms of mitophagy. *Nat Rev Mol Cell Biol.* 2011; 12(1):9-14.
- Youle RJ, van der Bliek AM. Mitochondrial fission, fusion, and stress. *Science.* 2012; 337(6098):1062-5.
- Yu-Wai-Man P, Sitarz KS, Samuels DC, Griffiths PG, Reeve AK, Bindoff LA, Horvath R, Chinnery PF. OPA1 mutations cause cytochrome c oxidase deficiency due to loss of wild-type mtDNA molecules. *Hum Mol Genet.* 2010; 19(15):3043-52.
- Yu-Wai-Man P, Lai-Cheong J, Borthwick GM, He L, Taylor GA, Greaves LC, Taylor RW, Griffiths PG, Turnbull DM. Somatic mitochondrial DNA deletions accumulate to high levels in aging human extraocular muscles. *Invest Ophthalmol Vis Sci.* 51(7):3347-53.
- Zeviani M, Servidei S, Gellera C, Bertini E, DiMauro S, DiDonato S. An autosomal dominant disorder with multiple deletions of mitochondrial DNA starting at the D-loop region. *Nature.* 1989; 339(6222):309-11.

Zeviani M, Bresolin N, Gellera C, Bordoni A, Pannacci M, Amati P, Moggio M, Servidei S, Scarlato G, DiDonato S. Nucleus-driven multiple large-scale deletions of the human mitochondrial genome: a new autosomal dominant disease. *Am J Hum Genet.* 1990; 47(6):904-14.

Zeviani M, Carelli V. Mitochondrial disorders. *Curr Opin Neurol.* 2003; 16(5):585-94. Review.

Züchner S, Mersiyanova IV, Muglia M, Bissar-Tadmouri N, Rochelle J, Dadali EL, Zappia M, Nelis E, Patitucci A, Senderek J, Parman Y, Evgrafov O, Jonghe PD, Takahashi Y, Tsuji S, Pericak-Vance MA, Quattrone A, Battaloglu E, Polyakov AV, Timmerman V, Schröder JM, Vance JM. Mutations in the mitochondrial GTPase mitofusin 2 cause Charcot-Marie-Tooth neuropathy type 2A. *Nat Genet.* 2004; 36(5):449-51.

